Diplomarbeit

Development of a UHF Frontend for a Comprehensive RFID Rapid Prototyping System

ausgeführt zum Zwecke der Erlangung des akademischen Grades eines Diplom-Ingenieurs unter Leitung von

Dipl.-Ing. Robert Langwieser

und

Ao. Univ.Prof. Arpad L. Scholtz

E389

Institut für Nachrichtentechnik und Hochfrequenztechnik

eingereicht an der Technischen Universität Wien

Fakultät für Elektrotechnik und Informationstechnik

von

Gregor Lasser

0125809

Pfadenhauerg.12/3/9, 1140 Wien

Wien, Oktober 2008

Abstract

Currently, Radio Frequency IDentification (RFID) is a booming area of research, especially the industry has high expectations for this technology. It should allow for tracking a product or components from production to customer on a convenient way. To achieve the higher reading range necessary for this applications, solutions in the UHF[1] range are getting increasingly into focus.

In this work I describe design and implementation of a frontend for a UHF RFID testbed. With this system novel RFID tags can be characterized. In addition, it allows to test new transmission modes for RFID.

In the first chapter fundamental characteristics and limits of UHF RFID systems are discussed. Furthermore, the system concept developed is described. In the next chapters the development and the characterization of the main components – transmitter, receiver and carrier compensation unit (CCU) – is illustrated. Finally, an experiment is presented, that has demonstrated the functionality and the outstanding capability of the frontend developed.

[1] Ultra High Frequency

Kurzfassung

Radio Frequency IDentification (RFID) ist derzeit ein boomendes Forschungsgebiet, besonders da die Industrie große Erwartungen an diese Technologie hat. Sie soll unter anderem die Verfolgung eines Produkts oder einzelner Komponenten von der Fertigung bis zum Kunden auf günstigem Wege ermöglichen. Um die dafür benötigten höheren Lesereichweiten zu erreichen wird zunehmend auf Lösungen im UHF[1] Bereich gesetzt.

In dieser Arbeit beschreibe ich Entwicklung und Aufbau des Hochfrequenzteils für ein UHF RFID Testsystem. Mit diesem System können neuartige RFID Transponder vermessen werden. Außerdem besteht die Möglichkeit neue Übertragungsverfahren für RFID zu testen.

Im ersten Kapitel werden grundlegende Eigenschaften und Grenzen von UHF RFID-Systemen besprochen. Im Weiteren wird das entwickelte Systemkonzept des Hochfrequenzteils beschrieben. In den nächsten Kapitel wird die Entwicklung und Vermessung der Hauptkomponenten Sender, Empfänger und Trägerkompensationseinheit (CCU) erläutert. Schließlich wird ein Experiment präsentiert, mit dem die Funktionalität und herausragende Leistungsfähigkeit des entwickelten Hochfrequenzteils demonstriert werden konnte.

[1] Ultra High Frequency

Contents

Chapter 1

Introduction

In our modern world there are many cases where large amounts of objects need to be identified. Radio Frequency IDentification (RFID) is a possible solution for such matters that has some advantages compared to conventional solutions like barcodes or smartcards.

While RFID systems were developed in World War II two distinguish between friend or foe, they have become quite popular today in many civil applications. These applications include enterprise supply chain management, electronic road pricing, access to public transport systems, libraries, inventory systems and animal identification [1].

Every RFID system can be split up in two parts: The **tag** or **transponder** that stores information and is placed on the object being identified, and the **reader** or **interrogator** that establishes the communication to one or more tags. The communication between reader and tag is performed with radio signals, whereas different frequencies are used. Common frequencies used for RFID are listed in Table 1.1 [2, p. 43].

System	Frequency
LF	135 kHz
HF	13.56 MHz
UHF Europe	865 - 868 MHz
UHF USA	902 - 928 MHz
Microwave	2.45 GHz

Table 1.1: Frequency ranges of different RFID systems

While RFID systems operated in the LF[1] and the HF[2] range use inductive coupling between tag and reader to exchange information, UHF[3] and microwave systems employ electromagnetic waves for the same purpose.

Another way to classify RFID systems is the method of supplying power to the tag. Usually the three varieties are called:

[1] Low Frequency
[2] High Frequency
[3] Ultra High Frequency

- **active**,
- **semi-passive**, and
- **passive**.

Active tags use a battery to supply memory cells, control electronics and a transmitter to send data to the reader. This allows for complex functions being implemented on the tag and enables long range communication. Active tags can also be used for data logging while not in direct contact with a reader. A disadvantage of active tags is that batteries are quite big and their lifetime is limited.

Passive tags do not have their own power supply, and therefore all power required for operation must be drawn from the electromagnetic field supplied by the reader. It is clear that no independent functions like data logging can be performed. Usually these tags just provide an amount of memory that can be read, and sometimes written from the interrogator. For data transfer to the reader a technique called backscattering or modulated RCS[4] is used.

Semi-passive tags combine active and passive tag technology. For data transmission power-saving backscattering is used but the tags electronics is supplied by battery. This combination enables active tag functionality but greatly enhances battery life and simplifies tag design due to the absence of an RF[5] transmitter.

1.1 Regulations

The focus of this work is on European RFID systems operating in the UHF band, so only regulations regarding this band are discussed.

Many European countries have implemented the ERC RECOMMENDATION 70-03 [3]. Here the UHF band is divided into 15 channels, each occupying a bandwidth of 200 kHz. The center frequency is therefore calculated by $864.9\,\text{MHz} + 0.2\,\text{MHz} \cdot n$, where n is the channel number.

In channels 4-13, corresponding to a frequency band of $865.6 - 867.6\,\text{MHz}$, the maximum allowed ERP[6] is 2 W. In the complete range of $865 - 868\,\text{MHz}$ only 0.5 W ERP is allowed.

1.2 Backscattering

As mentioned before, backscattering is the key technique for tag to reader communications in passive or semi-passive RFID systems. Figure 1.1 (compare to [4, p. 212]) illustrates a passive RFID system with special focus on backscattering.

[4] Radar Cross Section
[5] Radio Frequency
[6] Equivalent Radiated Power

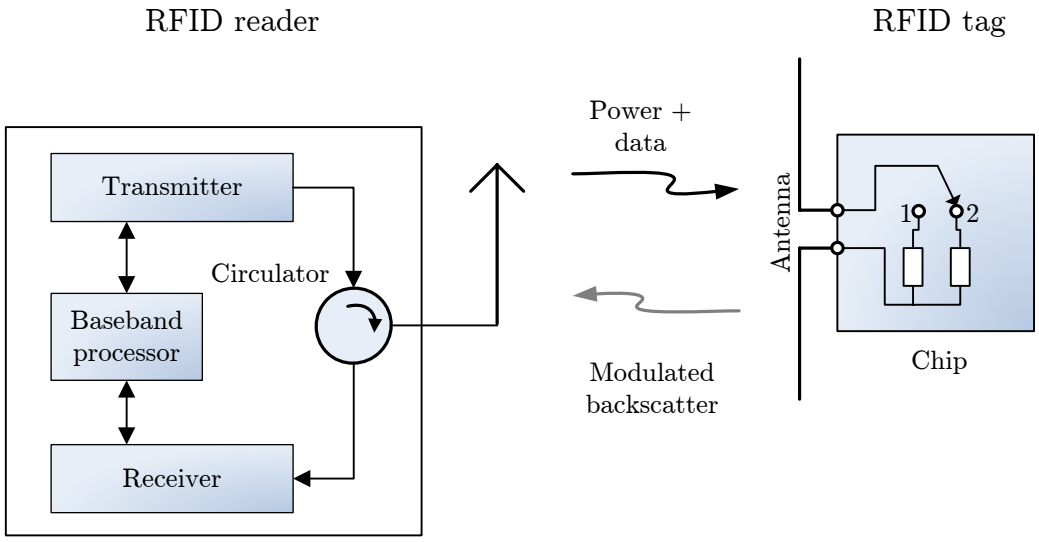

Figure 1.1: An overview of a passive RFID system [4, p. 212]

On the left hand side the reader is depicted. It consists of a transmitter part that produces an RF signal to power the tag and to send commands, and a receiver that takes care on amplifying and purifying received signals. Both, transmitter and receiver are connected to a single antenna via a circulator. Generation of baseband command sequences, demodulation of received signals and protocol control are implemented in a baseband processor.

The RFID tag, shown on the right side of the figure, consists of an antenna and an ASIC[7] chip. The focus of Figure 1.1 is on backscattering, so the tag-chip's frontend is drawn schematically to illustrate the chip's possibility to switch its input impedance between two states. This enables to change the amount of power being reradiated from the tag antenna due to antenna–chip mismatch. At an alternative point of view the impedance switching changes the RCS of the tag.

Most of the time an RFID reader tries to communicate with a tag it transmits a carrier signal to power the tag. Only in short reader to tag communication events, the unmodulated carrier is replaced by an ASK[8]-modulated signal that contains the reader's commands for the tag. Whenever a reader command requires a tag response, the tag starts its data transfer after a certain delay using backscattering. In this time period the reader again transmits a continuous wave signal that is partly reflected by the tag. The actual amount of power being reradiated depends on the antenna–chip mismatch. This dependency is now used at the tag to transmit data to the reader. The information-stream controls a switch that changes the antenna's load impedance and therefore acts as a modulator. It is now possible for the reader to retrieve this information by detection of the tag's

[7] Application-Specific Integrated Circuit
[8] Amplitude-Shift Keying

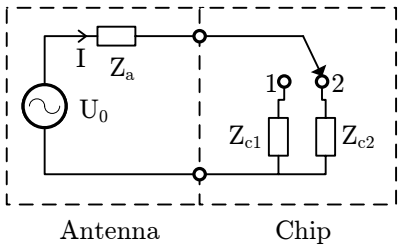

Figure 1.2: Tag equivalent circuit regarding backscattering [7]

backscattered signal.

The total backscattered field of any antenna can be decomposed in a constant part, the field scattered at the open-circuited antenna, and a variable part, the field scattered back due to antenna loading [5]. Antennas whose open-circuited backscattered part is zero are called minimum-scattering antennas [6]. The constant part of backscattered power does not bear any information and it is therefore sufficient to concentrate on the variable part, or at an other point of view, on minimum-scattering antennas. For such tag antennas an expression for their reradiated power has been derived in [4].

The power density S of an electromagnetic wave produced by a transmit antenna with antenna gain G_t fed with transmit power P_t in a distance r is given by

$$S = \frac{P_t G_t}{4\pi r^2}. \tag{1.1}$$

A receiver antenna with an effective antenna area

$$A_e = \frac{\lambda^2}{4\pi} G \tag{1.2}$$

collects the power P_a

$$P_a = S A_e \tag{1.3}$$

where G is the gain of the receiver antenna and λ is the wavelength. P_a represents the power provided at the antenna's port at matched conditions.

The reradiated power for a lossless antenna can be found from the equivalent circuit[9], Figure 1.2. The left side, with voltage source U_0 and source impedance Z_a, represents the antenna and the right side represents the switchable load impedances Z_{c1} and Z_{c2}. For the following derivation of the reradiated power and the RCS just Z_c is being used to represent both states.

The current I is easily calculated with Ohms law:

$$I = \frac{U_0}{|Z_a + Z_c|} \tag{1.4}$$

[9] Although this approach has several limitations [8], and is unsuited to analyze the backscattering behavior for arbitrary antennas, it is possible to successfully apply it here because only minimum-scattering antennas are considered [9].

When the impedances Z_a and Z_c are split up according to $Z_a = R_a + jX_a$ and $Z_c = R_c + jX_c$ the reradiated power P_{rerad} can be written as

$$P_{rerad} = I^2 \cdot R_a = \frac{U_0^2 \cdot R_a}{|Z_a + Z_c|^2} \tag{1.5}$$

The available power P_a can be calculated as the power P_L being absorbed in the load Z_c when we assume matched load conditions. In this case $Z_c = {Z_a}^*$ and therefore $R_c = R_a$. The voltages on the resistors R_c and R_a are equal and are $U_0/2$. So we find

$$P_a = P_L = \frac{(\frac{U_0}{2})^2}{R_a} = \frac{U_0^2}{4R_a}. \tag{1.6}$$

When we use the expression for U_0 in Equation 1.6 and insert this in Equation 1.5 we get

$$P_{rerad} = \frac{4P_a \cdot R_a^2}{|Z_a + Z_c|^2} \tag{1.7}$$

Finally, we use this expression to calculate the *EIRP* [10] reradiated from the tag

$$EIRP_{rerad} = P_{rerad} G = K P_a G \tag{1.8}$$

with the factor K given by

$$K = \frac{4R_a^2}{|Z_a + Z_c|^2}. \tag{1.9}$$

Equation (1.9) shows the influence of load-impedance mismatch on the amount of reradiated power. Some interesting values are printed in Table 1.2. Under matched load conditions, that permit maximum power transfer to the supply circuits of the tag, the reradiated power is qual to the power coupled to the power supply circuits.

Z_c	K
0	$\frac{4R_a^2}{R_a^2+X_a^2}$
Z_a^*	1
∞	0

Table 1.2: The K factor for different antenna load impedances. [4]

The radar cross section of the tag can now be calculated as

$$\sigma = \frac{EIRP_{rerad}}{S} = K A_e G \tag{1.10}$$

[10] Equivalent Isotropically Radiated Power

where the expression from (1.8) for the $EIRP_{rerad}$ has been used. By using the expressions for K and A_e from (1.9) and (1.2) we get

$$\sigma = \frac{\lambda^2 G^2 R_a^2}{\pi |Z_a + Z_c|^2}. \tag{1.11}$$

This equation is valid for tag and reader antennas being matched with respect to their polarizations and with the tag antenna pointing toward the reader.

When the tag transmits information to the reader, it switches between its two impedance states Z_{c1} and Z_{c2}. Therefore, the tag's RCS changes and a scalar differential radar cross section can be introduced:

$$\Delta\tilde{\sigma} = \sigma_1 - \sigma_2 = \frac{\lambda^2 G^2 R_a^2}{\pi} \left(\frac{1}{|Z_a + Z_{c1}|^2} - \frac{1}{|Z_a + Z_{c2}|^2} \right) \tag{1.12}$$

It is important to note, that the RCS presented in (1.11) and the scalar differential RCS $\Delta\tilde{\sigma}$ (1.12) is only a measure of the reflected **power** but not on the **phase** of the reflected signal. Therefore, even in situations where $\Delta\tilde{\sigma}$ is zero the phase-shift in the backscattered signal can be sufficient to successfully receive the tag's message. This can even be accomplished with a envelope detector, as discussed in the following section.

A true measure of the difference of the two states of backscattering offers the vector differential RCS [7]. With the introduction of complex power wave reflection coefficients

$$\rho_{1,2} = \frac{Z_{c1,2} - Z_a{}^*}{Z_{c1,2} + Z_a} \tag{1.13}$$

we get the vector differential RCS [7]

$$\Delta\sigma = \frac{\lambda^2 G^2}{4\pi} |\rho_1 - \rho_2|^2. \tag{1.14}$$

The vector differential RCS represents the difference of the two states of backscattering that can be measured using a coherent receiver.

1.3 Receiving Backscattered Signals

A major difference between conventional radio communication systems and passive RFID systems is the fact, that receiver and transmitter of an RFID system operate on the same frequency at the same time.

This is only possible when special care is taken to isolate the receiver from the transmitter. One possibility is to use different directional antennas for the receive and transmit path placed sufficiently apart from each other. Another possibility is to use one antenna, and connect receiver and transmitter through a circulator, as shown in Figure 1.1.

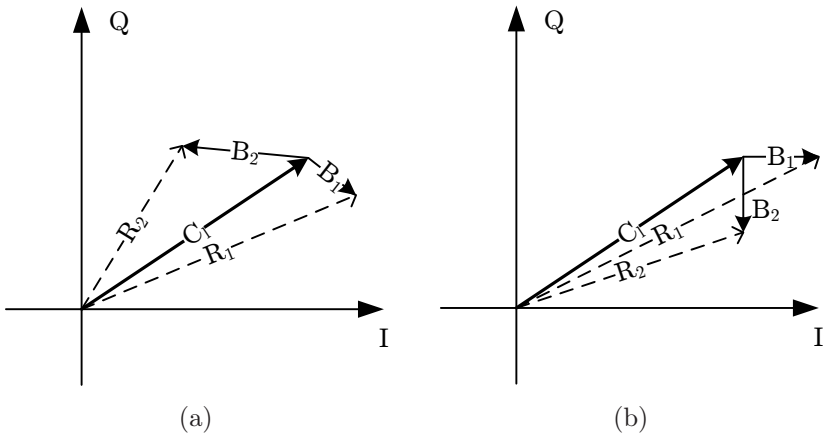

Figure 1.3: I/Q representation of the backscattered signals $B_{1,2}$, the leaking carrier C_l, and the resulting receiver signals $R_{1,2}$.

In both cases a part of the transmit signal will still leak into the receiver. The backscattered signal and the leaking carrier add up as vectors, forming the receiver input signal. Figure 1.3 depicts two possibilities of these signal constellations, that could be interpreted as receiver voltages or field quantities at the receiver antenna.

In Figure 1.3 the coordinate system represents the inphase (I) and quadrature (Q) components of some reference signal, for instance the transmit signal. Figure 1.3(a) shows the general case where the two states of backscattering B_1 and B_2 have different amplitude and phase. The difference in amplitude also results in a difference in power, therefore the backscattered signals can be characterized by some nonzero $\Delta\tilde{\sigma}$ as introduced in Section 1.2. The receiver input signals R_1 and R_2 are constructed by adding the leaking carrier C_l. In this case also the resulting received signals are different in amplitude and phase. Therefore, a simple non-coherent receiver like an envelope detector is able to detect the tag's message.

In Figure 1.3(b) the two backscattered signals have the same amplitude, representing a case where the scalar $\Delta\tilde{\sigma}$ is zero. One would suspect that such a tag signal can only be received with a coherent detector, but this is only true when no leaking carrier is present. The figure demonstrates that adding the leaking carrier C_l of matching phase results in two unequal received signals R_1 and R_2.

But also the opposite effect is possible: A bad matching leakage signal can remove any amplitude difference from the backscattered signals, as shown in Figure 1.4. The circle touching the tips of R_1 and R_2 demonstrates that the amplitudes of the received signals are equal.

This last example shows that a guaranteed detection of backscattered signals can only be achieved by using coherent receivers or rather I/Q detection.

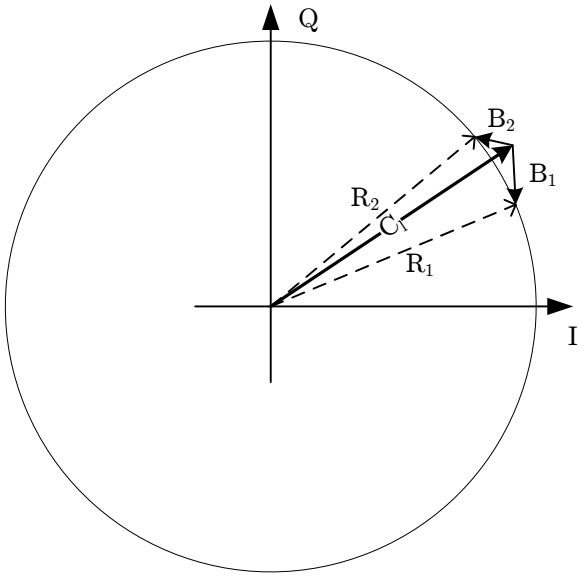

Figure 1.4: I/Q representation of the backscattered signals $B_{1,2}$, the leaking carrier C_l and the receiver signals $R_{1,2}$, here resulting in a loss of amplitude change in the receiver.

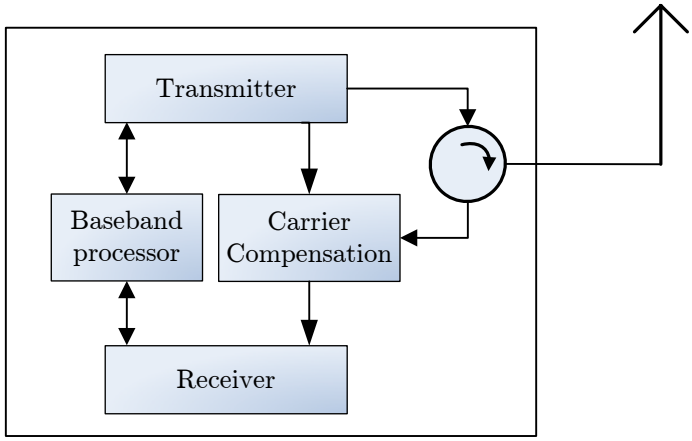

Figure 1.5: RFID reader with carrier compensation.

1.4 Carrier Compensation

As mentioned in Section 1.3 carrier leakage from the transmitter to the receiver is an important issue in RFID systems. The leaking carrier not only changes the modulation properties of the received signal, it also causes receiver blocking or even worse, destruction of the receiver.

To minimize such problems, some readers use some sort of leaking carrier canceler [10], also called carrier compensation or direct coupling compensation [2].

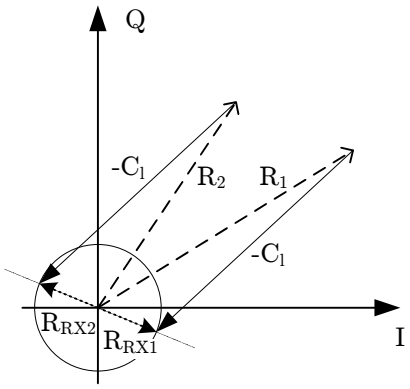

Figure 1.6: Effect of carrier compensation on an arbitrary backscattered signal

Figure 1.5 depicts a reader that incorporates a carrier compensation.

The idea is to cancel the leaking carrier by generating its inverse and then summing this signal with the received signal. In the context of carrier compensation a signal's inverse is its additive inverse often also called inverted signal. To generate the inverse of the leaking carrier, part of the transmit signal is fed into the carrier compensation block, where its polarity is inverted and it is attenuated to match the leaking carrier signal. The receiver antenna (in two antenna systems) or the receiver output of the circulator (in one antenna systems as drawn in Figure 1.5) is now connected to the carrier compensation module. The received signal is added to the reconstructed inverse leaking carrier resulting in a purified received signal that is fed to the receiver.

This concept reveals some new problems. First of all, amplitude and phase of the leaking carrier are usually unknown. Therefore, some estimation has to be used. One method is to minimize the receiver input signal by adjusting the amplitude and phase of the reconstructed leaking carrier signal. Besides the fact that this minimization is not easy in practice, this approach also modifies the modulation characteristics of the original backscattered signal.

When we assume that the two states of the backscattered signal are equally likely, the minimum received power approach results in a transformation of the original signal constellation to a BPSK[11]-signal. This situation is illustrated in Figure 1.6.

R_1 and R_2 represent the two reader input signals corresponding to the two states of backscattered signals. These reader input signals are the result of the backscattered signals and some leaking carrier, as was shown in Figure 1.3.

The estimated inverse leaking carrier is labeled $-C_l$. When it is added to the reader input signals R_1 and R_2, the receiver input signals (or carrier compensation output signals) R_{RX1} and R_{RX2} are generated. These resulting signals are antipodal. The receiver input signals are therefore very well suited for coherent

[11] Binary Phase Shift Keying

detection, but useless for envelope detection.

Where this result is quite interesting in theory, it should be quite rare in practical situations. The reason for this is that first of all usually one state is much more likely than the other. (When the tag listens to the reader or is waiting for a command it just remains in one dedicated state.)

The second reason is that in normal environments with moving tags and other scatterers, it is almost impossible to perfectly compensate for the leaking carrier. In this situations the resulting signal constellation will be more general with some reduction in receiver input power.

The worst case scenario is an estimated leaking carrier being 180° out of phase. Then the leaking carrier and its "canceling" counterpart would interfere constructively, resulting in a receiver input signal of twice the power of the original reader input signal. To avoid this the carrier compensation module continuously has to adjust the canceling carrier in amplitude and phase.

Chapter 2

System Concept

This chapter describes general RFID reader design considerations and presents an overview of the specific frontend I have designed in this work. This frontend supports different tags and test modes with different requirements. Therefore, the reader design has to be modular and flexible.

2.1 Link Budget

For a serious reader design a proper link budget is essential. The various requirements necessary to support different test scenarios are analyzed in the next subsections. Figure 2.1 presents the fundamental RFID scenarios underlying the following calculations.

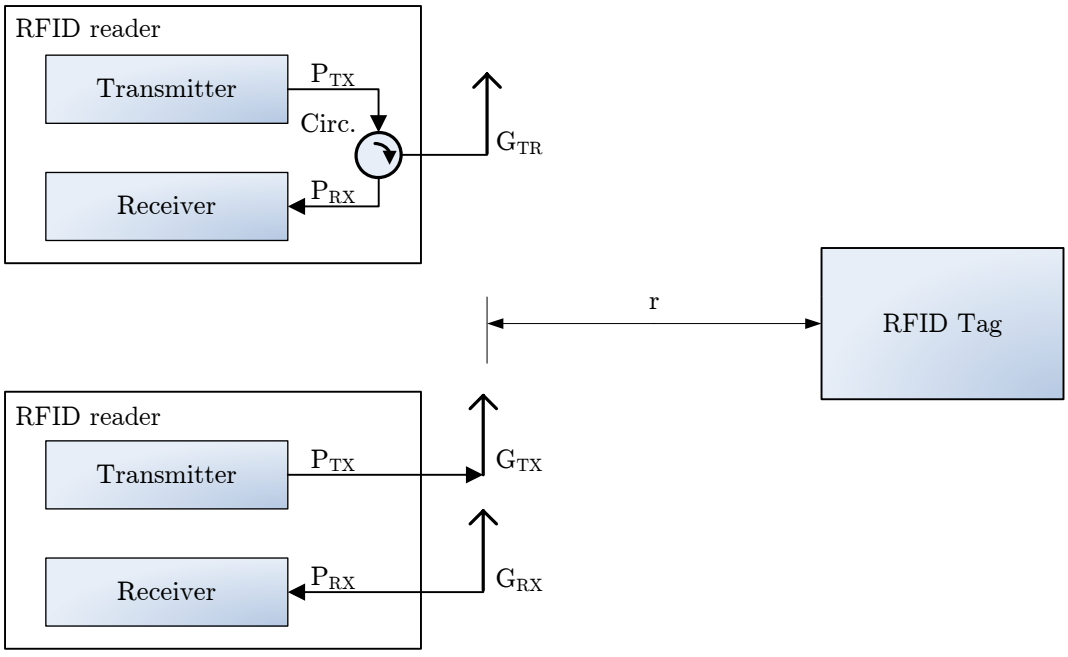

Figure 2.1: Simple RFID scenario showing single antenna- (top) and dual antenna reader (bottom).

2.1.1 Required Reader Sensitivity

First of all the maximum tag–reader distance has to be estimated. Current passive tags require about 5 µW to power their circuitry [10]. The tag input power P_{Tag} is calculated

$$P_{Tag} = G_{TX} P_{TX} G_{Tag} \left(\frac{\lambda}{4\pi r} \right)^2 \tag{2.1}$$

Where: P_{TX} is the transmitted power
G_{TX} is the reader's transmit antenna gain
G_{Tag} is the tag's antenna gain
λ is the wavelength
r is the distance between reader and tag

As indicated in Section 1.1 legal operation in Europe allows for a maximum transmit power of 2 W ERP. Therefore $G_{TX} P_{TX}$ in Equation 2.1 can be substituted by the *EIRP* , where the dipole's gain of 1.64 compared to an isotropic antenna has to be taken into account. So we get an EIRP[1] of 2 W·1.64 = 3.28 W.

$$P_{Tag} = EIRP\, G_{Tag} \left(\frac{\lambda}{4\pi r} \right)^2 \tag{2.2}$$

To calculate the maximum tag–reader distance we have to assume a certain gain of the tag antenna. Usual tags have small thin antennas with gains between 0 dBi[2] and −5 dBi [11]. From Equation 2.2 we get:

$$r = \sqrt{\frac{EIRP\, G_{Tag} \lambda^2}{(4\pi)^2 P_{Tag}}} \tag{2.3}$$

When we insert these assumptions, a tag antenna gain of −5 dBi[3], a minimum necessary tag power of 5 µW, legal limit operation at 3.28 W EIRP and a wavelength of 346 mm corresponding to a frequency of 866.5 MHz in Equation 2.3 we get a maximum achievable read-distance of 12.5 m.

To determine the required noise figure of the reader, the expected power levels at the receiver have to be calculated. The receiver input power P_{RX} of the reader is given by the radar equation [10]:

$$P_{RX} = \frac{P_{TX} G_{TX} G_{RX} \lambda^2 \sigma}{(4\pi)^3 r^4} \tag{2.4}$$

[1] Equivalent Isotropically Radiated Power
[2] Here the unit dBi indicates that this antenna gain is with respect to an isotropic antenna.
[3] The RCS calculated from this value, see Equation 2.5, also corresponds to the values found in literature [10].

Where: P_{TX} is the transmitted power
G_{TX} is the reader's transmit antenna gain
G_{RX} is the reader's receive antenna gain
λ is the wavelength
σ is the tag's radar cross section (RCS)
r is the distance between reader and tag

The RCS of the tag can be calculated from our assumed antenna gain of -5 dBi when we further presume that the tag, at least in its usual state, is perfectly matched to the tag antenna. This presumption is justified when we are discussing the maximum distance case, because good tag antenna matching is necessary for efficient power transfer to the tag, allowing long distances. When this matching condition ($Z_c = Z_a^*$) is inserted in Equation 1.11, then $Z_a + Z_c = 2R_a$ and we get:

$$\sigma = \frac{\lambda^2 G^2}{4\pi} \tag{2.5}$$

Our tag antenna with -5 dBi gain has a RCS of 9.53 cm^2 accordingly.

When we further assume equal reader transmit and receive dipole antennas, again use the legal limit transmit power of 2 W and the maximum distance of 12.5 m calculated before, and insert this in Equation 2.4 we get a received power of 12.66 pW or -79.0 dBm.

With this result we can proceed to calculate the admissible upper boundary of the reader's receiver noise figure. To achieve a reasonable SNR[4] of 10 dB the equivalent receiver input noise power P_{Ne} must not exceed -89.0 dBm. With a thermal noise floor of -174 dBm/Hz and a bandwidth of 5 MHz[5] we get a noise power P_N of -107 dBm.

The noise figure can now be calculated as the (in dB) difference of the equivalent receiver input noise power P_{Ne} and the noise power P_N, or as quotient:

$$F = \frac{P_{Ne}}{P_N} \tag{2.6}$$

With the assumptions stated before the maximum allowed noise figure F of the receiver is 18 dB.

2.1.2 Leaking Carrier Input

One phenomenon already mentioned in Section 1.4 is a strong direct coupled carrier present in RFID systems. The effects on the signal constellation of the backscattered data stream have already been discussed, now the focus is on receiver blocking. Figure 2.2 shows the direct coupling of the transmitted signal to

[4] Signal to Noise Ratio
[5] The bandwidth of 5 MHz was assumed because this corresponds to the testbeds nominal receiver bandwidth when no digital filtering is employed

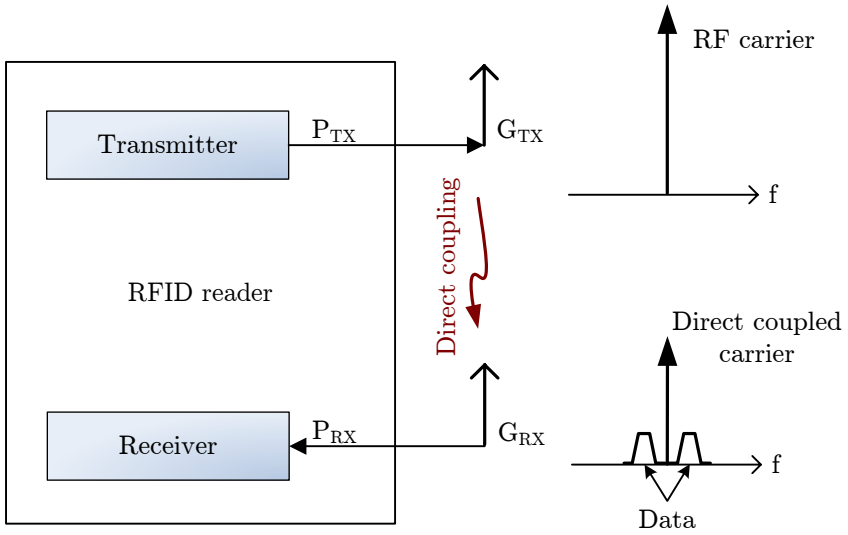

Figure 2.2: Direct coupling phenomenon in the dual antenna architecture, compare to [2, p. 121]

the receiver in a dual antenna constellation. The right side of the figure depicts the signals involved: A pure CW[6] carrier at the transmitter side on the upper part and the backscattered data signal superimposed with the direct coupled transmit carrier on the lower part.

In two antenna scenarios the amount of direct coupling depends on the type of antenna and their distance. To achieve good decoupling high gain antennas have to be used, so that their beams are parallel. Placing the antennas more apart also enhances isolation, but it gets more difficult to still hit the tag with both antenna beams. Typical transmitter–receiver isolation in dual antenna systems is in the range of $30 - 40$ dB.

To avoid bulky separate receiver and transmitter antennas and enable easier antenna pointing a single antenna can be employed. To separate the receive and transmit channels usually circulators are used. Figure 2.3 represents such a system.

An ideal circulator completely isolates port 3 (in this case the receiver input) from port 1 (the transmitter output) if port 2 (the antenna port) is perfectly matched to the characteristic impedance Z_0 of the circulator. Practical circulators have isolation values in the range of $20 - 25$ dB. The leaking carrier gets even stronger if the antenna is not perfectly matched to the circulator. Therefore, single antenna readers are more challenging to build and often some sort of carrier compensation or direct coupling compensation has to be used.

Another source of direct coupled carrier are conducting objects near the RFID reader. Depending on their size, conductivity and shape these objects act as reflectors and cause strong carrier components to appear at the receiver input.

[6] Continous Wave

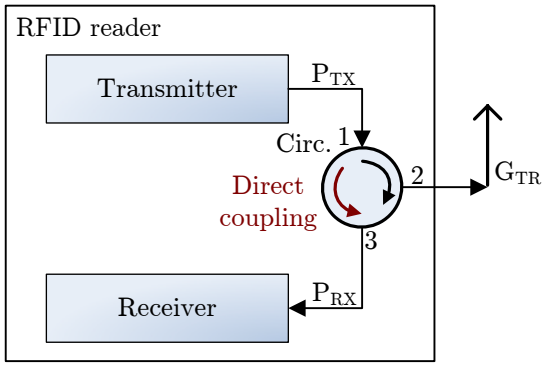

Figure 2.3: Direct coupling phenomenon in the single antenna architecture

This effect is especially dangerous for dual antenna readers that rely on good isolation of about 40 dB which can be effectively reduced to about 10 dB when a strong reflecting target is close to the antennas.

For those reasons a flexible reader has to withstand low transmitter–receiver isolations of about 10 dB and should be able to successfully communicate with tags under medium isolation situations of approximately 20 dB.

2.2 Main Design Concept

The goal of this work was to design and build the frontend for an UHF RFID testbed. While this UHF frontend had to be designed from scratch, a 13.56 MHz HF testbed had already been developed at the institute [12] using a rapid prototyping board from Austrian Research Centers.

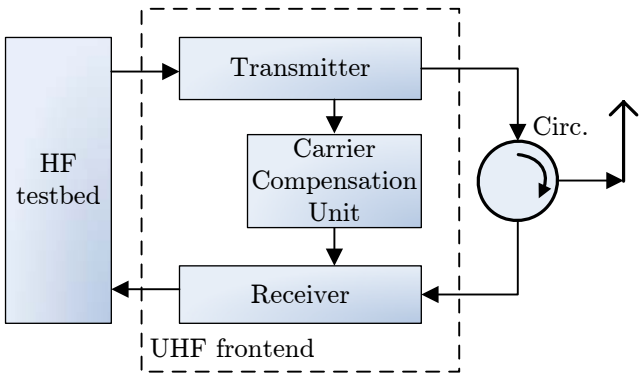

Figure 2.4: Testbed block diagram

The main concept was to reuse the modified HF testbed as a signal source for the UHF frontend that acts as a linear transponder. Figure 2.4 represents this concept. The frontend was divided in three physical and logical blocks: The transmitter, the receiver and the carrier compensation unit – CCU.

The upper part of the block diagram shows the transmitter section, which converts the low power HF signal provided from the rapid prototyping board into a medium power signal in the 865 - 868 MHz range.

The receiver section is shown on the lower part of the block diagram. Here the received signal is amplified, filtered and converted back to a low frequency signal suitable to the rapid prototyping board.

When the RFID reader system is configured as a single antenna reader, as shown on the block diagram, a circulator is needed to provide decoupling between transmitter and receiver. To further improve transmitter–receiver isolation an active carrier compensation is implemented between transmitter and receiver.

The main reason why this concept was chosen is flexibility: The use of digital baseband hardware allows to support practically all current and future RFID protocols. The only conceptual limitations are the frontends bandwidth and the frequency range. The use of separate transmitter and receiver modules further improves flexibility. Single and dual antenna operation is possible by choosing one antenna and an additional circulator or connecting separate receive and transmit antennas. Several test points, measurement couplers and outputs were implemented to allow for future extensions. By adding additional receiver, transmitter and CCU[7] modules, it is also possible to realize MIMO[8] readers.

While the UHF frontend described in this work was primary designed for passive UHF systems, it is also very well suited for active or semi-passive tags.

2.2.1 Power Level Considerations

For the frontend design it is necessary to know the expected output and necessary input levels of the rapid prototyping board. For verification a measurement of these levels was conducted.

The output of the rapid prototyping board, which was known to be equipped with a 16 bit digital to analog converter, was observed by a oscilloscope and terminated with 50 Ω. When operating as HF testbed, the output signals amplitude was 443 mVpp or −3.1 dBm. To measure the maximum output power a digital sawtooth signal of full height was sent to the DAC[9]. The observed output signal had an amplitude of 1 Vpp corresponding to 4 dBm in a 50 Ω load.

To characterize the input of the rapid prototyping board, which uses a 14 bit analog-to-digital converter, a signal generator was connected to the board input port. A sinewave at 13.56 MHz was injected in the board and the digital output was visually observed using a software tool on a PC[10] connected to the rapid prototyping board. The amplitude was increased till clipping could be observed on the monitored digital output. To achieve full modulation at a nominal input

[7] Carrier Compensation Unit
[8] Multiple Input Multiple Output
[9] Digital to Analogue Converter
[10] Personal Computer

impedance of 50 Ω, a 2.7 Vpp or 12.6 dBm signal was necessary. This corresponds to a board input voltage of 2 Vpp because the true input impedance of the rapid prototyping board was measured to be only 30 Ω.

As discussed in Section 1.4 not only the tag's backscattered signal is present at the receiver antenna, but also strong direct coupled carrier components which are introduced by antenna–antenna coupling, non-perfect circulator isolations, unmatched antennas and objects acting as reflectors. It is therefore necessary to ensure that the weak backscattered signal can be resolved by the limited resolution of the ADC[11] while also strong carrier components are present.

The SNR produced by quantizing a sinewave due to n bits of an ADC is given by [13]

$$SNR = 3 \cdot 2^{2n-1}. \tag{2.7}$$

It follows that two bits are needed to achieve a SNR of 10 dB. The used ADC has a resolution of 14 bit or 16384 steps. In best case, when the ADC is fully modulated with the leaking carrier and two bits remain for the backscattered signal, this signal is $20 \cdot \log(2^{14-2}) = 72.2$ dB lower.

For the weakest expected signal of -79.0 dBm calculated in Section 2.1.1 the maximum possible direct coupled carrier to successfully receive the tags message is therefore -79.0 + 72.2 = -6.8 dBm.

This result is quite interesting: When we assume a transmit power of 33 dBm a transmitter–receiver isolation of 39.8 dB is necessary to achieve the calculated input power of -6.8 dBm. Such high isolation values are only possible in very good dual antenna scenarios or with additional carrier compensation.

On the other side many practical LNA[12]s will be overloaded with a −6.8 dBm signal so the 14 bit ADC does not constitute a limiting factor. However, the effective resolution of a practical ADC might be much lower than the nominal value, so this result is only correct in theory.

2.2.2 Frequency Plan

Transmitter and receiver both employ a dual conversion scheme with a first IF[13] of 13.56 MHz produced by the rapid prototyping board and a second IF of 140 MHz. The conversion scheme is illustrated in Figure 2.5.

The first IF, called IF1, is filtered with a low pass filter with a cut-off frequency of 30 MHz. The overall selectivity of the frontend is determined at IF2 by a 140 MHz surface acoustic wave (SAW) filter with a 1 dB bandwidth of 5 MHz. This bandwidth is rather broad for classical RFID applications, but it enables broad-band measurements and further digital filtering is possible on the rapid prototyping board.

[11] Analogue to Digital Converter
[12] Low Noise Amplifier
[13] Intermediate Frequency

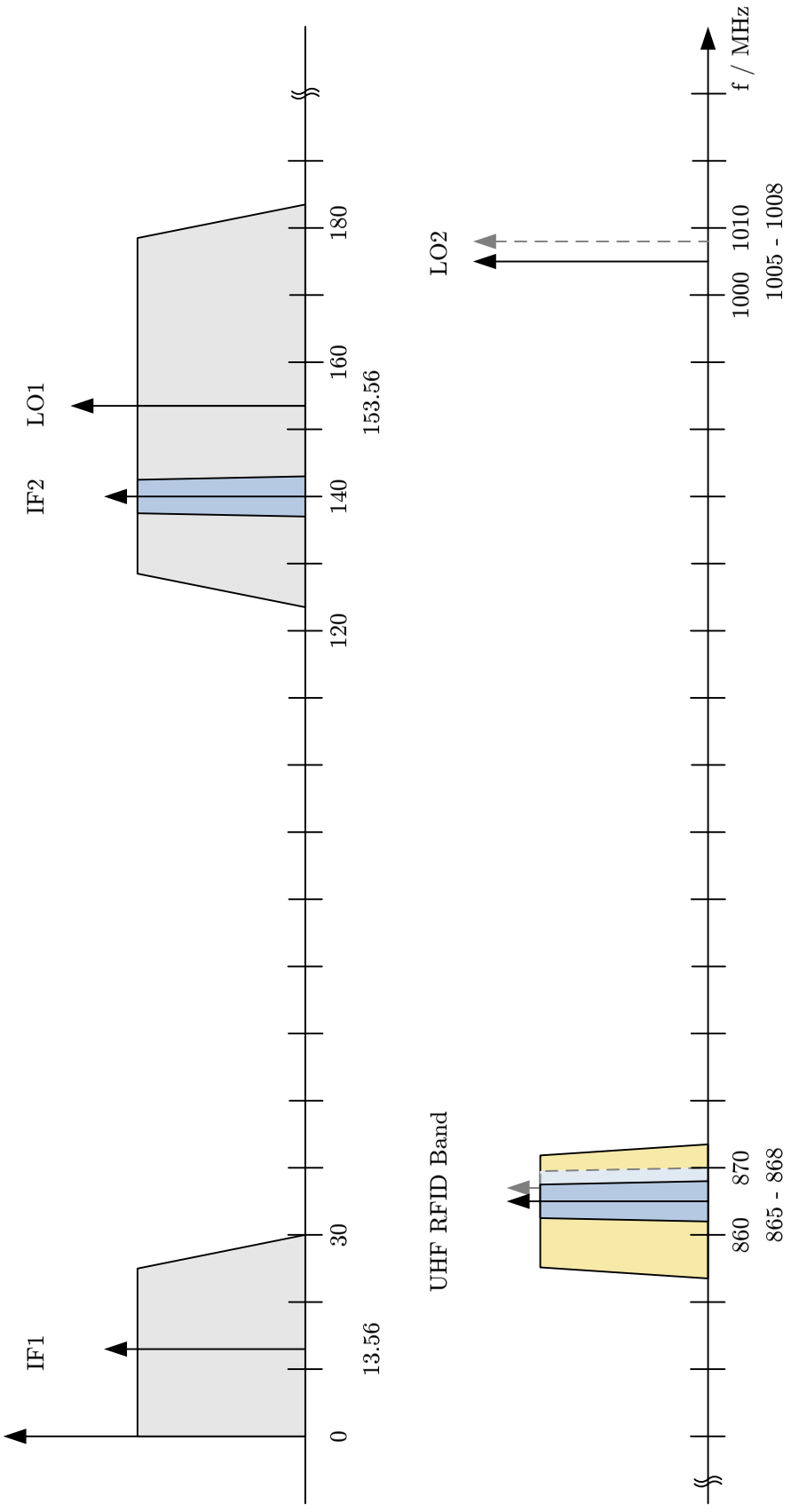

Figure 2.5: Spectral overview of the UHF frontend

Both mixers employ high-side LO[14] injection, therefore the fixed first LO frequency is 153.56 MHz. The second LO is used to choose the desired output frequency in the European UHF RFID band. LO2 frequencies of $1005 - 1008$ MHz are necessary to achieve an output frequency of $865 - 868$ MHz. This signal is filtered with a broad-band low loss SAW[15] to suppress the mirror image of $1145 - 1148$ MHz not drawn on Figure 2.5.

Identical filters are used for transmission and reception, so with respect to bandwidth the channel is symmetric. While the frontend was designed to operate on a first IF of 13.56 MHz the use of a low pass filter allows the first IF to be operated on virtually any frequency between a few MHz and 27.5 MHz. This gives some additional flexibility and the use of supplemental commercial band pass filters on this low IF (for example traditional 10.7 MHz filters) is possible if smaller bandwidths are desired.

2.3 The UHF Frontend

This section briefly describes the frontend designed in this diploma thesis. Detailed description and measurement results are given in the following chapters. Figure 2.6 gives a simplified block diagram of the frontend and the interaction between the various modules.

The upper part of Figure 2.6 shows the transmitter, with its input port to the left and the RF output port on the right side. Below the transmitter the two LO sources, power splitters, a microcontroller and the CCU are depicted. The receiver can be seen at the lower part of Figure 2.6.

The two local oscillators, which are provided by commercial signal generators, work on 153.56 and 1006.5 MHz respectively. These local oscillator signals are split up by power dividers and fed to the LO ports of receiver and transmitter.

The microcontroller shown in the middle of the block diagram is not required for basic operation of the RFID reader, but is part of the overall testbed design to control the various gain settings of the system automatically and for on-the-fly optimization of the carrier compensation. The microcontroller is not part of this diploma thesis, it is therefore drawn grew on Figure 2.6, but receiver, transmitter and CCU were designed to be easily controlled by the possible future expansion with this unit.

2.3.1 Transmitter

The 13.56 MHz signal from the rapid prototyping board enters the transmitter through a fixed attenuator. This provides some sort of enforced matching for the following low pass filter, and allows easy adaptation to higher signal level feeding.

[14] Local Oscillator
[15] Surface Acoustic Wave

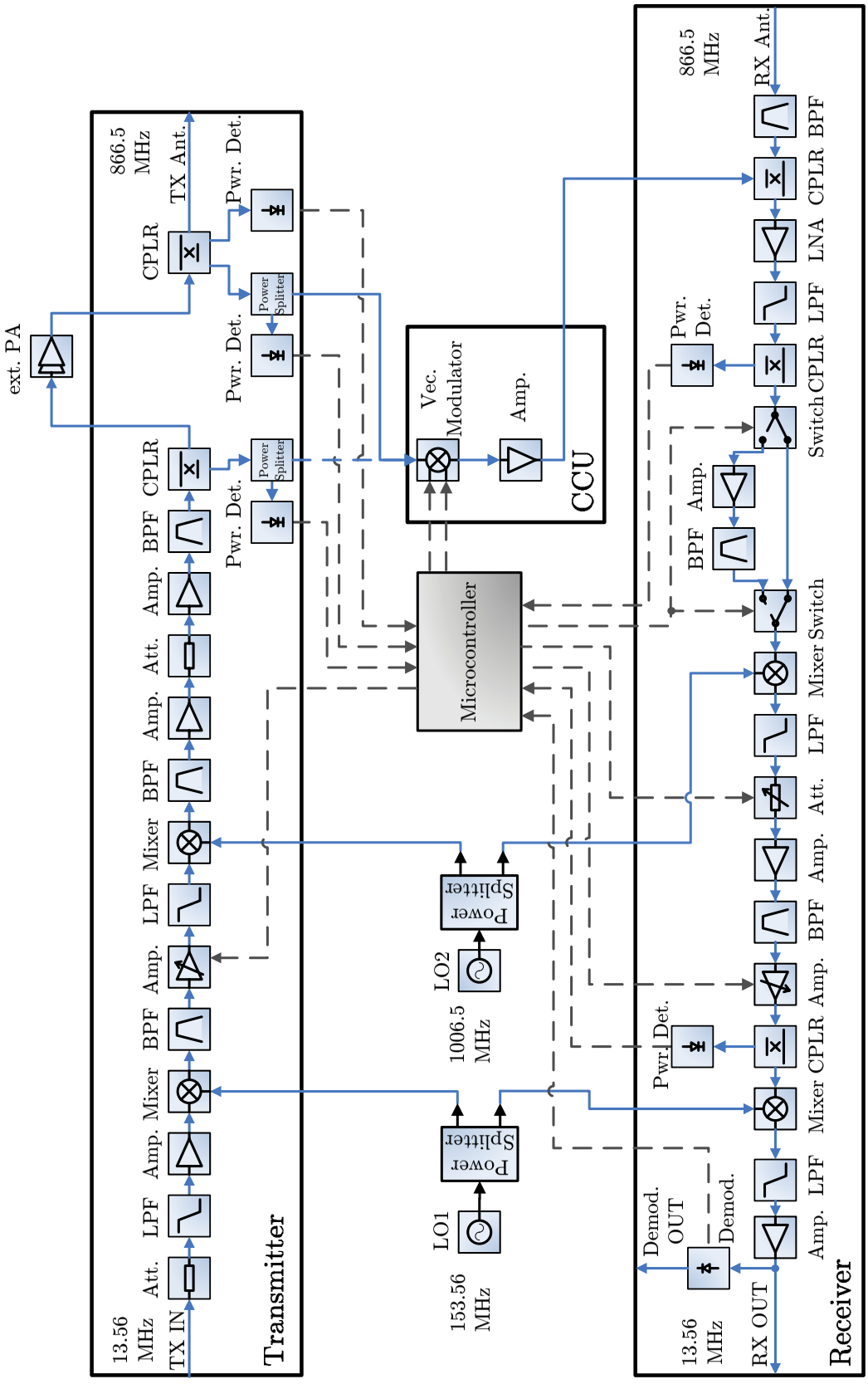

Figure 2.6: Simplified block diagram of the UHF frontend

The low pass filter provides suppression of aliasing products produced by the DAC on the rapid prototyping board. An amplifier compensates for the losses in the previous stages and provides isolation between the low pass filter and the first mixer. This double balanced mixer, fed by the 153.56 MHz local oscillator mentioned above, converts the first IF signal to the second IF at 140 MHz.

At the second IF the system overall bandwidth is fixed with a 5 MHz band pass filter and the upper sideband of the mixing process is suppressed. This filter is followed by a variable gain amplifier that is used to set the desired transmit level of the RFID transmitter. The output of this amplifier is low pass filtered and then fed into the second mixer for conversion to the UHF band.

The exact transmitter output frequency is determined by the second LO and can be freely chosen in the range of $865 - 868$ MHz. In Figure 2.6 a LO frequency of 1006.5 MHz was chosen to create an output signal of 866.5 MHz, the center frequency of the European RFID UHF band. The tuning range is determined by the SAW band pass filter following the second mixer. The same filter is also used after a two stage amplifier providing sufficient output power to drive an external power amplifier.

Directional couplers are implemented to measure the transmitter output power and provide a sample of the transmit signal for the carrier compensation unit. For reasons of flexibility this is done before and after the power amplifier, so the system can be used with different power amplifiers or even without a power amplifier.

The coupler directly following the transmitters last amplifier is only used to extract a sample of the forward power wave. This sample is then divided with a resistive power splitter to feed a power detector and the first output port to the CCU. The second coupler, which should be used when an external power amplifier is employed, also provides a sample of the reverse power. The power detector detached to this port of the final coupler provides a measure of reflections occurring at the TX[16] antenna port. This signal can be used to protect the external power amplifier from overloads due to reflected transmit power by reducing the power amplifier's drive power.

2.3.2 Receiver

At the receiver input both the backscattered signal from the tag and part of the transmit signal directly coupled from the transmitter are present. These signals are first band pass filtered with a SAW filter. This filter is followed by a directional coupler to allow insertion of the phase shifted carrier from the CCU to suppress most of the leaking carrier. The remaining signal is now amplified with a low noise amplifier and again filtered, now with a low pass filter. A small part of this signal is picked up by a coupler to enable power monitoring and adjustment of the CCU.

[16] Transmitter

The main goal at receiver design was immunity to overloading caused by high input levels of direct coupled carrier while maintaining a low noise figure. For that reason several methods of adjusting the gain of the different receiver subsections were implemented. At the RF stage a second amplifier followed by a SAW band pass filter can be inserted in the signal chain by means of an electronic switch. This additional amplification at RF frequencies improves the noise figure and can be used when high carrier suppression is present.

The RF signal is now converted to the first receiver IF at 140 MHz with a double balanced mixer, where its again low pass filtered. A switchable 10 dB attenuator provides adaption to low carrier suppression cases. The IF signal is further amplified by a fixed gain amplifier to overcompensate the losses of the 140 MHz SAW bandpass filter following this amplifier. This bandpass filter determines the receiver bandwidth of 5 MHz. It is followed by a variable gain amplifier, which has an adjustable gain from −8 dB to 15 dB. This gain can be set with 1 dB granularity by five digital control lines. To measure the power level of the IF signal a directional coupler is placed right after this variable gain amplifier. The coupled signal reaches a power detector that produces a voltage which corresponds to the signal level in a logarithmic scale.

The main part of the amplified IF signal is fed into the second receiver mixer, where it is converted to the second IF 13.56 MHz signal. The mixer is followed by a low pass filter to suppress other mixing products. The last amplifier raises the level of the second receiver IF and provides decoupling from the low pass filter. The level of the RX OUT signal at 13.56 MHz is now sufficient to directly drive the ADC on the rapid prototyping board.

An additional output provides a sample of the on board envelope demodulator. This output can be used for direct oscilloscope display and for simple measurement scenarios.

2.3.3 Carrier Compensation Unit – CCU

The carrier compensation unit consists of a vector modulator and a fixed gain amplifier.

A small part of the transmit signal is provided by one of two special CCU ports on the transmitter and is directly fed into the vector modulator. The vector modulator enables a true 360° adjustable phase and adjustable amplitude of the incoming signal. For that purpose the CCU provides two input lines, that control the inphase and quadrature components of the output signal.

To compensate for the coupler loss on the TX board and enable cancelation of strong carrier signals, the vector modulator is followed by a medium power amplifier.

2.4 Specification

The following tables summarize key parameters of the testbed's frontend and give the functions of the main power and control connector pins. Table 2.1 presents the specifications of the frontend structured in a common power supply part and the transmitter, receiver and CCU data. The transmitter's data is given for simple operation without an external PA[17]. In Table 2.2 and Table 2.3 the transmitters and receivers X1 main connector pinning is listed.

[17] Power Amplifier

Parameter	Conditions	Min	Typ	Max	Unit
Power Supply					
TX/RX Positive Supply Voltage		9.5	10	10.5	V
TX/RX Negative Supply Voltage		-10.5	-10	-9.5	V
TX/RX Positive Supply Current				1.65	A
TX/RX Negative Supply Current				70	mA
CCU Supply Voltage		4.75	5	5.25	V
CCU Supply Current				500	mA
Transmitter					
Abs. Maximum IF1 Input Power	Full Gain	3			dBm
Maximum IF1 Input Power	Lin. Op.		-3		dBm
Maximum RF Output Power	Lin. Op.		13.4		dBm
Maximum RF Output Power	Compr. Op.		25		dBm
Gain		-36		22	dB
CCU Driver Output Attenuation			8.2		dB
CCU PA Output Attenuation			31.7		dB
Input IP_3	Full Gain		14.4		dBm
Noise Figure	Full Gain		22		dB
Receiver					
Abs. Maximum RF Input Power		2			dBm
Abs. Maximum CCU Input Power		28			dBm
Maximum RF Input Power	No CCU		-6.4		dBm
Maximum CCU Input Power			28		dBm
Maximum IF1 Output Power			12.6		dBm
Gain		4.2		44	dB
CCU Compensation Power Offset			4.5		dB
Noise Figure	Full Gain		5.03		dB
CCU					
Abs. Maximum RF Input Power		13			dBm
Maximum RF Input Power	Lin. Op.		-1		dBm
Maximum RF Output Power	Compr. Op.		27		dBm
Gain		-12		18	dB

Table 2.1: Specifications of the UHF frontend

Pins	Use
1-3, 14-16	Ground
4	External Gain Control
5	External Gain Control Ground
6	Driver Forward Power Detector
7	Driver Forward Power Detector Ground
9	Enable Line 1
10	Enable Line 2
11-13, 23-25	Positive Power Supply
17	VGA Reference Voltage Output
18	VGA Reference Voltage Output Ground
19	PA Reverse Power Detector
20	PA Reverse Power Detector Ground
21	PA Forward Power Detector
22	PA Forward Power Detector Ground

Table 2.2: Transmitter connector X1 pin functions

Pins	Use
1-3, 14-16	Ground
4	IF1 Detector DC Output
5	Second RF Amplifier Control Line
6	VGA 16 dB Attenuator Control Line
7	VGA 8 dB Attenuator Control Line
8	VGA 4 dB Attenuator Control Line
9	VGA 2 dB Attenuator Control Line
10	VGA 1 dB Attenuator Control Line
11	Auxiliary Line 1
12-13, 24-25	Positive Power Supply
17	IF2 10 dB Attenuator Control Line
18, 22	Negative Power Supply
19	IF2 Power Detector
20	Measurement Ground
21	RF Power Detector
23	Auxiliary Line 2

Table 2.3: Receiver connector X1 pin functions

Chapter 3

Transmitter

The following chapter describes the transmitter I have designed in this diploma thesis. Its main purpose is to generate UHF output signals from the HF feeding signals provided by the rapid prototyping board. These UHF signals are used in the RFID testbed to send messages to the tag and power up passive RFID tag chips.

3.1 Concept

As mentioned in Section 2.2.2 a double conversion scheme is used for the transmitter. Both necessary LO sources are not implemented in the transmitter but must be supplied by external sources. For that purpose dedicated SMA[1] connectors are used. All RF connections and their circuitry was designed for a characteristic impedance Z_0 of $50\,\Omega$.

3.1.1 Mechanical Concept

The transmitter is implemented on a four-layer printed circuit board in Eurocard format (160×100 mm). This board is enclosed in a steel frame housing with the internal dimensions of $160 \times 100 \times 35$ mm. Top and bottom of this frame are closed with removable fingered lids.

All RF signals like IF and LO input, are fed to the transmitter using SMA connectors. For measurement, performance verification and future use several RF test points are present on the transmitter PCB[2]. These signals are also accessible via SMA connectors, but these connectors are not placed on the transmitter housing but directly on the PCB.

For power and control signals a 25 pin Sub-D connector is provided. To manually control the transmitter, jumpers and a trimmer resistor can be used. Four LED[3]s provide an optical status message of the power and control circuits.

[1] SubMiniature version A (connector)
[2] Printed Circuit Board
[3] Light Emitting Diode

3.1.2 Input Power Levels

The maximum 13.56 MHz IF input level for linear operation is −3 dBm. The absolute maximum save continuous input level is 3 dBm. The transmitter can easily be adapted to higher input levels by changing three resistors that form an input attenuator. A detailed power level analysis can be found in Section 3.2.6.

The local oscillators require different drive levels. The first LO requires a 153.56 MHz signal of −5 dBm. This level was chosen to meet the requirements of both the transmitter and the receiver mixers. Therefore a simple power splitter and a single source can be used to supply both of them .

The second mixer requires 0 dBm of LO drive at the corresponding SMA connector.

3.1.3 Output Power Levels

The output power level depends on the first IF drive level, the setting of the transmitter variable gain amplifier and the use of an external power amplifier.

The transmitter gain without power amplifier $P_{PA_{IN}}/P_{IF1}$ can be controlled from −36 dBm to 22 dBm. The maximum output power under linear conditions are 13.4 dBm. To achieve this output a minimum IF input of −8.6 dBm is required.

For classical RFID protocols linear transmitter operation is not really essential. The reason are the modulation formats and detectors used in reader to tag communications. In this mode approximately 25 dBm output power is possible.

Limitations in output power are low if an external power amplifier is used. When the internal measurement coupler and power detectors should be used after the external PA, the power limit is 50 dBm or 100 W. It seems very questionable if such high power levels are ever needed in RFID systems. For normal operation an external power amplifier with 20 - 30 dB gain should be used to achieve about 33 dBm output power.

For the carrier compensation two output ports are provided: The first picks up part of the transmitter's last amplifier signal, called CARCOMP_DR, the second provides a sample off the signal leaving the external power amplifier, called CARCOMP_PA. These outputs are also illustrated in Figure 2.6.

The CARCOMP_DR output is 8.2 dB lower than the corresponding output of the transmitter driver TO_PA. To compensate for the gain of the external amplifier, the CARCOMP_PA output is 31.7 dB lower than the external PAs output called ANT.

3.2 Realisation

3.2.1 Input Stage

The output signals of the rapid prototyping board are first processed by the transmitter input stage, its schematic can be seen on Figure 3.3.

The input signal enters the transmitter through the IF_IN connector and passes a 3 dB attenuator pad formed by R38–R40. This attenuator serves two purposes: It enables easy adaption to higher input levels by changing the resistor values and provides some amount of enforced matching.

The LPF[4] module F2 is supplied by Coilcraft. It is a P7LP-306L seven-pole elliptical LPF with a −3 dB cutoff frequency at 30 MHz. This filter module can be substituted for a 15 MHz variety if smaller bandwidth or lower IF frequencies are desired. Figure 3.1 shows the measured frequency response of the filter, which was placed on a small test print for this measurement.

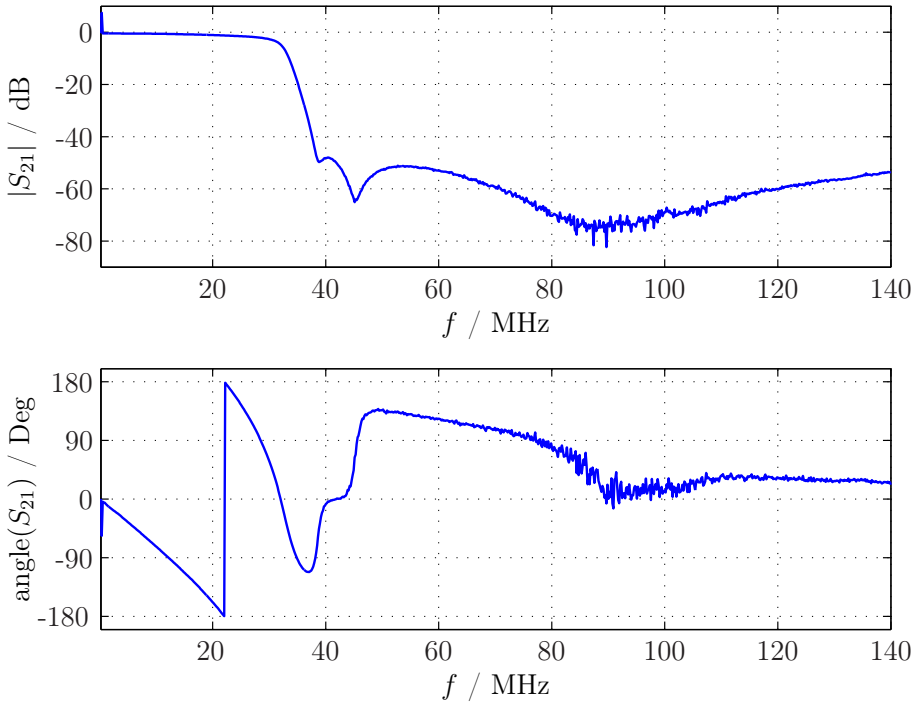

Figure 3.1: Measured frequency response of the Coilcraft LPF P7LP-306L.

After the filter an amplifier boosts the signal level and decouples the LPF from the first mixer. For that purpose a MAR-4SM from Mini-Circuits is used. This is a monolithic amplifier in Darlington configuration, as can be seen in Figure 3.2. It has a typical gain of 8 dB. Figure 3.3 indicates that the amplifier is supplied from the 10 V rail. L32, C92 and C93 form a filter network to prevent coupling of

[4] Low Pass Filter

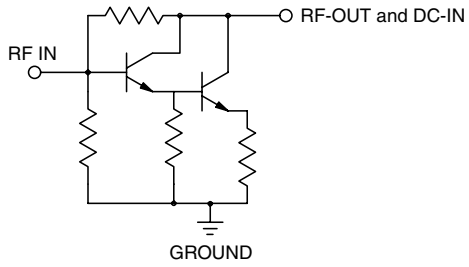

Figure 3.2: Simplified schematic and pin description of the amplifier MAR-4SM [14].

IF signals over this supply line. R41 - R43 and the radio frequency choke L29 form the load impedance of the amplifier and provide DC[5] biasing. The amplifier's output is AC[6] coupled with C91 and again passes a 3 dB-pad. This attenuator can be removed when lower IF drive levels are desired.

The transmitter's first mixer converts the 13.56 MHz first IF signal to the second IF of 140 MHz. An LT5511 active double balanced mixer with integrated LO-buffer from Linear Technology is used for that purpose.

The mixer IC[7] requires a differential low impedance IF input signal which is provided by Coilcrafts TTWB-4-A 4:1 transformer. Best mixer performance is obtained when both mixer IF input ports, which connect to the emitters of the mixers switching transistors, are DC isolated and draw the same current. For that reason 0.1% precision resistors (R32 and R33) are used for DC biasing and C85 and C86 provide blocking of the DC path through the secondary transformer winding.

The mixer's output ports, called RF+ and RF-, are internally connected to the collectors of the output switching transistors, thus having a high impedance. This symmetric high impedance output is matched to the asymmetric 50 Ω system impedance by L26, L27, TR2 and C83. TR2 is a center tapped 1:4 transformer from M/A-COM which is also used to feed the mixer output transistors with the 5 V supply. L26, L27 and C83 were chosen for best output return loss. This was done using a small test print which carries the mixer-IC and input and output matching elements.

The LO input is terminated in a 62 Ω resistor R37 which forms an easy match to 50 Ω in conjunction with the LT5511s LO port input impedance.

The power supply circuits are decoupled by double L/C- filter networks. While L30 rejects lower frequency components, L31 and L28 suppress LO and second IF components on the 5 V supply line.

[5] Direct Current
[6] Alternating Current
[7] Integrated Circuit

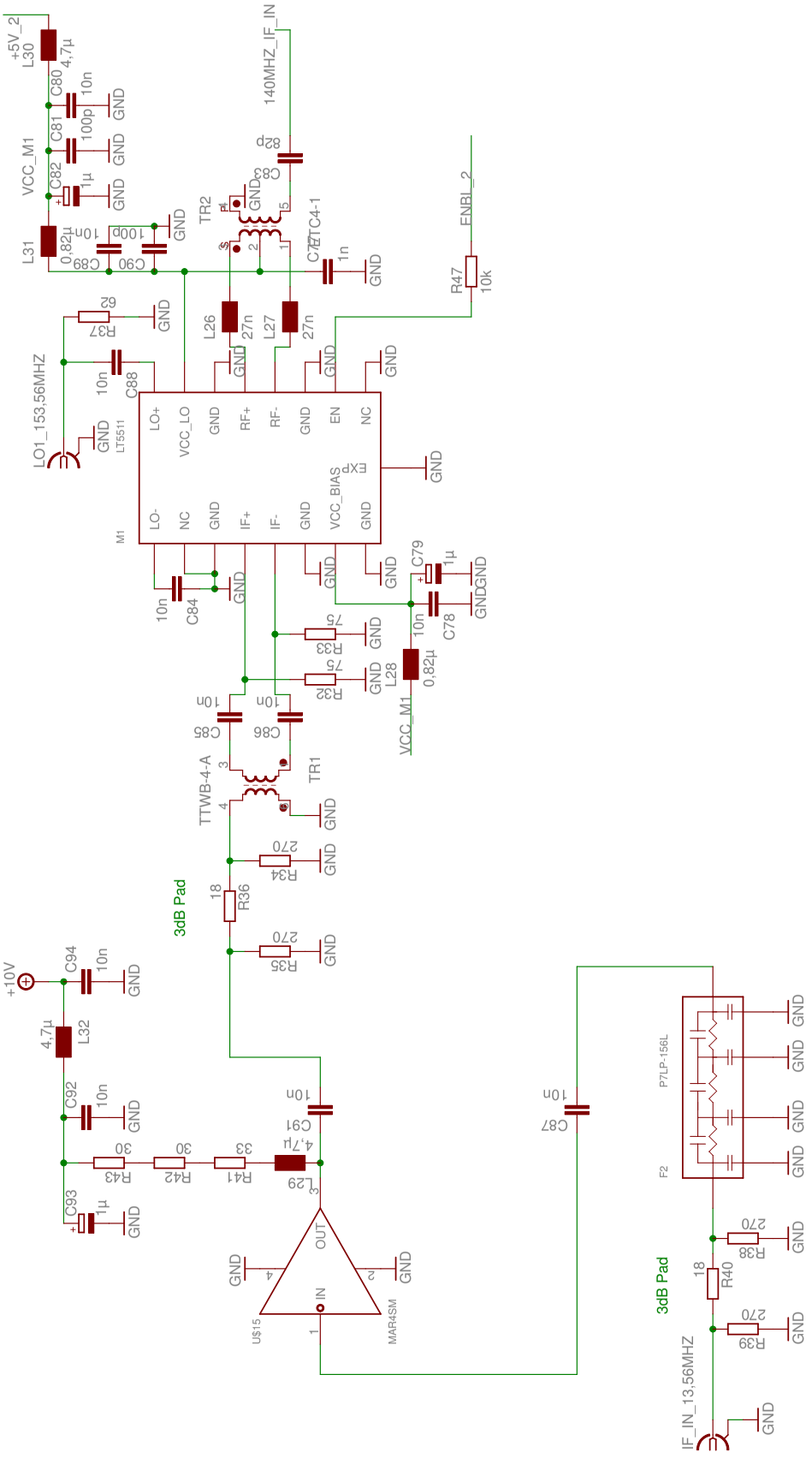

Figure 3.3: Transmitter input stage schematic

3.2.2 Second Intermediate Frequency Stage

At the second IF section the overall transmitter selectivity is reached and the possibility to adjust the gain of the transmitter is implemented. The schematic is depicted in Figure 3.4. Leaving the first mixer circuits of the input stage the 140 MHz second IF signal is filtered by a SAW filter from Telefilter called TFS140AV. L22 and C55 form the input, L24 and C56 the output matching network. The values were found using the s-parameter file supplied by the manufacturer and simulations in Microwave Office. For verification a test print was built and measured.

To set the transmit level and adapt to different IF1 input levels a variable gain amplifier is used in the signal chain directly after the second IF SAW filter. The main component is the ADL5330 from Analog Devices. It is a voltage controlled variable gain amplifier with a minimum gain setting of -35 dB and a maximum gain setting of 23 dB. RF input and output pins are 50 Ω differential so on both sides a BALUN[8] is used to adapt to the asymmetric transmission line used on the transmitter board.

The BALUNs both are M/A-COM ETC1-1-13 which have about 0.32 dB insertion loss. The inputs INHI and INLO are internally biased on a DC level, therefore coupling capacitors C68 and C69 are used. At the outputs OPLO and OPHI RF chokes L17 and L19 provide DC biasing to the decoupled 5 V line. The differential output is adapted to the asymmetric transmission line again using a ETC1-1-13 BALUN.

The gain control line is filtered with L21 and C75 and C76 to prevent RF signals to enter the gain control circuitry of the VGA[9]-IC. With R30 and R31 an additional resistive divider can be installed to reduce external gain control signals to an appropriate level, which is 0 - 1.4 V.

The VGA output is connected to a 200 MHz LPF realized with discrete inductors and capacitors. It is used to suppress second order intermodulation products of the VGA and improve rejection of higher frequency components leaking through the IF2 SAW filter.

A special test port, X2, can be used to analyze the signal leaving the LPF or inject IF2 signals in the following transmitter stages. To select one of those possibilities the coupling capacitors C102-C104 are used. Under normal operation conditions a 1 nF capacitor is used for C102, and C103 and C104 are left blank. To analyze the IF2 signal leaving the VGA and the LPF C103 is used and the other ones are removed. Finally C104 enables to inject an IF2 signal in the second mixer and following stages.

[8] BALanced - UNbalanced converter
[9] Variable Gain Amplifier

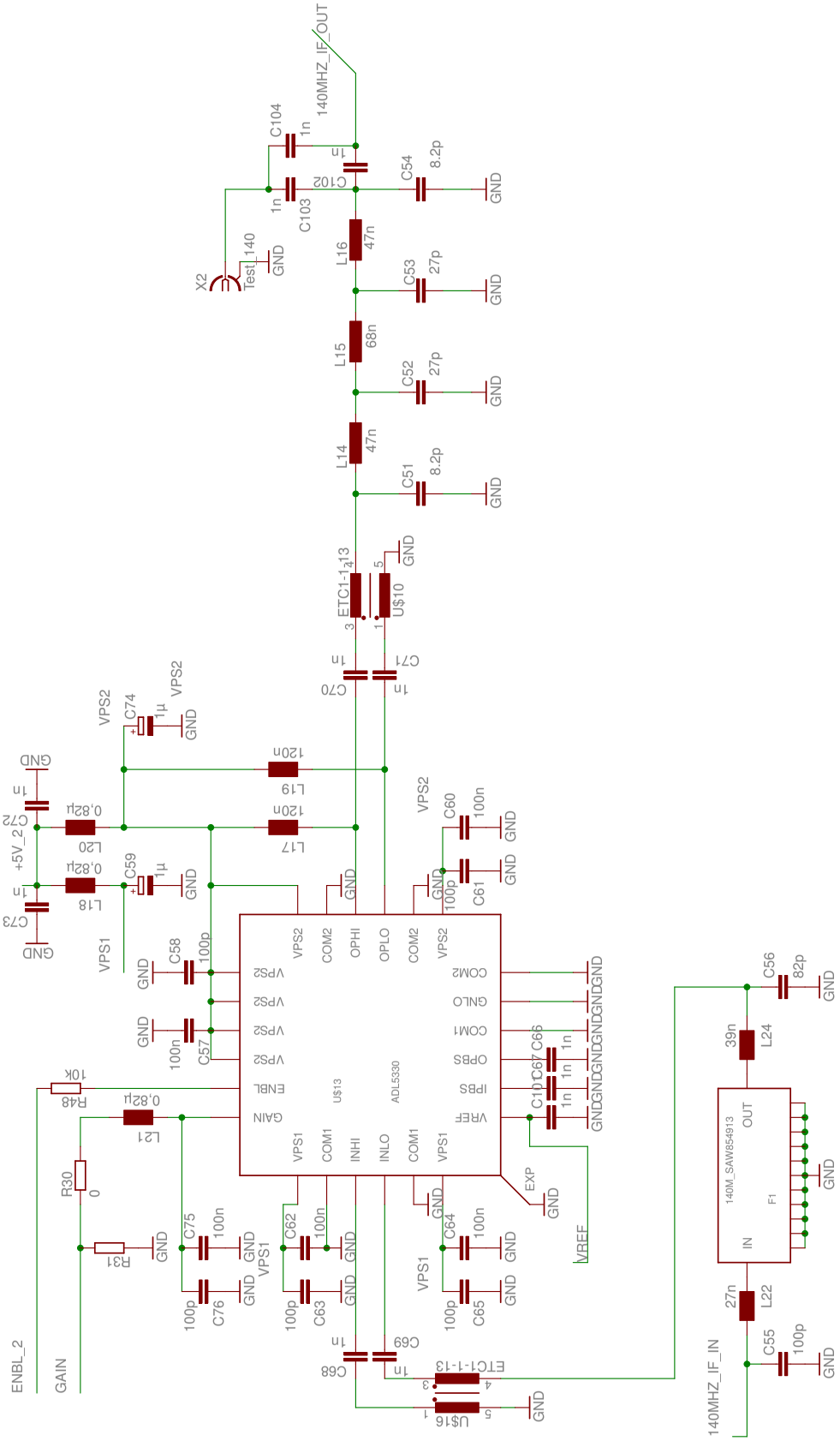

Figure 3.4: Transmitter second IF stage schematic

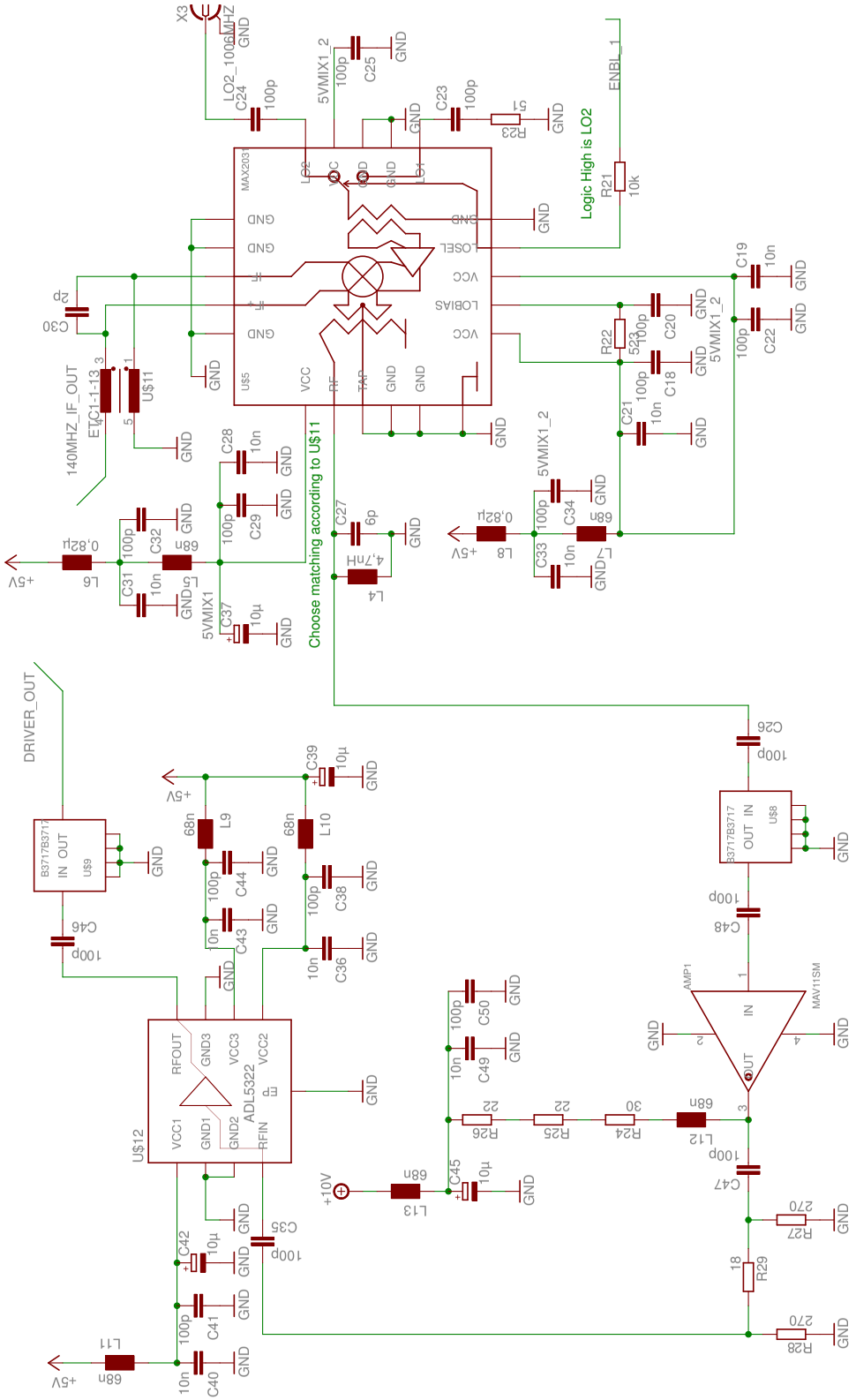

Figure 3.5: Transmitter output stage schematic

3.2.3 Output Stage

The first element of the output stage, which is shown on Figure 3.5, is the second transmitter mixer that converts the 140 MHz IF2 signal to the final transmit frequency in the RFID UHF band. A passive double balanced mixer IC with integrated LO buffer, the MAX2031 from Maxim, is used.

This mixer requires a differential input. A BALUN with good phase and amplitude balance is necessary to achieve high LO suppression. The circuit and layout were designed to support two different BALUNs, the MABACT0060 and the pin compatible ETC1-1-13. While the first transformer promised a slightly better phase balance, the latter has already been used at the transmitter, so it was chosen for implementation. Measurements on the testprint designed for this mixer revealed that the use of the ETC1-1-13 transformer also makes the matching capacitor C30 and the output tank circuit C27/L4 unnecessary and even counterproductive.

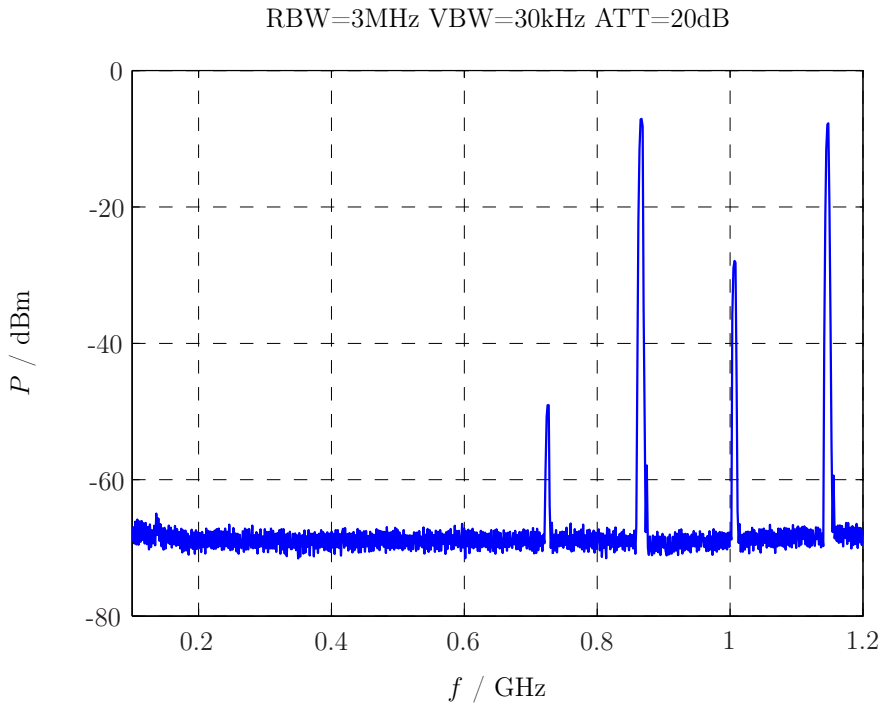

Figure 3.6: Output spectrum of the MAX2031-testprint in upconverter operation

Figure 3.6 shows the result of one of several measurements carried out with the testprint using no external matching components but the ETC1-1-13 transformer. Here a spectrum analyzer from Advantest and two signal generators have been used. The input signal was a 0 dBm sinewave at 140 MHz, the LO drive was also 0 dBm at 1006 MHz. The output shows the desired frequency at 866 MHz and the mirror image at 1146 MHz. Due to imperfect symmetry of the mixer, and phase and amplitude imbalance of the feeding transformer, the LO is also

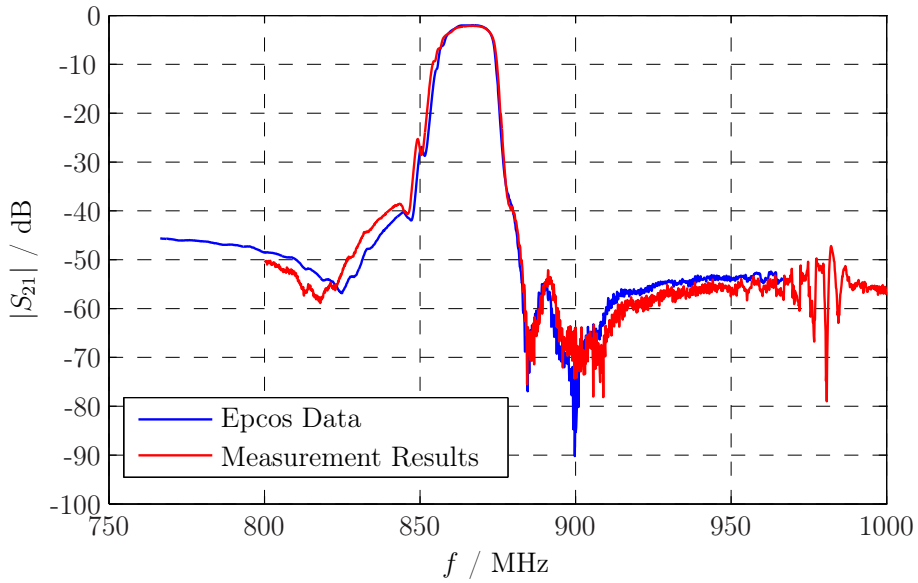

Figure 3.7: B3717 frequency response

present at the output and is only about 20 dB lower than the desired output signal. Another product that can be observed when driven with such high input levels is an intermodulation of third order, $f_{LO} - 2f_{IF2}$, at 726 MHz. This signal is more than 40 dB below the carrier output and is eliminated by the following filters.

The MAX2031 has two LO inputs and an integrated LO switch to select one of those inputs for actual use. At the transmitter only the second LO input is used and the LO switch is connected to an enable line for possible shutdown.

For the internal LO buffer it is necessary to connect the LOBIAS pin with a 523 Ω high precision resistor (R22) to the 5 V line. All supply pins are blocked with suitable capacitors and decoupling networks are provided.

To eliminate the mirror image and the leaking LO the mixers output signal is filtered in a B3717 SAW filter from Epcos. This is a low loss device that was specially designed for UHF RFID applications. The frequency response of the filter was again measured with a small testprint containing only the filter and two SMA connectors. Figure 3.7 shows the comparison between the measurement results and data supplied by Epcos. The curves show strong matching and good suppression of undesired signal components as the LO and mirror images.

The filtered signal is amplified with a MAV11SM from Mini-Circuits which is very similar to the MAR-4SM described in Section 3.2.1, but provides a slightly higher gain of 9 dB and a higher output compression point. R24-R26 and L12 form the load impedance of the amplifier and allow DC biasing. The output of the amplifier is AC coupled to a 3 dB attenuator that provides decoupling from the following amplifier. Here a ADL5322 from Analog Devices serves as the final onboard amplifier of the transmitter.

This amplifier, also called driver, has a gain of 20 dB and an output compression point of 27 dBm. The amplifier's three supply pins are decoupled using two 100 pF and 10 nF capacitors in parallel and a 68 nH choke at each input. The amplifier's output is again filtered using a B3717 filter.

3.2.4 Power Detectors and CCU Couplers

It was already discussed in Section 2.3 that the transmitter utilizes couplers to feed part of the transmitted signal to the CCU and measure the output power generated by the transmitter. The necessary circuitry can be seen on Figure 3.8.

The first directional coupler is placed right after the drivers output. Here a BDCA-6-16 from Mini-Circuits with a nominal coupling of −6.5 dB was used. The output of this coupler is fed to a SMA port called TO_PA because its intention is to provide the input signal of an external power amplifier. When there is no need for an external PA the TO_PA output can be directly connected to a transmit antenna or a circulator for single antenna operation.

If an external power amplifier is used its output should be connected to the FROM_PA SMA connector because the signal applied to this port is routed through a low loss high power directional coupler (Mini-Circuits SYBD-26-13HP+) before it reaches the ANT output port of the transmitter module. The two outputs of the directional coupler are both connected to resistor power divider networks that ensure that the coupled ports of the directional coupler are properly terminated and the right amount of power is fed to the power detectors from Linear Technology. The power divider connected to the forward port of the coupler also provides an attenuated sample of the transmit signal at the CARCOMP_PA output to drive the CCU module.

The total attenuation from the FROM_PA port to the CARCOMP_PA output are about 31.7 dB, where 26.8 dB is the coupling loss of the directional coupler and 4.9 dB result from the R2–R3 divider. R4 and R5 form the input attenuator for the power detector measuring the forward power, R7 and R8 form the input attenuator for the reverse power detector, both having an attenuation of about 26.7 dB. The LT5537 power detector has a high input impedance so for simplicity transformers or discrete baluns were omitted. Instead, the detector input pins were placed in parallel to a low impedance resistor, so the detector's load impedance basically does not affect the attenuation of the resistor power dividers described above.

The usable dynamic range of the detector at this frequency is 70 dB and the lowest detectable value is −60 dBm [15]. So the dynamic range of the complete on board PA power detector system including the directional coupler loss of 26.8 dB, the power dividers loss of 26.7 dB and the detector IC is −6.5 dBm to 63.5 dBm, for both forward and reverse power.

The slope of the output voltage of all power detector ICs is set to 20 mV/dB and can be controlled by R15, R16 and R17.

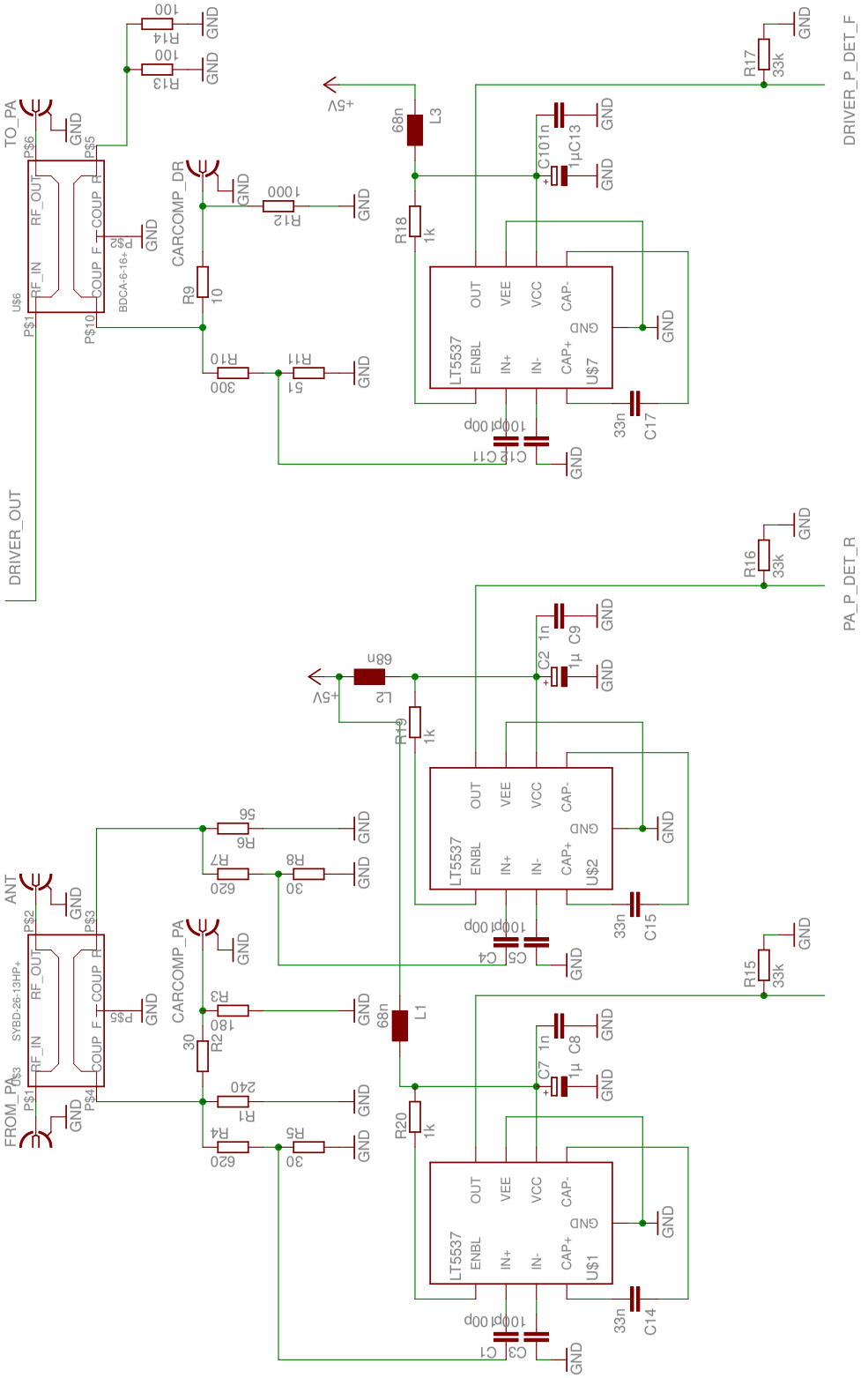

Figure 3.8: Transmitter power detectors and CCU couplers schematic

The attenuation network and power sensor circuitry attached to the driver's directional coupler is a slightly simplified copy of the PA coupler circuitry described above. The CARCOMP_DR output provides a 8.2 dB attenuated copy of the driver signal, where 1.7 dB account on the R9–R12 divider network. While the reverse power detector was omitted, the forward power detector receives a 23.3 dB attenuated driver output sample through R10-R11. This results in a driver detector operating range of −36.7 dBm to 33.3 dBm. R13 and R14 ensure proper matching of the directional coupler and terminate its reverse port.

3.2.5 Power Supply and Control Circuits

The whole transmitter module is designed for a single supply voltage of 10 V that enters the unit through a male 25 pin Sub-D connector that also carries control and measurement lines. The connector and the power supply input circuit is drawn in Figure 3.9.

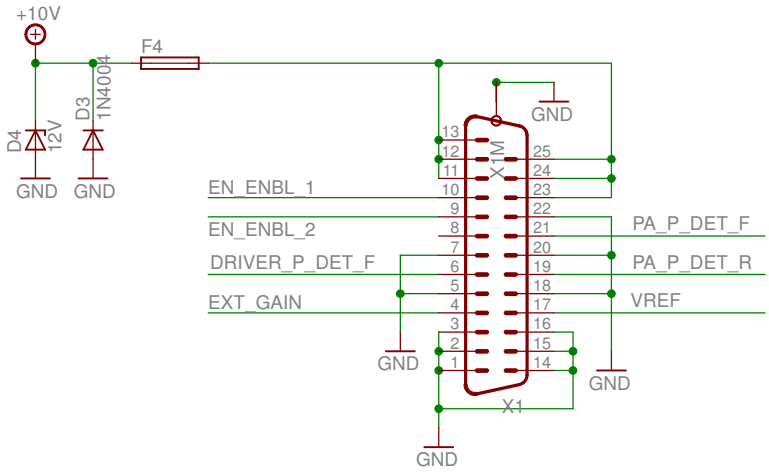

Figure 3.9: Transmitter power and control connector circuit

The pins 11-13, 24 and 25 are connected to the internal positive supply lines through a 1.5 A fuse F4. The transmitter is further protected by D3 and D4. While both diodes conduct if the polarity of the supply voltage is reversed, D4 also starts conducting when the supply voltage reaches levels above 12 V. In both cases F4 blows and prevents further damage to the transmitter.

Only two amplifier ICs directly operate on the 10 V line, all other components require a 5 V supply. This voltage is generated by two identical MC7805ABD2T linear voltage regulators. Figure 3.10 shows the fist one that supplies the second mixer, the driver and the power detectors. The rest is supplied by an identical second regulator and filter capacitors.

To shut down the transmitter two enable lines are provided which correspond to the two 5 V supply lines, see Figure 3.11. EN_ENBL_1 activates the second

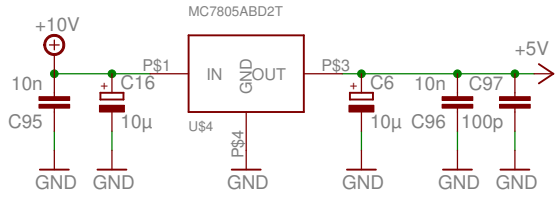

Figure 3.10: Transmitter 5 V supply (one of two)

mixer, EN_ENBL_2 the first mixer and the VGA. The enable lines connect to switching transistors through 10 kΩ protection resistors for easy connection to an external microprocessor board. When the enable lines are "high" corresponding LEDs (LED1 and LED6) light up to indicate transmitter operation. LED4 and LED5 indicate the presence of supply voltage on the two 5 V supply lines.

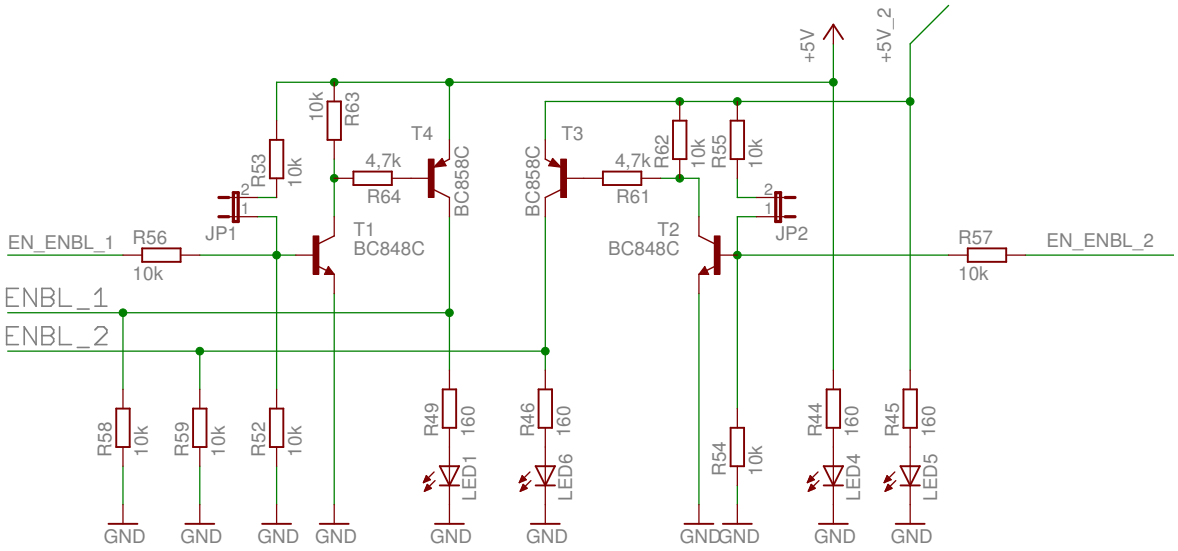

Figure 3.11: Transmitter enable circuits

When the transmitter is not connected to a microprocessor board, the gain of the VGA can be set by an on-board variable resistor (R51) and the enable lines can be permanently set "high". For this operation mode the enabling jumpers JP1 and JP2 have to be used and pins 2 and 3 of SV1 have to be connected. As a reference voltage for the VGA either the second 5 V supply line or the internal VGA-IC reference can be used. In the first case R60 is omitted, in the second case R50; see Figure 3.12.

3.2.6 Power Level Plan

During the design process I created a detailed level plan which was very helpful to simultaneously register the power levels at the different transmitter stages. In

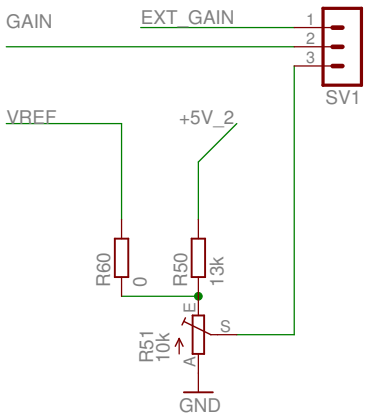

Figure 3.12: Transmitter gain resistors

Figure 3.13(a) the gain, noise figure, 1 dB output compression point, and absolute maximum output power are written down for every transmitter stage. The signal and noise levels at every stage were calculated, here an effective bandwidth of 7 MHz was used, which corresponds to the 140 MHz second IF SAW filter. An input level of −5 dBm, and as an external amplifier, a ZHL-2-12 from Mini-Circuits was assumed.[10]

The gain of the VGA was set to 13 dB to get an output power of about 33 dBm. The rows of carrier power, 1 dB output compression point called "OP1dB", and absolute maximum output power are visualized in Figure 3.13(b). The graphs also show that under the conditions assumed here the transmitter itself is operating in linear mode; the carrier graph is always more than 10 dB lower than the OP1dB graph. The external PA however is operating in strong compression so the total output signal will be compressed. As mentioned before this is no problem for current RFID protocols as long as the modulation index of the ASK signal does not get too small due to clipping of the high level signals. To achieve linear operation a power amplifier with higher 1 dB output compression point has to be used.

3.2.7 Circuit Board Layout

The transmitter was implemented on a four layer FR4 printed circuit board in Eurocard format (160 × 100 mm). The PCB core has a height of 0.7 mm, the outer layers have 0.4 mm isolation. All copper layers are 35 µm thick.

All parts were placed on the top of the PCB, and with exception of the protection diodes and connectors only surface mounted devices were used. Most RF signal lines were fabricated as microstrip lines with a characteristic impedance of 50 Ω, running on the top layer. It was therefore necessary to define the second

[10]This amplifier was actually used for RFID experiments, see Chapter 6

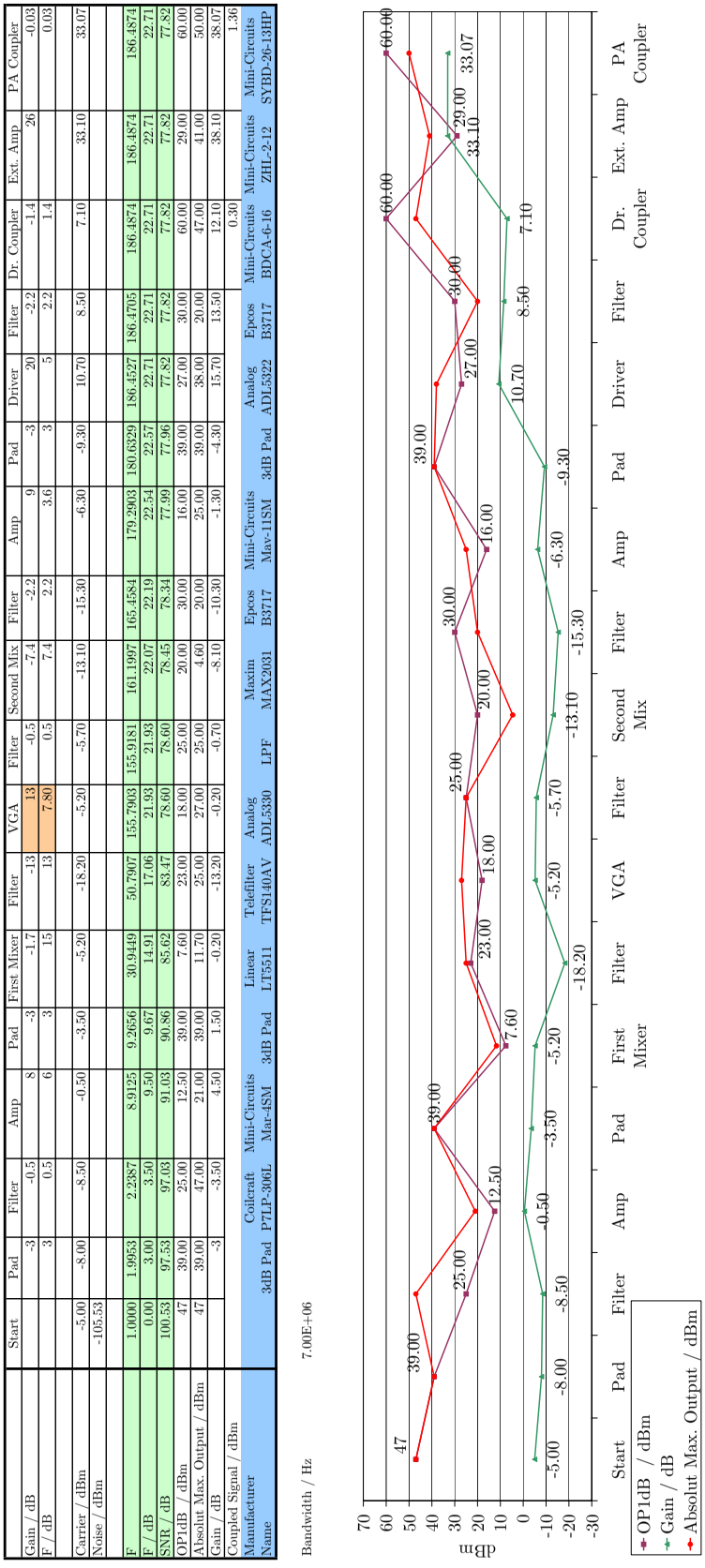

	Start	Pad	Filter	Amp	Pad	First Mixer	Filter	VGA	Filter	Second Mix	Filter	Amp	Pad	Driver	Filter	Dr. Coupler	Ext. Amp	PA Coupler
Gain / dB		-3	-0.5	8	-3	-1.7	-13	13	-0.5	-7.4	-2.2	9	-3	20	-2.2	-1.4	26	-0.03
F / dB		3	0.5	6	3	15	13	7.80	0.5	7.4	2.2	3.6	3	5	2.2	1.4		0.03
Carrier / dBm	-5.00	-8.00	-8.50	-0.50	-3.50	-5.20	-18.20	-5.20	-5.70	-13.10	-15.30	-6.30	-9.30	10.70	8.50	7.10	33.10	33.07
Noise / dBm	-105.53																	
F	1.0000	1.9953	2.2387	8.9125	9.2656	30.9449	50.7907	155.7903	155.9181	161.1997	165.4584	179.2903	180.6329	186.4527	186.4705	186.4874	186.4874	186.4874
F / dB	0.00	3.00	3.50	9.50	9.67	14.91	17.06	21.93	21.93	22.07	22.19	22.54	22.57	22.71	22.71	22.71	22.71	22.71
SNR / dB	100.53	97.53	97.03	91.03	90.86	85.62	83.47	78.60	78.60	78.45	78.34	77.99	77.96	77.82	77.82	77.82	77.82	77.82
OP1dB / dBm	47	39.00	25.00	12.50	39.00	7.60	23.00	18.00	25.00	20.00	30.00	16.00	39.00	27.00	30.00	60.00	29.00	60.00
Absolut Max. Output / dBm	47	39.00	47.00	21.00	39.00	11.70	25.00	27.00	25.00	4.60	20.00	25.00	39.00	38.00	20.00	47.00	41.00	50.00
Gain / dB		-3	-3.50	4.50	1.50	-0.20	-13.20	-0.20	-0.70	-8.10	-10.30	-1.30	-4.30	15.70	13.50	12.10	38.10	38.07
Coupled Signal / dBm																0.30		1.36
Manufacturer			Coilcraft	Mini-Circuits		Linear	Telefilter	Analog		Maxim	Epcos	Mini-Circuits		Analog	Epcos	Mini-Circuits	Mini-Circuits	Mini-Circuits
Name		3dB Pad	P7LP-306L	Mar-4SM	3dB Pad	LT5511	TFS1440AV	ADL5330	LPF	MAX2031	B3717	Mav-11SM	3dB Pad	ADL5322	B3717	BDCA-6-16	ZHL-2-12	SYBD-26-13HP

Bandwidth / Hz 7.00E+06

(a)

(b)

Figure 3.13: Transmitter power level plan

layer as a ground layer, being completely covered with copper. The distance of 0.4 mm between the top and second layer and the properties of FR4, summarized in Table 3.1, lead to microstrip lines of 0.702 mm width at 866 MHz. The lay-

Parameter		Value	Unit
Relative permittivity	ε_r	4.7	
Dielectric loss	$\tan\delta$	0.014	
Height	h	0.4	mm
Copper plating thickness	d	35	µm
50 Ω microstrip line width for 866 MHz	w	0.702	mm

Table 3.1: Properties of FR4 PCB material used at the transmitter (typical values, upper layer)

out of the transmitter PCB can be seen on Figure 3.14, where the top layer was printed in grey. The board is divided in two parts by the footprint of a shielding plate that can be soldered onto the PCB. It divides the IF1 and IF2 elements on the lower side of Figure 3.14 from the second mixer, RF and control circuits on the upper part.

The jumpers for manual enabling of the transmitter and the gain control trimmer resistor are right below the Sub-D connector on the upper right part of the layout figure. The upper left part is occupied by the PA directional coupler and power detector circuitry. The 13.56 MHz IF1 signal enters the board through the lower right SMA connector and follows an U-shaped path through the first IF stage on the lower right part of the transmitter board. The first mixer M1 is placed on the middle of the lower side, here also the LO1 connector can be seen. After entering the SAW filter on the lower left side the signal is routed up through the VGA to the second mixer. The RF signal leaves the mixer traveling right, is further amplified and finally reaches the TO_PA connector at the right side of the board after running through the driver directional coupler. The CARCOMP_DR output is right above the TO_PA connector. I have chosen this design to minimize the length of the lossy microstrip lines but provide enough room at critical stages to prevent crosscoupling between different microstrip lines.

The two linear voltage regulators are mounted on big copper rectangles which act as heat sinks. These rectangles and all central pads of of the RF-ICs were connected with multiple vias to the ground layer to further improve heat transfer and provide a good RF ground necessary for RF components. For these vias a diameter of 0.3 mm was chosen, which corresponds to the smallest value available in the PCB manufacturer's standard process.

Figure 3.15 shows a picture of the board already equipped with components. For testing the transmitter was not placed in its housing with flange mount SMA connectors but PCB SMA connectors were used.

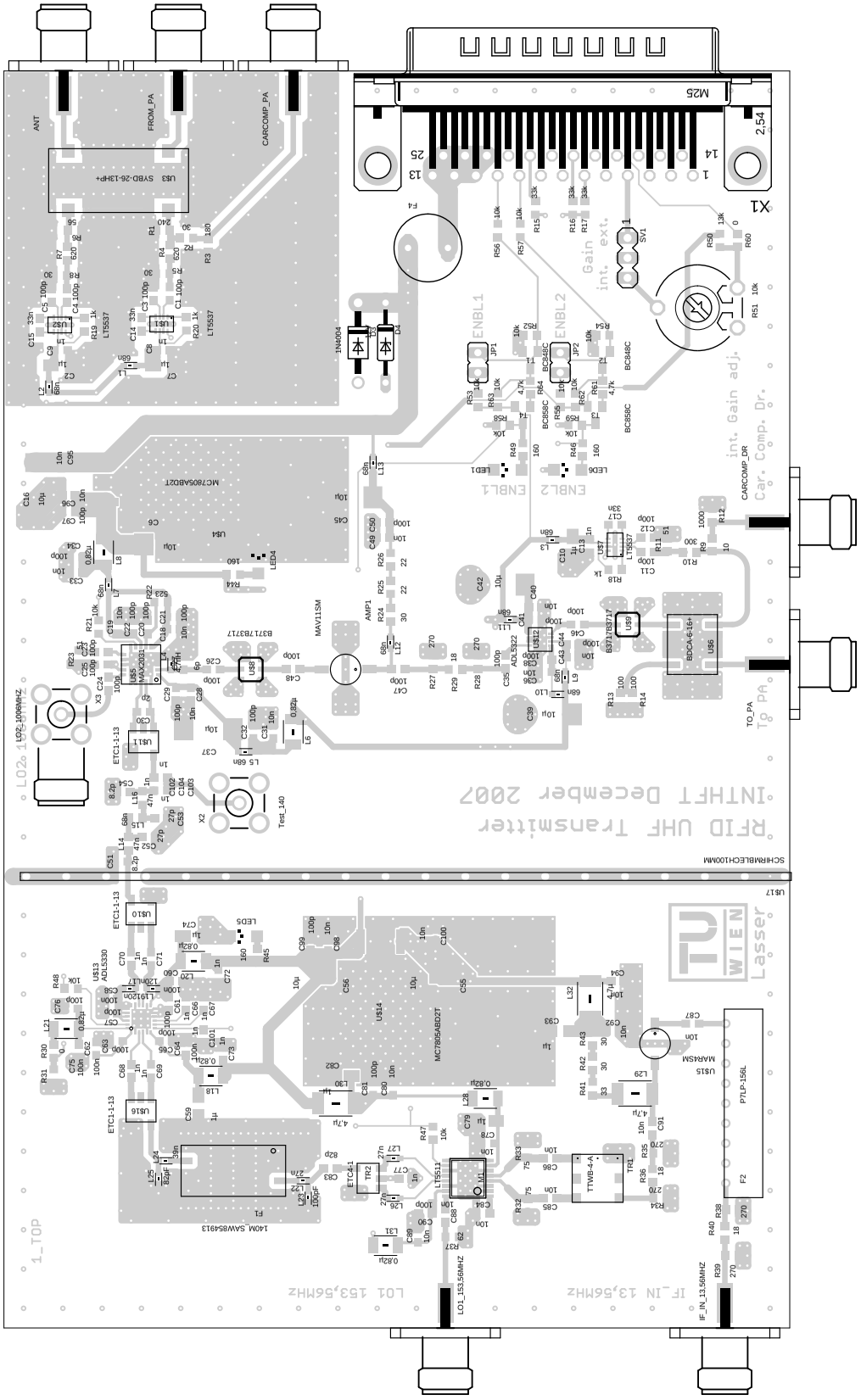

Figure 3.14: Transmitter PCB layout

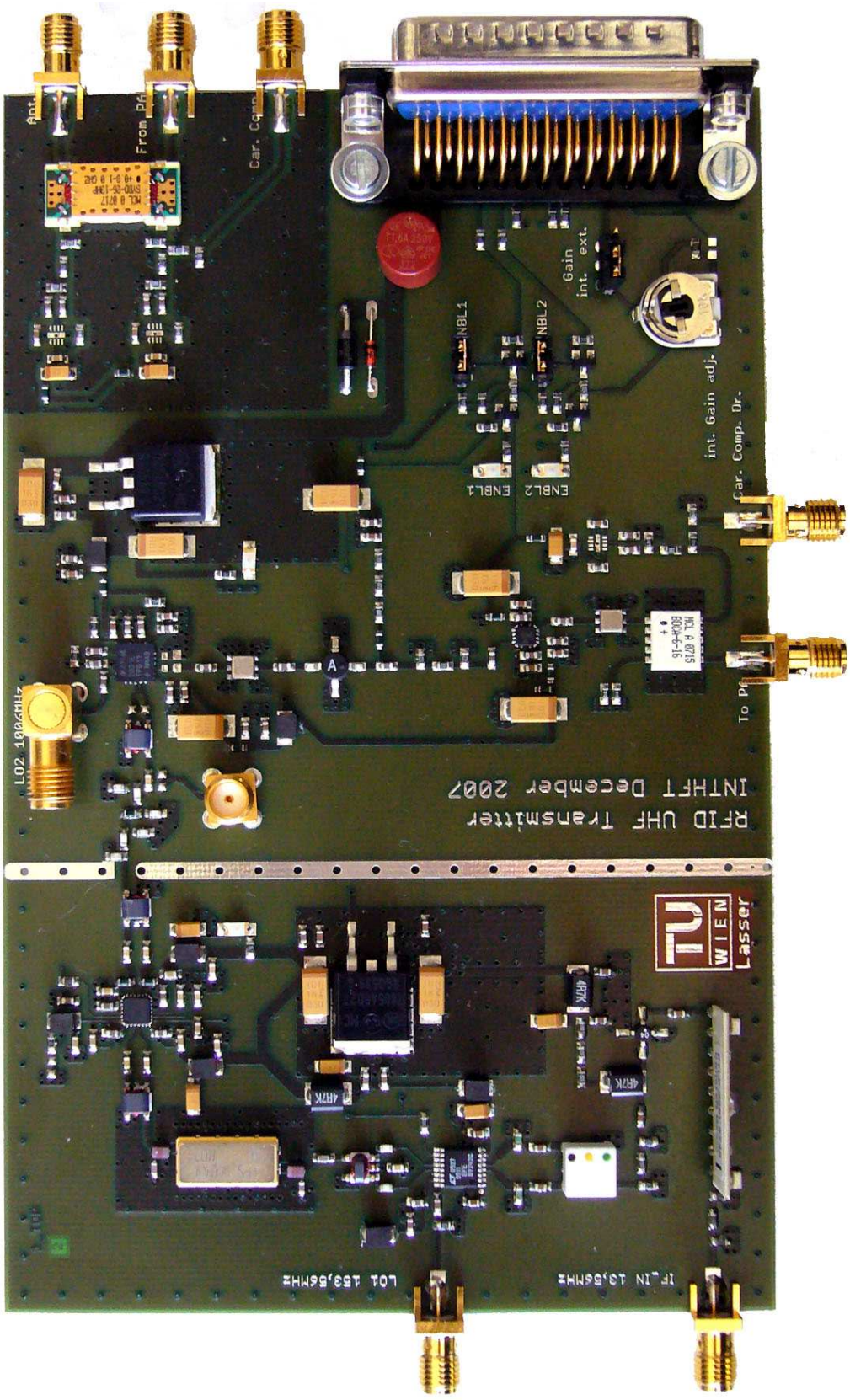

Figure 3.15: Transmitter board

3.3 Measurements

3.3.1 Frequency Response

The frequency response of the transmitter was measured using a VNA[11] and two auxiliary RF-generators, one only used for calibration.

The VNA, here a ZVA24 from Rhode & Schwarz had been used, was operated in scalar mode with different receive and transmit frequencies. One port of the ZVA24 was used as a LO source. This is possible because this four-port VNA has two independent generators. The second LO frequency was produced by an SMU200A signal generator which was also controlled by the VNA. A second signal generator, an SME06, was utilized for VNA receiver calibration. Figure 3.16 shows a block diagram of the measurement setup used to conduct this test.

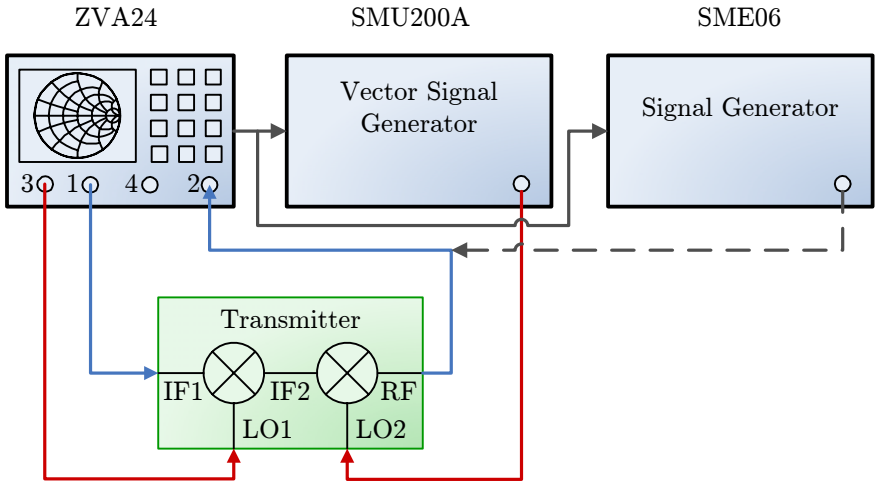

Figure 3.16: Transmitter frequency response measurement setup

The measurement setup was calibrated using a power detector connected to the VNA and measuring the output power of all sources at all used frequency points with this sensor. Afterwards the now calibrated sources were used as a reference for VNA receiver calibration. Table 3.2 summarizes the frequencies of the different VNA and RF generator ports.

Figure 3.17 presents the result of the measurement. While the LO frequencies were kept constant, the transmitter input frequency f_{IF1} was swept from 10 to 30 MHz resulting in an RF output frequency range from 862.44 MHz to 882.44 MHz. This frequency response was measured with the transmitter set to full gain and −10 dBm IF1 input power.

The frequency response of the transmitter is a direct consequence of the SAW filter used in the second intermediate frequency stage. The passband ripple was

[11] Vector Network Analyzer

Port	Use	Value	Unit
ZVA24 port 1	IF1 Output	10 - 30	MHz
ZVA24 port 2	RF Input	862.44 - 882.44	MHz
ZVA24 port 3	LO1 Output	153.56	MHz
SMU200A	LO2 Output	1006	MHz
SME06	VNA Receiver Cal. Generator	862.44 - 882.44	MHz

Table 3.2: Transmitter frequency response test equipment frequencies

measured to be smaller than 0.8 dB, where the nominal 5 MHz bandwidth has been used.

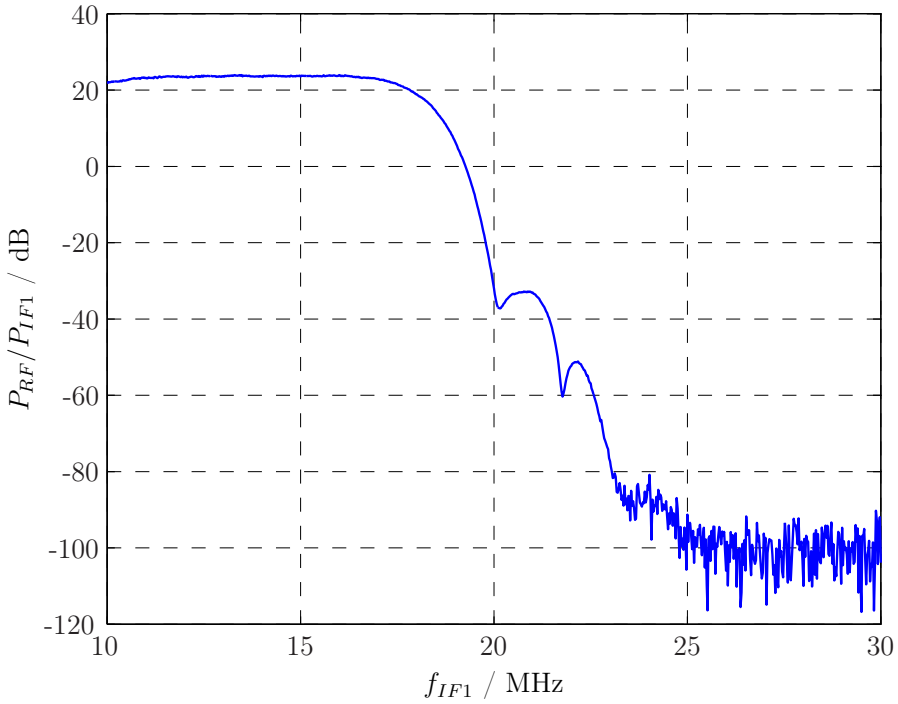

Figure 3.17: Transmitter frequency response

3.3.2 Powersweep

When the transmitter input power is increased, at some point the transmitter's components will start to saturate and compression of the output signals will be present. To measure this phenomenon a power sweep was performed. The measurement setup was quite similar to the one used for measuring the frequency response, but now the IF1 frequency f_{IF1} was constant at 13.56 MHz. Again the transmitter was set to maximum gain.

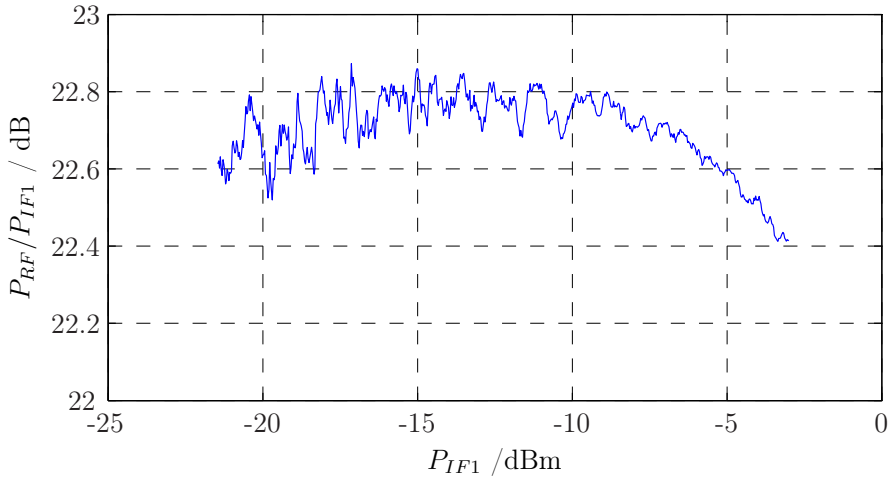

Figure 3.18: Transmitter power sweep

The result of the measurement is printed in Figure 3.18. The input level was limited to −3 dBm. This power limitation made it impossible to directly measure the 1 dB compression point of the transmitter, at −3 dBm a gain degradation of about 0.4 dB was measured.

3.3.3 Intermodulation

To qualify the transmitter's intermodulation properties a two-tone test was carried out. As signal source a SMU200A RF signal generator was used, that is capable of producing a two-tone test signal. The two test signals were spaced 500 kHz apart. Test series with different power levels were conducted, in the first one each tone had a signal power $P_{IF_{Tone}}$ of −13 dBm, while −8 dBm was used in the second series. The transmitter's output was attenuated by 20 dB and observed with an spectrum analyzer.

Figure 3.19 and Figure 3.20 show the results of the tests carried out with the transmitter set to full gain. The same measurements were also carried out with reduced transmitter gain, it was set to approximately 6 dB, these results show a slightly better intermodulation performance. The reason for that behavior is that at high gain settings the driver amplifier is first driven into saturation, while at lower gain settings the IF1 amplifier and the first mixer begin to saturate.

The numerical results of the measurements were summed up in Table 3.3. While the absolute values of the measured output powers are of the usual accuracy of spectrum analyzers, the IM_3[12] results are quite precise because only differential accuracy is required here. For every measurement the 3rdorder input intercept point IP_3 was calculated, here only the absolute input power per tone $P_{IF_{Tone}}$ is critical. This fact is also expressed in Equation 3.1, which is valid for

[12] 3rd Order Intermodulation Ratio

logarithmic units.

$$IP_3 = \frac{IM_3}{2} + P_{IF_{Tone}} \tag{3.1}$$

In theory the 3$^{\text{rd}}$order intercept point should not depend on the input power. However in practical systems the slope of the intermodulation products is not constant and so the slightly different IP_3 values for the same gain setting found in Table 3.3 are not suspicious at all.

Gain Setting	Full	Full	Reduced	Reduced	Unit
$P_{IF_{Tone}}$	-13	-8	-13	-8	dBm
$P_{RF_{Tone}}$	6	10.66	-10.41	-6.16	dBm
P_{IM3}	-48.75	-31.78	-74.06	-61.13	dBm
P_{IM5}	$\leq$-74.09	-56.09	$\leq$-83.6	-73.69	dBm
IM_3	54.75	42.44	63.65	54.97	dB
IP_3	14.4	13.22	18.83	18.49	dBm

Table 3.3: Transmitter intermodulation test summary

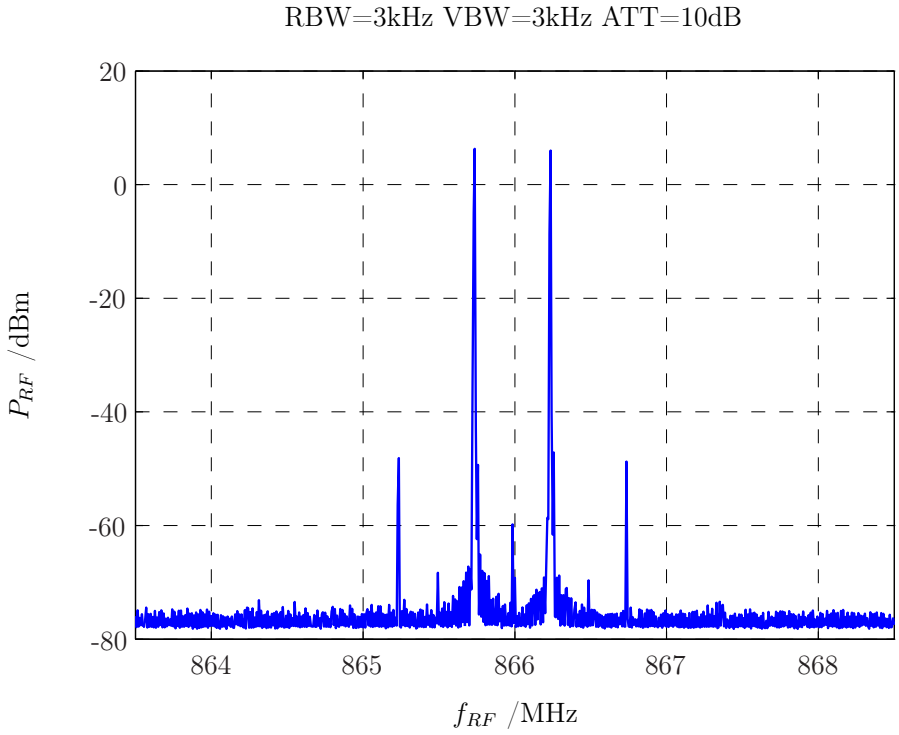

Figure 3.19: Transmitter intermodulation test: full gain, −13 dBm test signals

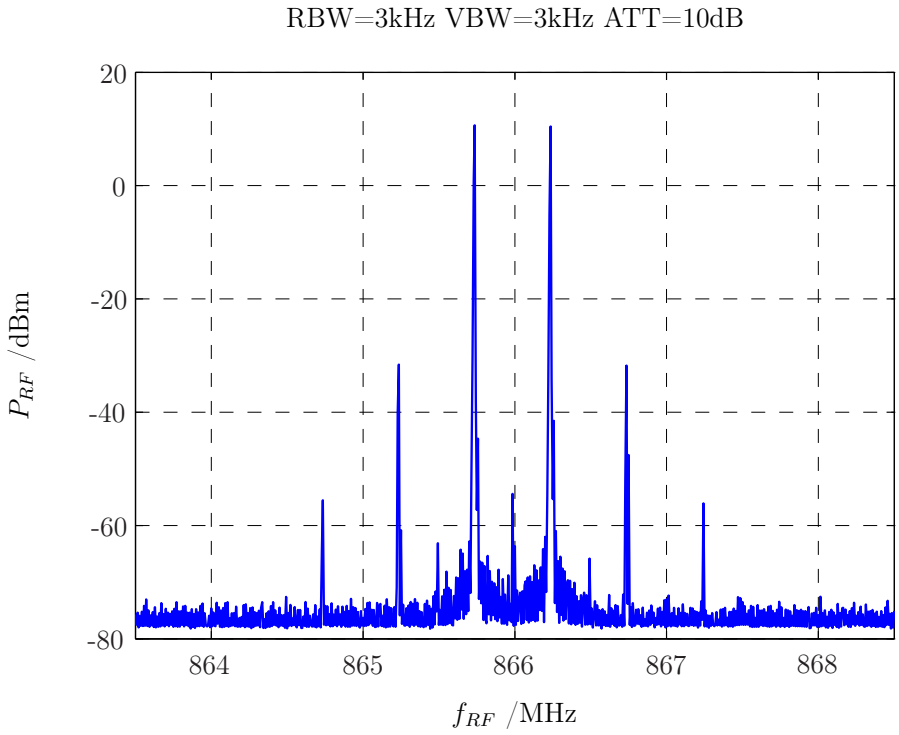

Figure 3.20: Transmitter intermodulation test: full gain, −8 dBm test signals

Chapter 4

Receiver

While the transmitter described in the previous chapter is essentially a quite conventional linear transponder, the receiver required for the RFID testbed is far more challenging. As described in Section 1.3 carrier components of very high amplitude from the transmitter can be present at the receiver input. However, a low receiver noise figure is essential when the messages of far tags should still be decoded. This chapter describes the receiver module that I have designed, built and successfully tested in this diploma thesis.

4.1 Concept

Transmitter and receiver share the same double conversion high side LO injection concept that was already described in previous chapters. Also the mechanical concept is identical to the transmitter, the same housing and PCB material was used.

4.1.1 Input Power Levels

The LO input power levels were chosen to meet the transmitter and receiver needs, so for both the LO1 is fed with a -5 dBm signal and LO2 with a 0 dBm signal.

The maximum allowed receiver input power on the RX_ANT connector depends on the possible extinction of parts of this input signal by an injected CAR_COMP_IN signal. If carrier compensation is omitted linear operation is possible up to an input power of -6.4 dBm. The absolute maximum input power is 2 dBm.

When a carrier compensation signal is injected by an external compensation module, the input power level is only limited by the maximum allowed input level at the CAR_COMP_IN connector. 28 dBm of compensation signal can be applied at this connector, so when this compensation is perfectly matched, a 4.5 dB lower receiver input signal is maximally allowed. The reason for this difference can be found in the attenuation of the received signal by the receiver input filter and the coupling losses of the receiver's CCU coupler, for further details see Section 4.2.1.

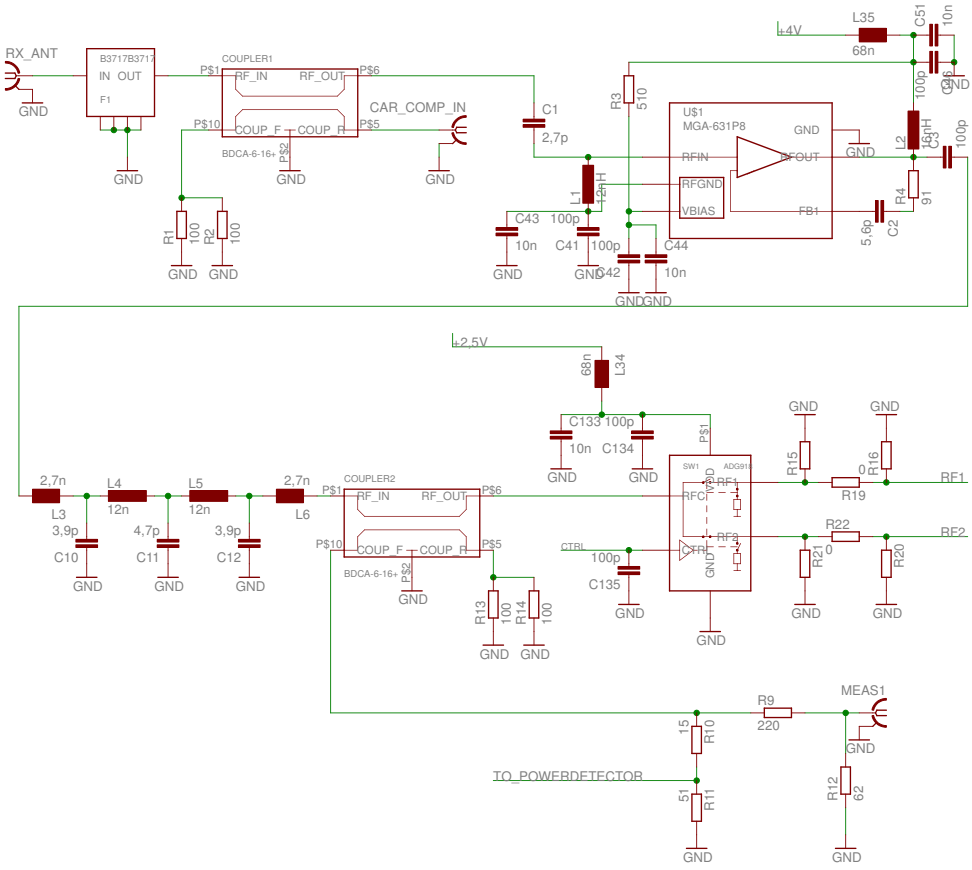

Figure 4.1: Receiver LNA and CCU coupler schematic

When using the CCU module described in Chapter 5 about 20 dBm of leaking carrier input power at the RX_ANT can be compensated.

4.1.2 Output Power Levels

As described in Section 2.2.1 the necessary receiver output power to drive the rapid prototyping board is 12.6 dBm, so the receiver has been designed support this value.

4.2 Realisation

Many components used in the receiver were also used in the transmitter with almost identical circuitry and have already been described in Section 3.2. Therefore, description of these identical parts is omitted here.

4.2.1 LNA and CCU Coupler

The receiver input signal is first routed through an Epcos B3717 low loss SAW filter that was already described in the receiver chapter. Its main purpose is to attenuate out of band signals, specially at the receiver mirror frequency at about 1145 MHz. Strong GSM[1] radio signals, which are also located near the RFID frequency band, are also an issue here.

The input signal is fed in the CCU directional coupler to allow injection of an inverted copy of the leaking carrier component for cancelation. The forward coupled port of this directional coupler is terminated with two parallel 100 Ω resistors in 1206 style. While most resistors used in the receiver are of the 0603 type, here the power handling capabilities of the bigger resistors of 0.25 W per resistor allow for an injection of a 28 dBm carrier compensation signal, where the coupler's mainline losses are taken into account.

The carrier compensation directional coupler is a BDCA-6-16 from Mini-Circuits with typical 6.7 dB of coupling loss and a mainline loss of 1.4 dB. The coupler was placed after the input filter to benefit from the filter attenuation of about 2.2 dB and prevent intermodulation caused by strong GSM signals at the carrier compensation module output amplifier.

The partly compensated antenna signal is then amplified in a LNA from Avago, the MGA-631P8. This type was chosen for its high output 1 dB compression point of 18 dBm. The matching components C1, L1 and L2 were selected as good compromise between input return loss, gain and noise figure. This selection was based on simulations carried out in Microwave Office with data files supplied by the manufacturers of the LNA and the inductors.

The LNA is followed by a LPF and afterwards a measurement coupler. Here again a BDCA-6-16 was used. The forward coupled output of COUPLER2 is divided by a resistor network into a 2.2 dB attenuated signal for a LT5537 power detector, and a 13.2 dB attenuated signal for the first measurement connector MEAS1. This port can be used to adjust the cable length of the CCU interconnect cables for an equal delay between the direct coupled TX–RX path, and the TX–CCU–RX compensation path to achieve best carrier suppression performance.

To enable a switchable second RF amplifier after the LNA an RF switch from Analog Devices, the ADG918, is placed right after the measurement coupler. Both outputs lead to Π-attenuator structures, where only R19 and R22 are fitted with 0 Ω resistors to disable the attenuators. These structures were just inserted to improve flexibility and allow RF attenuation when necessary.

4.2.2 Switchable second RF Amplifier and first Mixer

As a second RF amplifier a MAV11SM is used. The biasing circuit equals the one used in the transmitter, as can be seen on Figure 4.2. The gain of this amplifier

[1] Global System for Mobile Communications

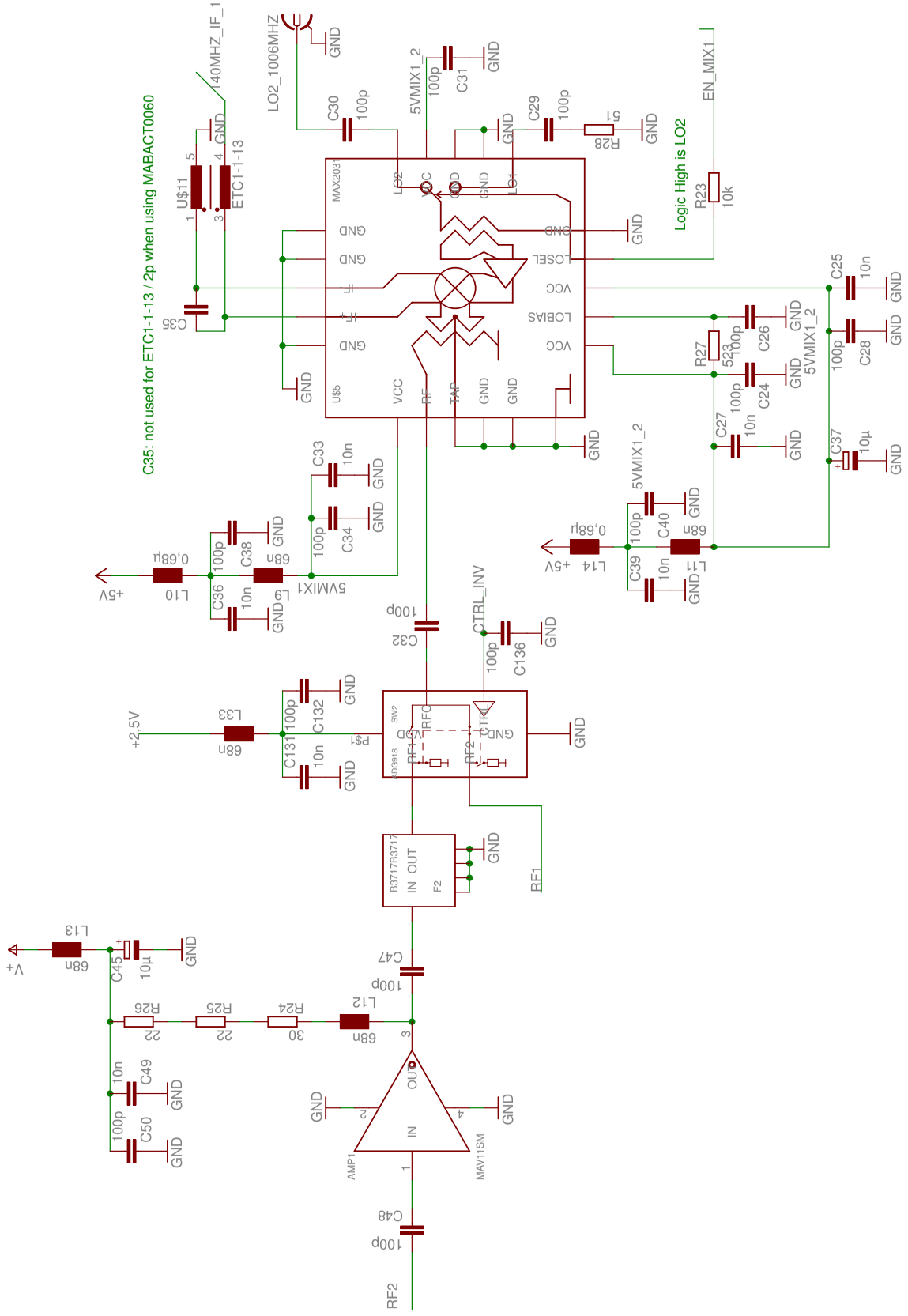

Figure 4.2: Receiver second RF amplifier and first mixer schematic

enables the use of a second B3717 RF SAW filter to further improve RF selectivity. The amplified and nonamplified pathes merge together at a second ADG918 switch IC where now RF1 and RF2 are interchanged for layout considerations. To enable proper switching the ICs are driven with complementary drive signals from the control circuits.

The first mixer is a MAX2031 used in an identical circuitry as in the transmitter upconverter case, so here no further description is given.

4.2.3 First IF Stage

The output 140MHZ_IF_1 of the first receiver mixer enters the IF stage depicted in Figure 4.3 through a LPF to suppress undesired mixing products. At the filter input C102, C103 and C104 also enable to switch from regular receiver operation to IF signal injection or IF signal measurement output at connector X2 called Test_140.

To keep the noise figure low, a high gain (20 dB) amplifier is used prior to the IF SAW filter to overcompensate for the filter losses. To prevent overloading this amplifier and further IF stages in high input signal situations, a switchable 10 dB attenuator is provided between the IF-LPF and the amplifier. Here a HMC541LP3 from Hittite was used, for operation only DC blocking capacitors C56 and C57 and filter capacitors C58 and C59 are necessary. Like all other stages the switchable attenuator and the following amplifier are not directly connected to their supply lines, but decoupling is provided by an L/C network.

The amplifier, an Analog Devices ADL5542 just needs an RF choke (L21) on its output port for DC biasing and a 1 µF capacitor (C62) connected to the CB pin to filter AC components from the internal biasing circuitry of the amplifier.

The SAW filter and its matching components are identical to the one described in Section 3.2

The filter is followed by a MAX2027 VGA from Maxim, that essentially is a switchable attenuator and an amplifier in one housing. The attenuator part is switchable between 0 and 23 dB attenuation in 1 dB steps and is followed by a fixed gain amplifier. At the maximum gain setting, corresponding to minimal attenuation, the whole IC has a gain of 15.5 dB at a noise figure of 4.7 dB

The internal biasing circuit needs a DC path to the AMP_IN pin that is provided by L22. The bias current is set with R29. The output of the amplifier is DC biased with the radio frequency choke L23. The IC is again supplied by the locally filtered 5 V line.

4.2.4 IF Coupler and second Mixer

To enable automatic gain control at the first receiver IF a measurement coupler is implemented before the second mixer. Here an ADC-10-1R from Mini-Circuits was used, which has a forward coupling loss of 10.6 dB. The resistor divider network,

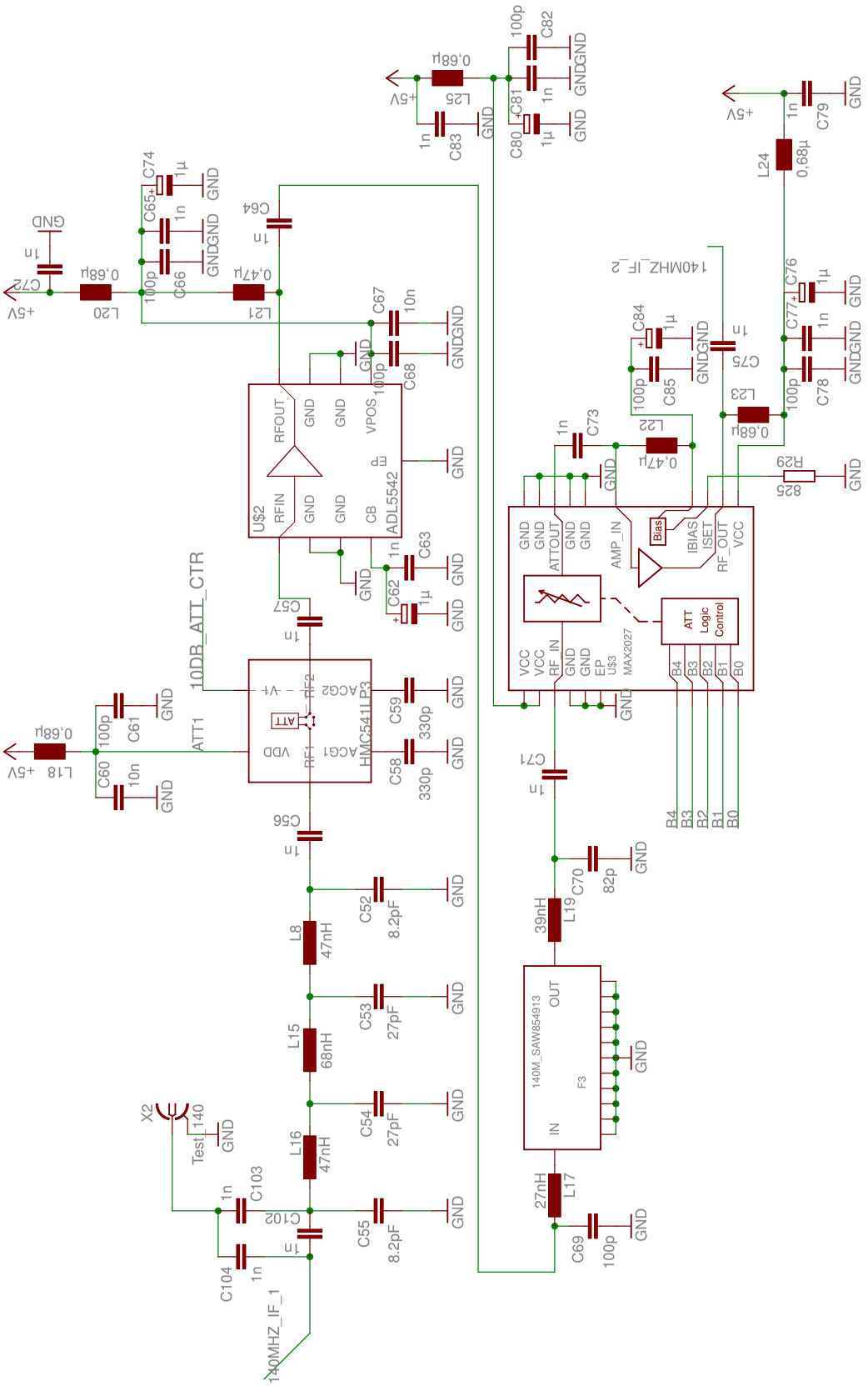

Figure 4.3: Receiver 140 MHz IF schematic

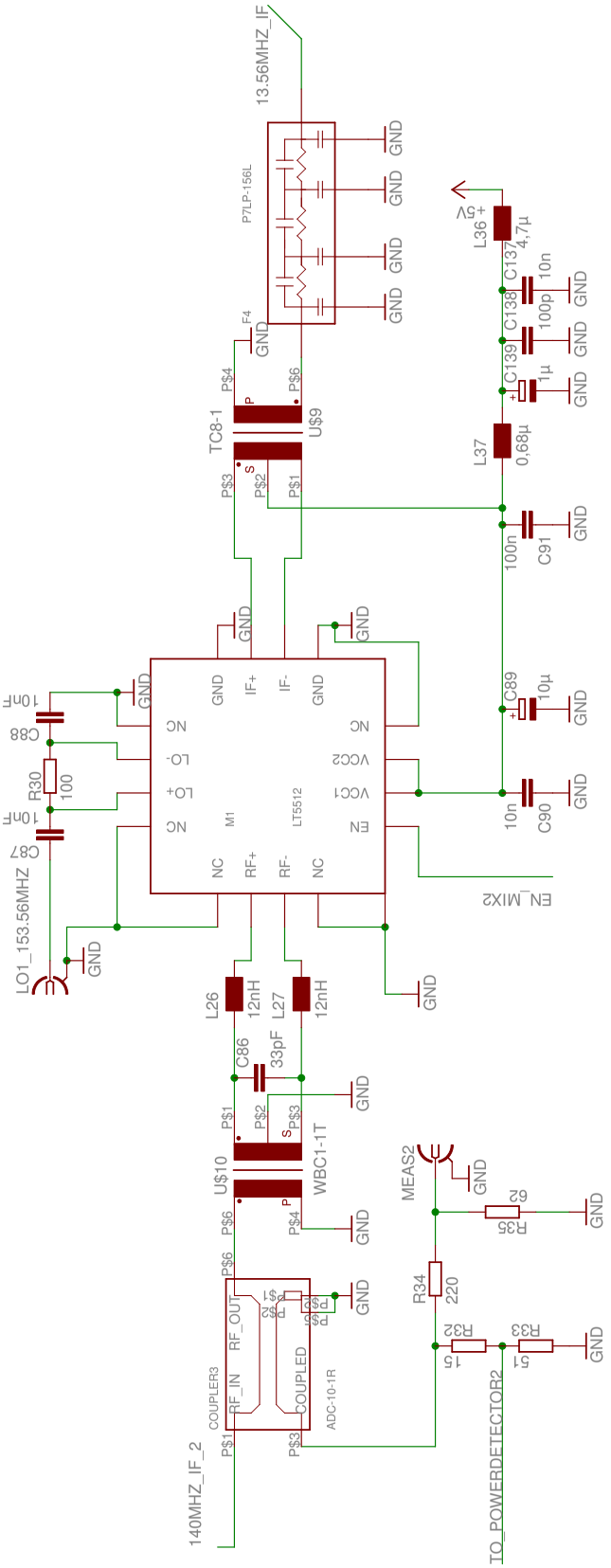

Figure 4.4: Receiver IF coupler and second mixer schematic

used for dividing the coupled signal into a detector input and measurement output signal, is identical to the one implemented on the first measurement coupler at the RF stage.

The second mixer is realized using a double balanced active mixer IC from Linear Technology, the LT5512. The matching network was provided by the manufacturers recommendation [16]. The input transformer WBC1-1T from Coilcraft is a 1:1 transformer that is used to convert the asymmetric IF signal into a balanced drive signal for the mixer input. The transformer center tap also provides a DC path necessary for proper mixer operation. C86, L26 and L27 form an input matching network with low pass characteristics. The output transformer, a Mini-Circuits TC8-1, converts the high impedance balanced output back to a 50 Ω asymmetric signal that is again filtered by Coilcrafts P7LP-156 LPF. The output transformer's center tap also provides DC bias for the mixer output switching transistors.

4.2.5 Output Stage and Envelope Detector

The second IF stage, which boosts the IF signal to an appropriate level for interfacing the rapid prototyping board, is shown in Figure 4.5.

Before entering the final amplifier, the IF signal is routed through two solder jumpers SJ2 and SJ3. These jumpers enable the IF signal to be routed to board-to-board connectors to attach second IF add-on boards. Possible uses include a second IF VGA for higher dynamic range, a narrow band notch filter to suppress the carrier component and further filtering to improve selectivity. For powering such add-on cards a separate power connector is available.

The output amplifier was realized using a high speed operational amplifier. For the complete amplifier circuitry a voltage gain of 4 or 12 dB was planned. To better adapt to the low impedance drive a TC8-1 with an impedance ratio of 1:8 was utilized. The secondary side of TR1 was originally terminated with a 400 Ω resistor R39. The value was later changed to 442 Ω because measurements revealed that with this value of R39 a slightly better matching and higher gain is possible.

The op-amp[2] is used in a conventional noninverting configuration. R40 and R41 set the gain of the operational amplifier. The transformer helps to reach the desired gain of 12 dB by increasing the input voltage according to $1 : \sqrt{8} = 1 : 2.83$, but at the op-amp's output the easy match to 50 Ω by adding R42 contributes to the whole amplifier gain as a factor of 1/2. This leads to a necessary gain of the op-amp of $\frac{4 \cdot 2}{2.83} = 2.83$ and so R40 and R41 were chosen to reach this gain. C112 can be used to add a low pass character, and R38 helps to prevent high frequency oscillations. To reach a nominal output impedance of 50 Ω a series resistor, R42, is used.

[2] operational amplifier

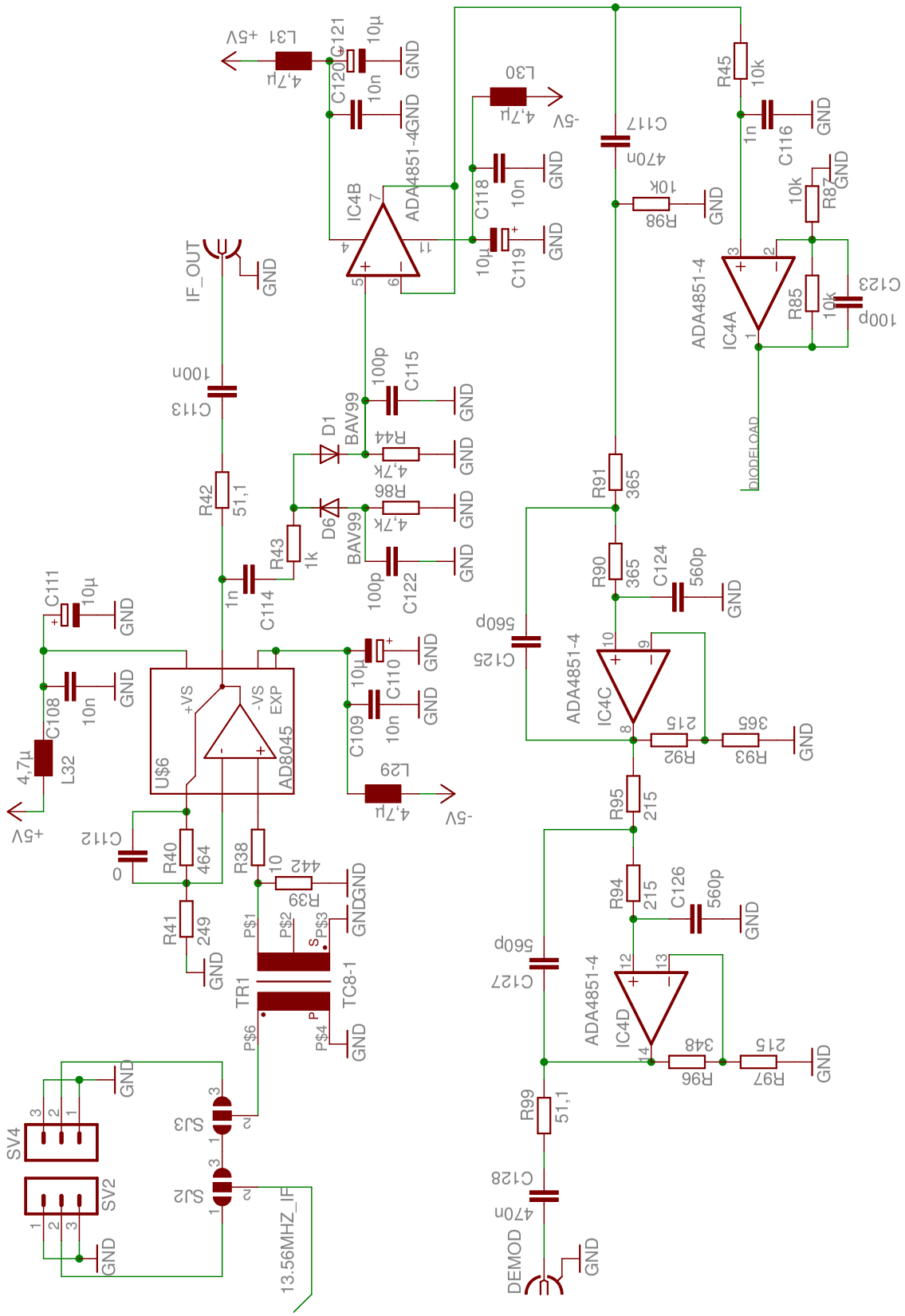

Figure 4.5: Receiver output stage and envelope detector schematic

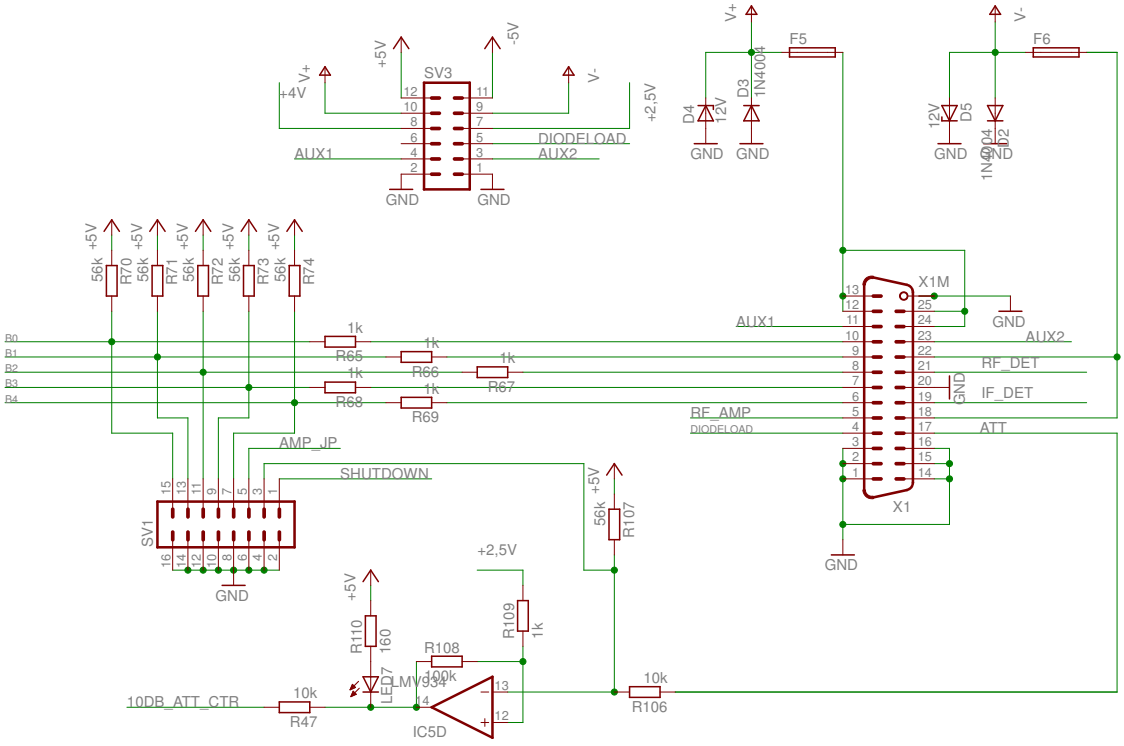

Figure 4.6: Receiver power and control connector schematic

The envelope detector is formed by D1 and C115. To prevent C114 from accumulating charge due to the rectification of only the positive halfwave by D1, a second rectifier stage, D6, C122 has been applied to balance the current through C114. The rectifiers output is buffered with an op-amp follower stage IC4B and then divided in a DC component for automatic gain control, and an AC component for direct observation of the tag signal.

The DC and lower frequency components of the IF signals envelope are amplified in IC4A and are fed to the power and control connector for external use.

The AC component still includes IF signal components. To remove them without disturbing the demodulated output signal an active filter was used. IC4C and IC4D and their associated circuitry form a four pole 0.5 dB ripple Chebyshev filter with a cut-off frequency of 1.3 MHz. The values of R90 to R97 were chosen to match the necessary time constants and gains (1.582 for the first and 2.66 for the second stage) as indicated in [17]. The output of the filter is routed to the DEMOD SMA connector after passing R99 and C128 to remove DC components and guarantee 50 Ω output impedance.

4.2.6 Power Supply and Control Circuits

The main control and power connector X1, a 25 pin Sub-D connector, can be seen on Figure 4.6. The receiver needs five different voltages for operation, see

Voltage	Use
10 V	Second RF Amplifier
5 V	Most Components
4 V	LNA
2.5 V	RF Switch
-5 V	Operational Amplifiers

Table 4.1: Receiver supply voltages

Table 4.1.

These voltages are all derived from ±10 V supplied from an external power source using linear voltage regulators. Both, positive and negative supply input lines are protected with fuses and protection diodes against high voltage and reverse voltage connection.

All control input lines were equipped with pull-up resistors to ensure that the receiver is operating in minimum gain mode when powered up with no control lines connected. Besides the Sub-D connector X1 for external use there is also a 16 pin connector SV1 for local receiver control. Table 4.2 gives a summary of the control lines, their function and logical activation level.

Pin SV1	Pin X1	Element/Function	Active on
1	-	Shutdown	L
3	17	10 dB Attenuator	H
5	5	RF Amp	L
7	6	VGA 16 dB Att.[3]	H
9	7	VGA 8 dB Att.	H
11	8	VGA 4 dB Att.	H
13	9	VGA 2 dB Att.	H
15	10	VGA 1 dB Att.	H

Table 4.2: Receiver control lines

As mentioned before, all control lines set the receiver in "save" low gain mode when driven high. To achieve this, some internal control lines need to be inverted. For example, the 10 dB attenuator line is inverted by IC5D. The op-amp in conjunction with R108 also provides a small hysteresis and drives a LED to show the attenuators status. Here the 2.5 V line is used as a reference. IC5 is a rail-to-rail input and output op-amp running on 5 V.

Connector SV3 provides power connections for an optional add-on second IF card. Two control lines, AUX1 and AUX2 are directly connected to the X1 main connector and could be used for gain control or notch filter frequency adjustment

[3]The use of the VGA 16 dB attenuator disables the VGA 8 dB attenuator automatically.

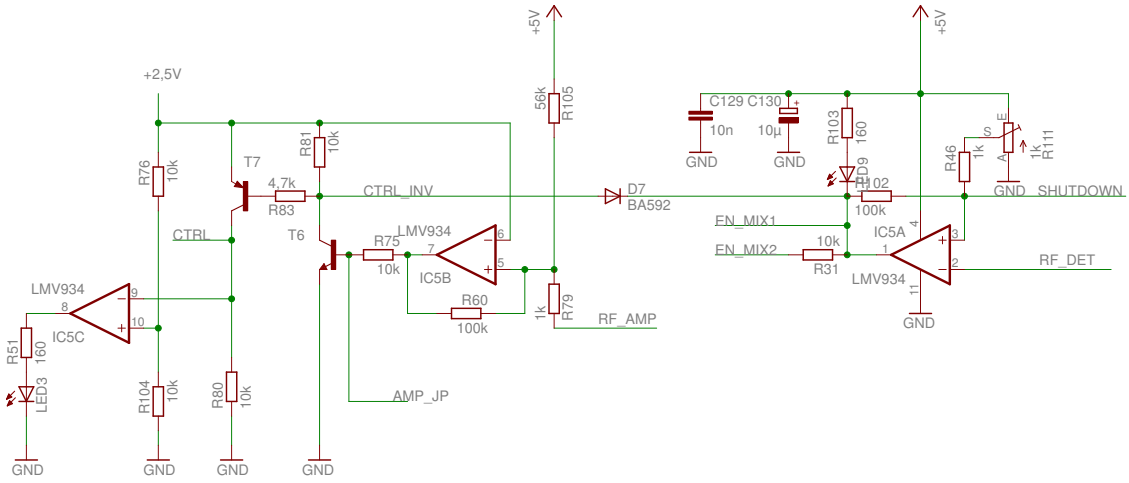

Figure 4.7: Receiver control and shutdown schematic

of this optional add-on card. To enable the implementation of an analog AGC[4] on this card, the DIODELOAD signal from the envelope detector is also available on SV3.

As mentioned in Section 4.2.2 the RF switches that control the second RF amplifier are differentially driven. IC5B, that is drawn on Figure 4.7, acts as a buffer amplifier and adds a small switching hysteresis. The output of the op-amp is fed in a level converter and an inverter build by T6 and T7. The level conversion is necessary because the switches run on the 2.5 V line. IC5C monitors the switches CTRL input line and drives a LED when the second RF amp is inserted in the signal path by the RF switches.

A protection circuit is implemented using IC5A. The output voltage of the RF power detector RF_DET is compared with an adjustable voltage derived from R111. When the input power reaches the level set by R111, IC5A pulls the mixer enable lines low, D7 starts to conduct and turns off the second RF amp. The red LED LED9 lights up to show the overload status.

While the protection circuit, when tripped, sets an optical alarm and shuts down the first and second IF stages for protection, it cannot however prevent destruction of the LNA, the RF switches and the first mixer when the RF input power is further increased above the maximum ratings.

4.2.7 Power Level Plan

The level plan presented in Figure 4.8(a) is quite similar to the one used for transmitter design. However, here the received signal is decomposed in a (leaking) carrier component, and the modulated signal component. While the carrier component depends on the transmit power, the effectiveness of the CCU and

[4] Automatic Gain Control

the transmitter–receiver leakage, the modulated signal component depends on tag antenna size, orientation and reader–tag distance. To illustrate the effects of carrier leakage and compensation a weak data signal of −80 dBm was assumed here.

For the level plan a transmit power of 33 dBm, corresponding to the legal limit at a dipole antenna, and a transmitter–receiver isolation of 20 dB was assumed. This equals a carrier component of 13 dBm at the receiver input. Therefore, for linear operation a minimum carrier suppression of 19.4 dB is necessary. Figure 4.8(a) and Figure 4.8(b) depict this situation, the second RF-amplifier is switched off, the 10 dB attenuator is switched on and the attenuator of the VGA is set to medium gain to produce an output power of approximately 12 dBm for full ADC coverage.

In this mode of operation the noise figure is quite high (17 dB), but still 1 dB lower than the maximum allowed noise figure for long distance reception calculated in Section 2.1.1.

Figure 4.9 shows the growth of the noise figure from stage to stage when further stages are added to the first receiver part.

While the heaviest increase clearly takes place at the later receiver stages, especially at the switchable 10 dB attenuator, the reason for this lies in the lack of gain in the RF section of the receiver. However, a higher gain, that could be realized by switching on the RF amplifier, is not possible here without overloading many following receiver components.

A totally different situation is depicted in Figure 4.10(a). Now the suppression ratio of the CCU is significantly higher, 45 dB, so that it is possible to use the highest available receiver gain of 44 dB. A graphical representation can be found at Figure 4.10(b).

The added receiver gain also improves the noise figure of the receiver. At highest gain the receiver has a noise figure of 5 dB. For this situation the noise figure build-up is again graphically represented in Figure 4.11.

Now the stages that contribute the biggest part of the noise figure are the filter, coupler and LNA. Further improvement is only possible by substituting the filter and coupler for lower loss types. Where lower loss SAW filters are currently not available, bulkier helix filters could be used. Lower loss couplers automatically lead to couplers with higher coupling loss, that would inhibit the compensation of high leaking carrier components, when the same cancelation power is preconditioned. However, a noise figure of 5 dB is quite low and is certainly low enough for passive RFID systems and should even be sufficient for most active RFID systems.

Table 4.3 lists all optimum receiver settings for different carrier suppression ratios in 2 dB steps. In this context optimum means that the highest possible gain was chosen to fully modulate the ADC and work under minimum noise figure. Higher attenuation settings of the VGA are possible when lower ADC drive is desired.

	Start	Filter	Coupler	LNA	Filter	Coupler	Switch	Pad	2nd RF Amp	Filter	Switch	First Mixer	Filter	ATT sw.	10dB ATT	IF Amp1	Filter	var. ATT	IF Amp2	Coupler	2nd Mixer	LPF	Amplifier
Gain / dB		-2.2	-1.4	18	-1	-1.4	-1	0	0	0	-1	-7	-0.5	-0.8	-10	20	-13	-9	15.5	-0.5	2	-0.5	12
F / dB		2.2	1.4	0.7	1	1.4	1	0	0	0	1	7	0.5	0.8	10	2.7	13	9	4.7	0.5	10.3	0.5	1.23
Signal / dBm	-80.00	-82.20	-83.60	-65.60	-66.60	-68.00	-69.00	-69.00	-69.00	-69.00	-70.00	-77.00	-77.50	-78.30	-88.30	-68.30	-81.30	-90.30	-74.80	-75.30	-73.30	-73.80	-61.80
Carrier / dBm	13.00	10.80	-10.00	8.00	7.00	5.60	4.60	4.60	4.60	4.60	3.60	-3.40	-3.90	-4.70	-14.70	5.30	-7.70	-16.70	-1.20	-1.70	0.30	-0.20	11.80
Signal/Carrier / dB	-93.00	-93.00	-73.60	-73.60	-73.60	-73.60	-73.60	-73.60	-73.60	-73.60	-73.60	-73.60	-73.60	-73.60	-73.60	-73.60	-73.60	-73.60	-73.60	-73.60	-73.60	-73.60	-73.60
F	1.0000	1.6596	2.2909	2.6915	2.7009	2.7183	2.7347	2.7347	2.7347	2.7347	2.7552	3.1564	3.2176	3.3313	9.4161	15.2445	16.5258	25.8921	46.7996	46.8365	50.1284	50.1545	50.2331
F / dB	0.00	2.20	3.60	4.30	4.32	4.34	4.37	4.37	4.37	4.37	4.40	4.99	5.08	5.23	9.74	11.83	12.18	14.13	16.70	16.71	17.00	17.00	17.01
SNR / dB	25.53	23.33	21.93	21.23	21.21	21.18	21.16	21.16	21.16	21.16	21.12	20.53	20.45	20.30	15.79	13.70	13.34	11.39	8.82	8.82	8.53	8.52	8.52
OP1dB / dBm	47	30.00	25.00	18.00	25.00	25.00	17.00	47.00	17.50	30.00	17.00	20.00	25.00	17.00	30.00	19.60	23.00	5.10	20.60	25.00	12.50	25.00	17.50
Abs. Max. Output / dBm	39	20.00	47.00	31.00	25.00	47.00	18.00	47.00	25.00	20.00	18.00	5.00	25.00	18.00	30.00	38.00	25.00	5.10	30.00	47.00	13.00	25.00	
Gain / dB	0	-2.20	-3.60	14.40	13.40	12.00	11.00	11.00	11.00	11.00	10.00	3.00	2.50	1.70	-8.30	11.70	-1.30	-10.30	5.20	4.70	6.70	6.20	18.20
Manufacturer		Epcos	MiniCircuits	Avago		MiniCircuits	Analog		MiniCircuits	Epcos	Analog	Maxim		Hittite		Analog	Telefilter	MAXIM		MiniCircuits	Linear Tech.		Analog
Name		B3717	BDCA-6-16	MAG-631P8	LPF	BDCA-6-16	ADG918	Pad	Mav-11SM	B3717	ADG918	MAX2031	LPF	HMC541LP3		ADL5542	TFS140AV	MAX2027		ADC-10-1R	LT5512	LPF	AD8045

Bandwidth / Hz 7.00E+06
Circ. Isolation / dB 20
Carrier Suppression / dB 19.4

(a)

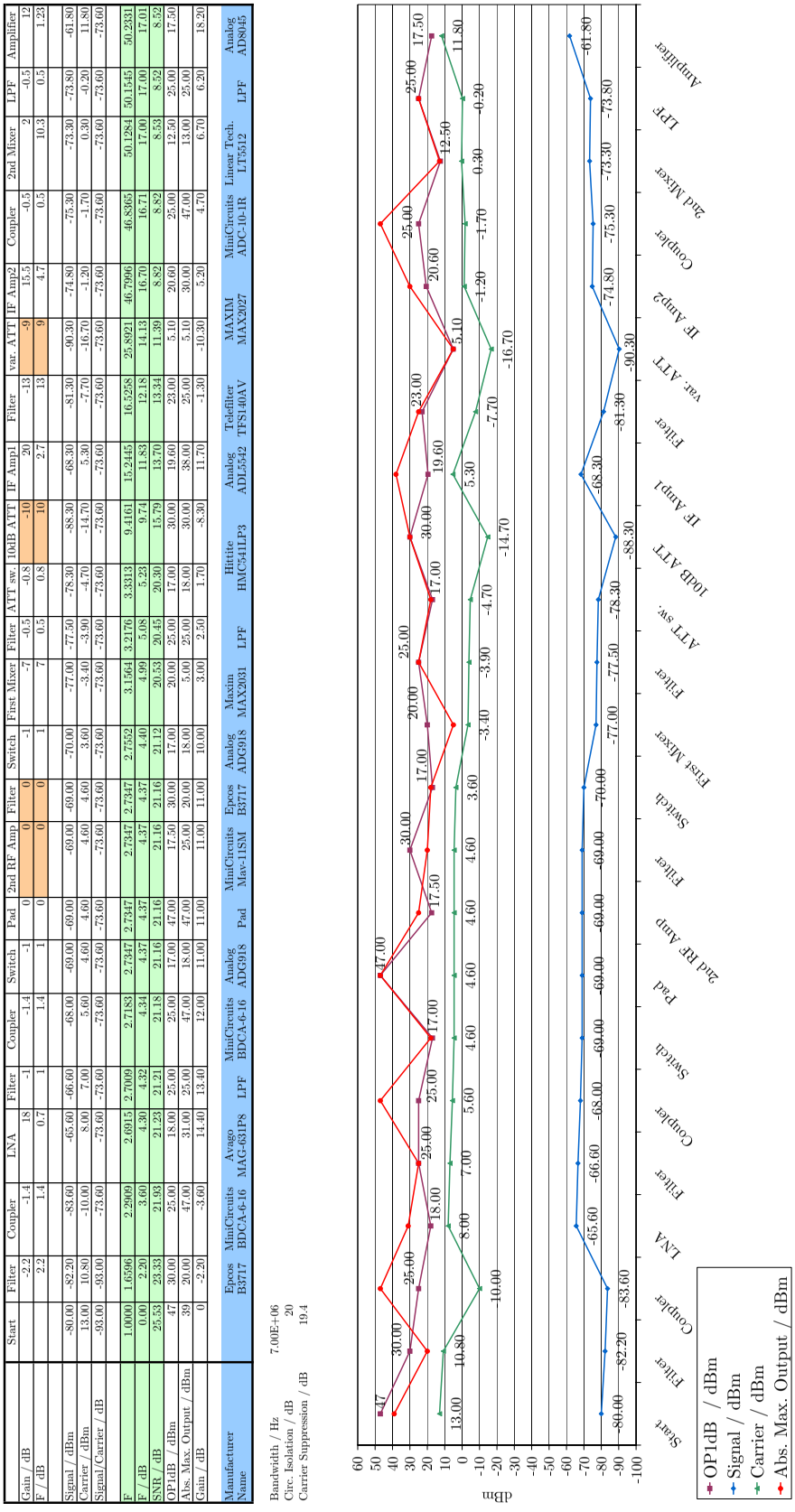

(b)

Figure 4.8: Receiver power level plan at low gain

Carrier Suppression /dB	Equiv. Input Power /dBm	RF Amp.	10 dB-Att.	VGA Att. Setting /dB	F /dB
19.4	-6.4	off	on	-9	17.0
20	-7	off	on	-9	17.0
22	-9	off	on	-7	15.7
24	-11	off	on	-5	14.6
26	-13	on	on	-9	11.1
28	-15	on	on	-7	10.0
30	-17	on	on	-5	9.2
32	-19	on	off	-13	6.9
34	-21	on	off	-11	6.3
36	-23	on	off	-9	5.8
38	-25	on	off	-7	5.5
40	-27	on	off	-5	5.3
42	-29	on	off	-3	5.2
44	-31	on	off	-1	5.1
45	-32	on	off	0	5.0

Table 4.3: Receiver gain settings, noise figures (F) and corresponding necessary minimum carrier suppressions in conjunction with 20 dB intrinsic TX–RX isolation and 33 dBm TX power

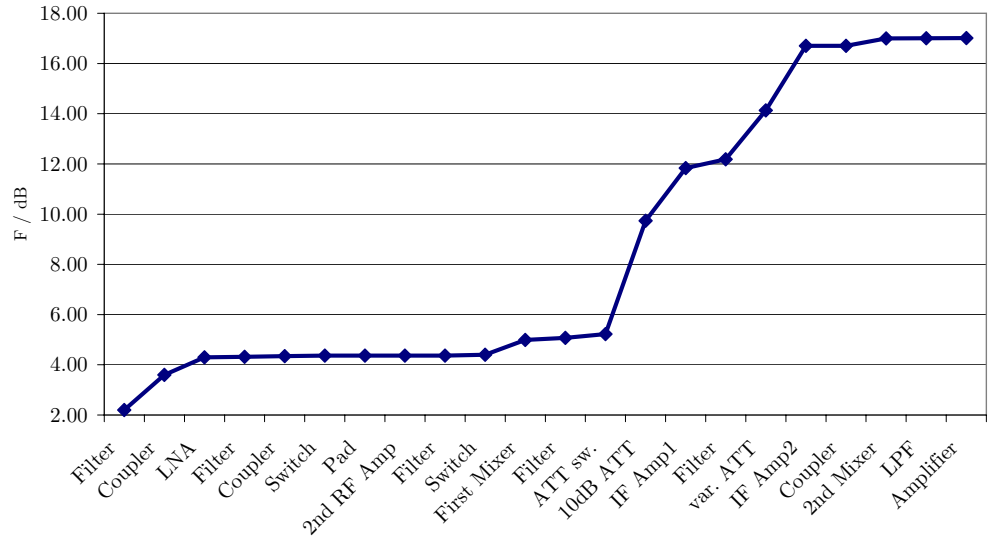

Figure 4.9: Receiver noise figure plan at low gain

The second column of Table 4.3 lists the equivalent carrier input power, which is the power of a leaking carrier signal that would produce the same level of output power when no carrier compensation would be used.

In Section 2.2.1 the maximum allowed carrier level to successfully receive the weakest expected RFID signals with a 14 bit ADC and 10 dB SNR was calculated to be −6.8 dBm. This value is was calculated without any active carrier compensation, so it is fully comparable to the equivalent input power used in Table 4.3. At this theoretical limit the receiver already operates on a noise figure slightly lower than the maximum allowed noise figure as calculated in Section 2.1.1.

To cut a long argument short the receiver designed in this diploma thesis constitutes no limit in receiving signals from any current passive RFID tag.

4.2.8 Circuit Board Layout

The receiver shares all construction details with the transmitter described in Section 3.2.7, including the PCB size, characteristics and microstrip design, so no details are given here.

Figure 4.12 shows the layout of the receiver board. The signal path on the receiver board is shaped like a lying “S”. The receiver input signal enters the board through the Antenna SMA connector right beside the sub-D connector. After passing the CCU coupler it is filtered and amplified and reaches the first mixer on the left lower edge of Figure 4.12. The IF signal passes a shielding plate and now moves up through attenuator, amplifier and filter stages towards the VGA, where it makes a right turn, passes a measurement coupler and enters the second mixer. Now it goes back down through the second IF filter module, solder jumpers and enters the last amplifier before it reaches the SMA output connector

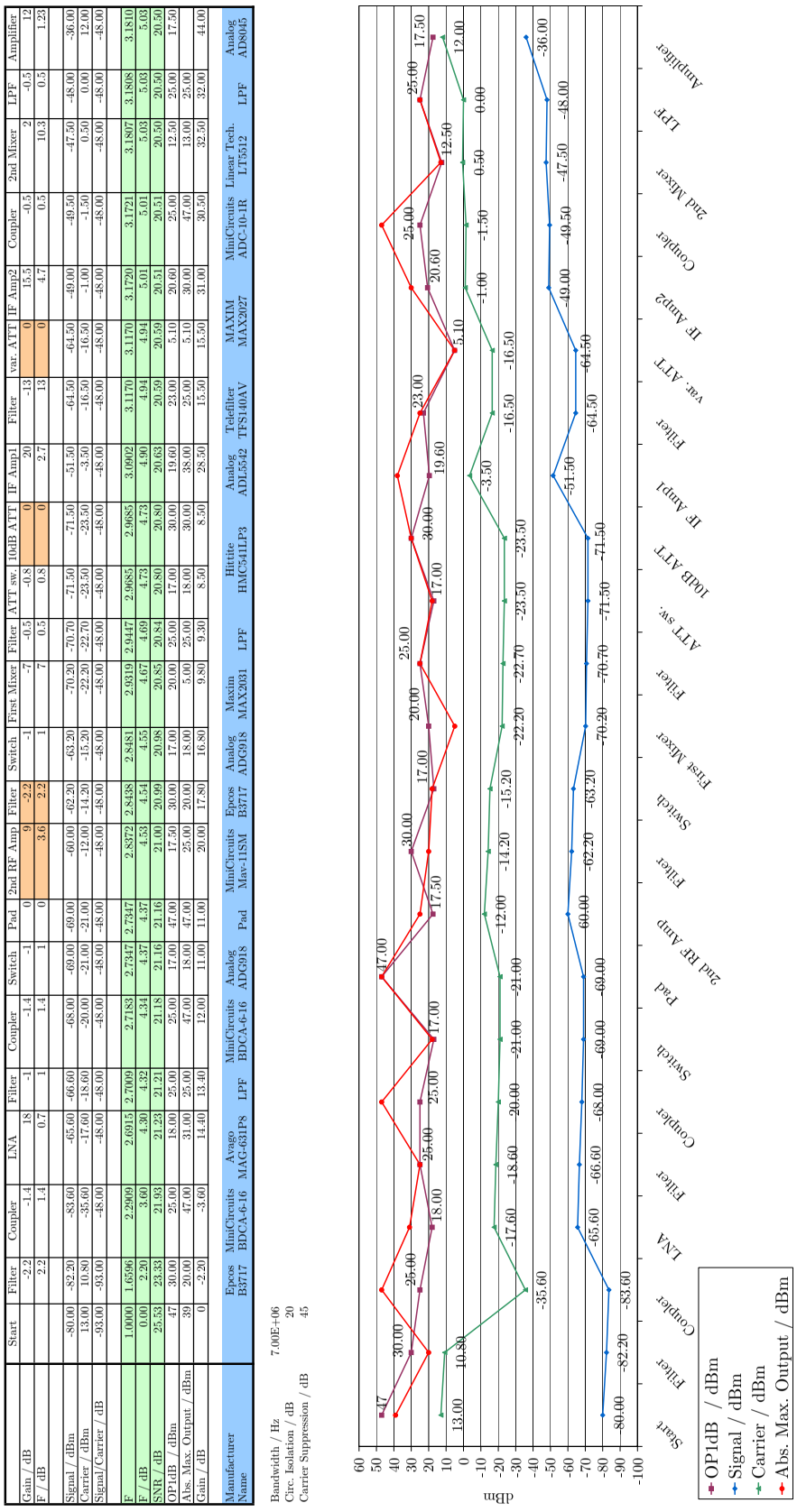

	Start	Filter	Coupler	LNA	Filter	Coupler	Switch	Pad	2nd RF Amp	Filter	Switch	First Mixer	Filter	ATT sw.	10dB ATT	IF Amp1	Filter	var. ATT	IF Amp2	Coupler	2nd Mixer	LPF	Amplifier
Gain / dB		-2.2	-1.4	18	-1	-1.4	-1	0	9	-2.2	-1	-7	-0.5	-0.8	0	20	-13	0	15.5	-0.5	2	-0.5	12
F / dB		2.2	1.4	0.7	1	1.4	1	0	3.6	2.2	1	7	0.5	0.8	0	2.7	13	0	4.7	0.5	10.3	0.5	1.23
Signal / dBm		-80.00	-82.20	-83.60	-65.60	-66.60	-68.00	-69.00	-69.00	-60.00	-62.20	-63.20	-70.20	-70.70	-71.50	-71.50	-51.50	-64.50	-64.50	-49.00	-49.50	-47.50	-48.00	-36.00
Carrier / dBm		13.00	10.80	-35.60	-17.60	-18.60	-20.00	-21.00	-21.00	-12.00	-14.20	-15.20	-22.20	-22.70	-23.50	-23.50	-3.50	-16.50	-16.50	-1.00	-1.50	0.50	0.00	12.00
Signal/Carrier / dB		-93.00	-93.00	-48.00	-48.00	-48.00	-48.00	-48.00	-48.00	-48.00	-48.00	-48.00	-48.00	-48.00	-48.00	-48.00	-48.00	-48.00	-48.00	-48.00	-48.00	-48.00	-48.00	-48.00
F		1.00000	1.6596	2.2909	2.6915	2.7009	2.7183	2.7347	2.7347	2.8372	2.8438	2.8481	2.9319	2.9447	2.9685	2.9685	3.0902	3.1170	3.1170	3.1720	3.1721	3.1807	3.1808	3.1810
F / dB		0.00	2.20	3.60	4.30	4.32	4.34	4.37	4.37	4.53	4.54	4.55	4.67	4.69	4.73	4.73	4.90	4.94	4.94	5.01	5.01	5.03	5.03	5.03
SNR / dB		25.53	23.33	21.93	21.23	21.21	21.18	21.16	21.16	21.00	20.99	20.98	20.85	20.84	20.80	20.80	20.63	20.59	20.59	20.51	20.51	20.50	20.50	20.50
OP1dB / dBm		47	30.00	25.00	18.00	25.00	25.00	17.00	47.00	17.50	30.00	17.00	20.00	25.00	17.00	30.00	19.60	23.00	5.10	20.60	25.00	12.50	25.00	17.50
Abs. Max. Output / dBm		39	20.00	47.00	31.00	25.00	47.00	18.00	47.00	25.00	20.00	18.00	5.00	25.00	18.00	30.00	38.00	25.00	5.10	30.00	47.00	13.00	25.00	
Gain / dB		0	-2.20	-3.60	14.40	13.40	12.00	11.00	11.00	20.00	17.80	16.80	9.80	9.30	8.50	8.50	28.50	15.50	15.50	31.00	30.50	32.50	32.00	44.00
Manufacturer		Epcos	MiniCircuits	Avago		MiniCircuits	Analog		MiniCircuits	Epcos	Analog	Maxim			Hittite		Analog	Telefilter	MAXIM		MiniCircuits	Linear Tech.		Analog
Name		B3717	BDCA-6-16	MAG-631P8	LPF	BDCA-6-16	ADG918	Pad	Mav-11SM	B3717	ADG918	MAX2031	LPF		HMC541LP3		ADL5542	TFS140AV	MAX2027		ADC-10-1R	LT5512	LPF	AD8045

Bandwidth / Hz 7.00E+06
Circ. Isolation / dB 20
Carrier Suppression / dB 45

(a)

(b)

Figure 4.10: Receiver power level plan at high gain

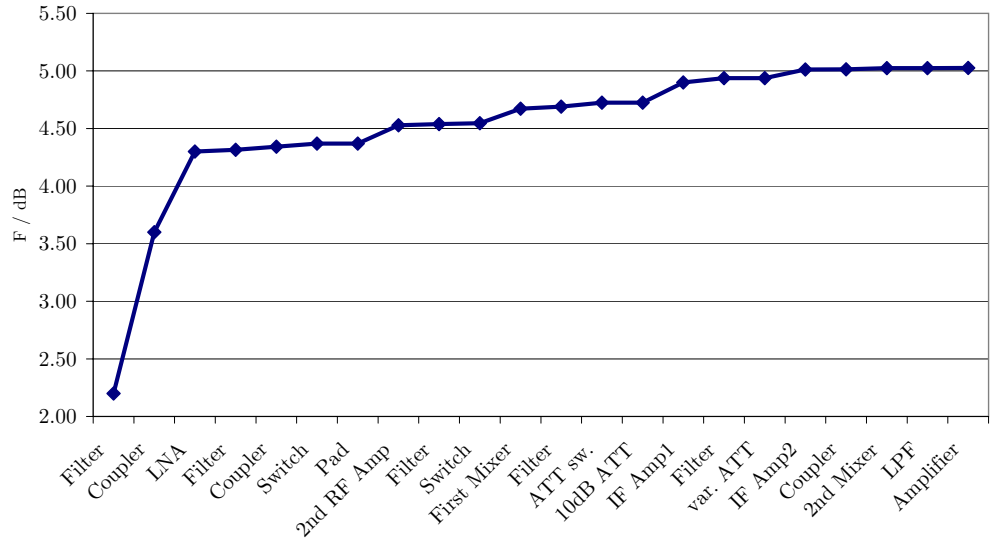

Figure 4.11: Receiver noise figure plan at high gain

on the right lower part of the receiver PCB board.

In the right lower part of the transmitter layout diagram the power and signal connectors for an optional add-on card can be seen. All components for manual control are grouped together right below the sub-D connector.

4.3 Measurements

4.3.1 Frequency Response

The measurement of the receiver frequency response was conducted using a very similar setup to the one described in Figure 3.16. The only difference is the slightly modified frequency range and the swapped frequencies of the ZVA ports 1 and 2, as indicated in Table 4.4, now port 1 acts as RF output and port 2 as an IF input.

Port	Use	Value	Unit
ZVA24 port 1	RF output	862.44 - 900	MHz
ZVA24 port 2	IF1 input	10 - 47.56	MHz
ZVA24 port 3	LO1 output	153.56	MHz
SMU200A	LO2 output	1006	MHz
SME06	VNA receiver cal. generator	10 - 47.56	MHz

Table 4.4: Receiver frequency response test equipment frequencies

Four different frequency response measurements are presented here: Figure 4.14 represents the receiver at the highest possible gain setting, while the RF amplifier

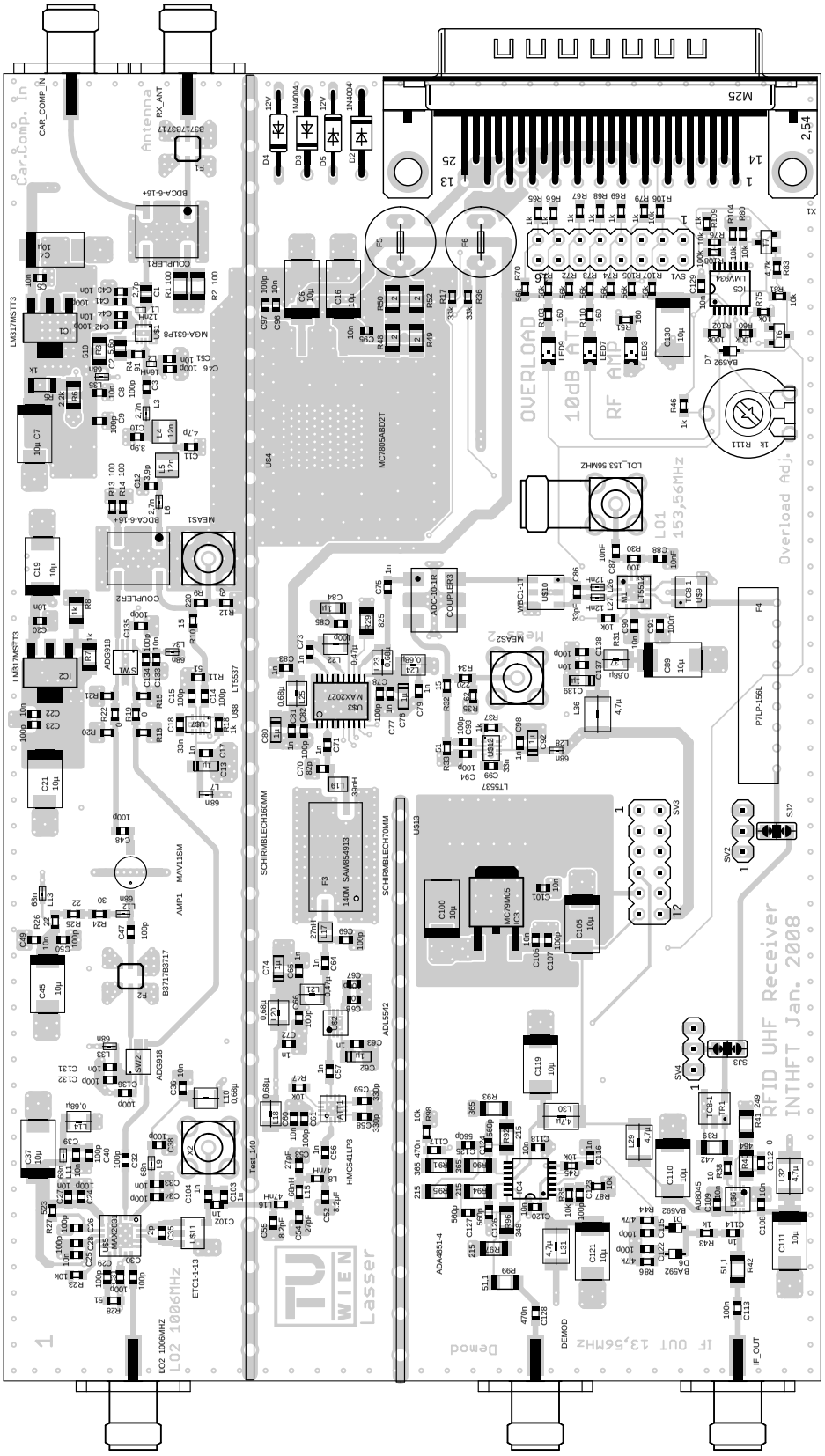

Figure 4.12: Receiver PCB layout

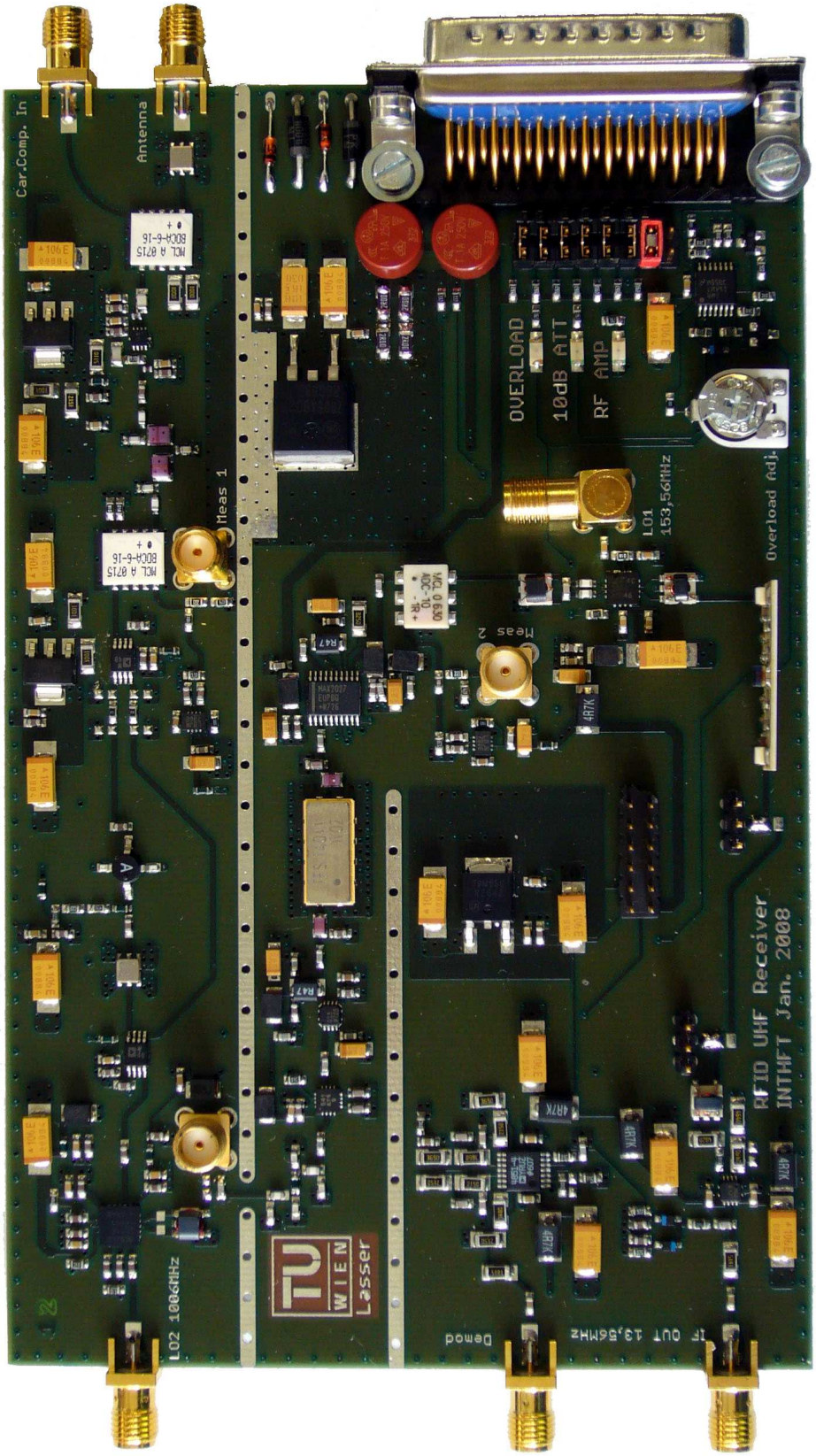

Figure 4.13: Receiver board

was switched off during the measurement of Figure 4.15. Figure 4.16 was measured with reduced gain by switching the attenuator on and finally Figure 4.17 was taken at lowest possible gain mode.

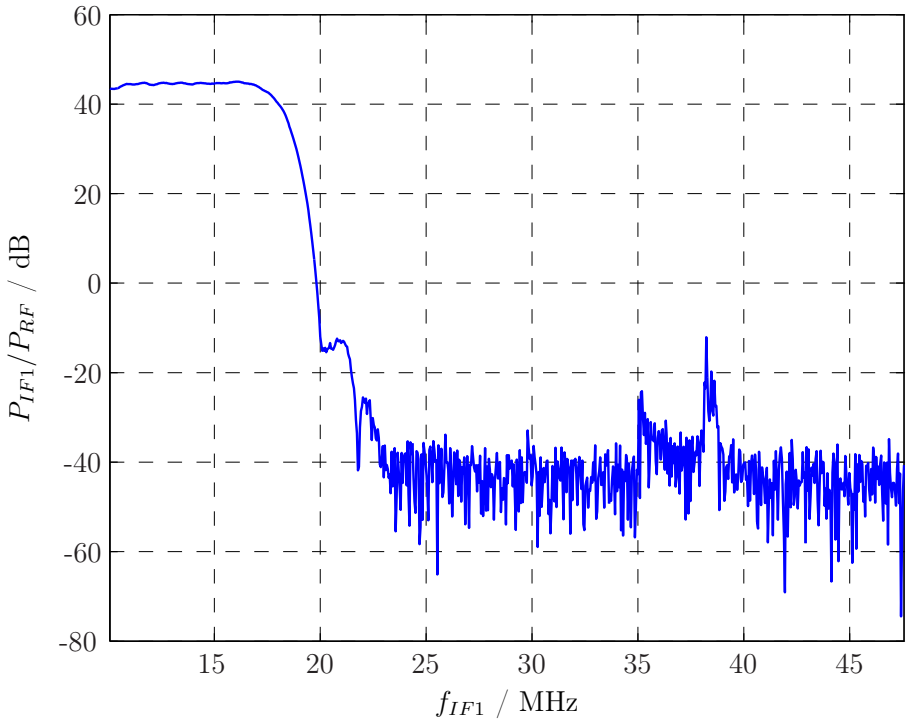

Figure 4.14: Receiver frequency response: full VGA gain, Att. off, RF amp. on

There is a spurious signal present on all measurements at about 35 - 38 MHz. In fact, the spurious signal proved to be present in the laboratory even when the receiver was switched off completely and could be detected using a spectrum analyzer and a short piece of wire as a probe antenna. It can also be noted that the amplitude of the spurious signal is the same for all four measurement plots regardless of the receiver gain setting. So it is clear that the cause of the spurious signals can only be found in the second receiver IF, called IF1. Otherwise, an RF signal mixed down by the receiver would have been affected by its gain setting.

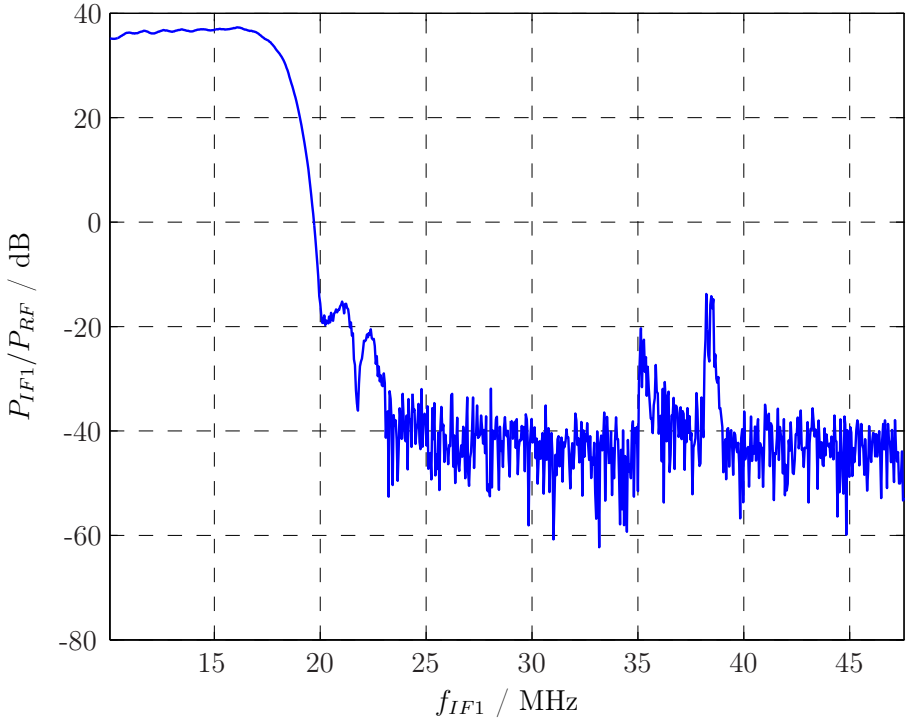

Figure 4.15: Receiver frequency response: full VGA gain, Att. off, RF amp. off

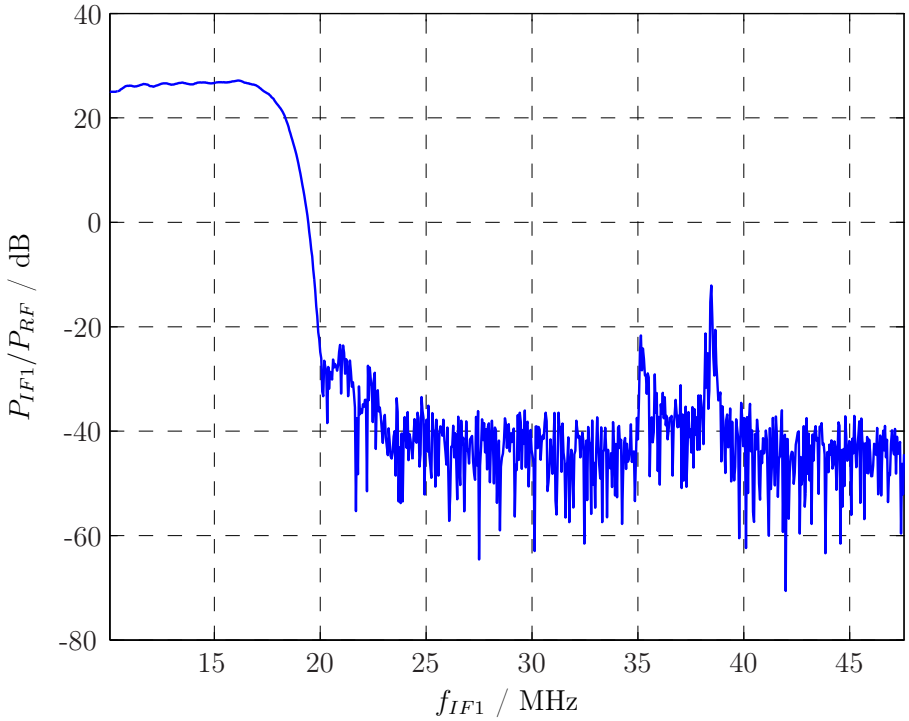

Figure 4.16: Receiver frequency response: full VGA gain, Att. on, RF amp. off

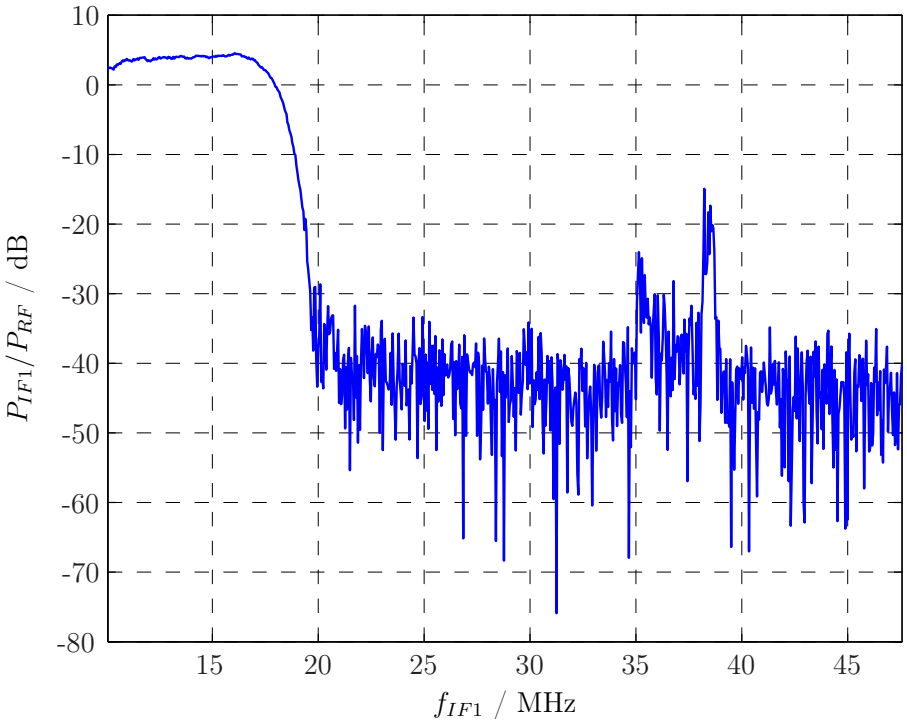

Figure 4.17: Receiver frequency response: min. VGA gain, Att. on, RF amp. off

4.3.2 Powersweep

The powersweep conducted with the receiver was carried out using the same measurement setup as described before for the frequency response. An RF test frequency of 866 MHz has been used. Two tests were carried out, one at full receiver gain, represented in Figure 4.18 and one at minimum gain, shown in Figure 4.19.

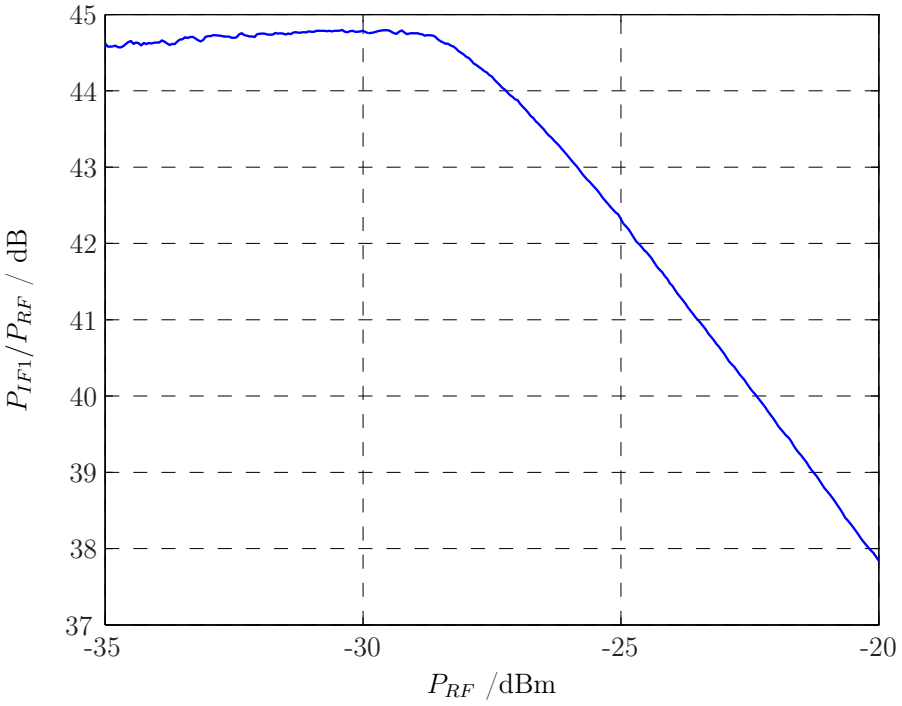

Figure 4.18: Receiver powersweep: max. VGA gain, Att. off, RF amp. on

When the two graphs are compared, they show totally different behavior of the receiver at different gain settings. This effect can be explained by inspecting the level plan and keeping in mind that the last receiver amplifier is an operational amplifier.

At high receiver gains two stages are first affected by too high input power levels: The second mixer and, even more seriously, the op-amp presenting the last stage. Unlike the other conventional stages, the output of the op-amp follows the amplifiers input even at higher degrees of modulation, because the non-linearities are canceled by the effects of negative feedback that set the op-amp's gain, as long as the closed loop gain is high enough.

But if the input power is pushed too high the output is limited by the maximum possible output swing depending on the op-amp's supply voltage. This effect can be observed on Figure 4.18. Above a critical point, at about -29 dBm input power, the gain drops almost linear. Between -25 dBm and -20 dBm the receiver gain degrades 4.5 dB. The reason for not dropping full 5 dB is the clipping of the

output signal, that more and more becomes a square wave, which has a higher fundamental component amplitude than a sinewave with the same amplitude.

The situation is totally different in the low gain case. The first components to be driven into saturation in this case are the LNA, the second RF amp switches and the first IF amplifier, the $P_{1\text{dB}}$[5] of all three of them are within a range of 4.3 dB. This leads to a slowly (note the scaling) dropping graph depicted in Figure 4.19. Between −1 dBm and 3 dBm input power the gain only drops 1.4 dB. However the slope is permanently increasing and not constant as in the high gain case.

The spike at −5 dBm is the result of an unrepeatable offset in a switching process in the VNA or the associated calibration generator.

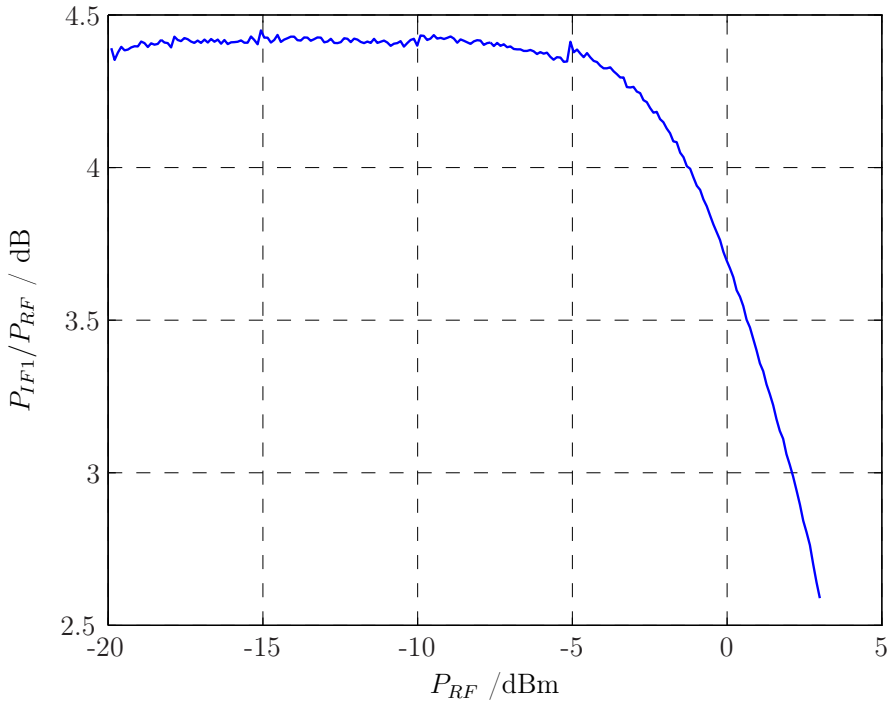

Figure 4.19: Receiver powersweep: min. VGA gain, Att. on, RF amp. off

[5] 1 dB Compression Point

Chapter 5

Carrier Compensation Unit – CCU

This chapter describes the carrier compensation unit, which is responsible for providing a well matched compensation signal with regards to phase and amplitude. The functionality of the CCU is essential for proper RFID testbed operation.

5.1 Concept

In contrast to the transmitter and receiver modules the carrier compensation unit has been designed not only to operate in the RFID testbed, but also as a testprint to validate the possibilities of carrier compensation. Therefore, the CCU module also contains a directional coupler to inject test signals and to observe the combined output.

5.1.1 Mechanical Concept

Unlike receiver and transmitter the CCU was primarily intended as a test print so no provisions for housing have been made. The CCU is placed on a double-sided PCB. For the RF connections again SMA connectors are used. Power is supplied to the board using copper braid cables soldered to the PCB.

5.1.2 CCU Power Levels

The maximum input power for linear operation is -1 dBm. However, higher input levels up to 13 dBm are possible when compression is accepted.

In linear operation mode the gain of the CCU can be controlled between -12 dB and 18 dB. It follows that 17 dBm output power can be reached under linear conditions. Usually, the CCU was operated at a maximum output level of 20 dBm to enable the cancelation of higher leaking carrier input signals. As long as second order intermodulation products do not block the receiver, intermodulation is not an issue here because during reception the CCU only operates on unmodulated carrier signals.

5.2 Realisation

5.2.1 Circuit Description

The CCU mainly consists of two parts: A vector modulator IC and a medium power output amplifier. The CCUs schematic is drawn in Figure 5.1.

The vector modulator functionality is provided by an IC from Analog Devices, the AD8340. This IC splits up the input signal in an inphase and a quadrature component with an integrated polyphase network and provides separate balanced variable gain attenuators for the I and Q channel. These internal balanced attenuators also allow to change the corresponding channel's polarity, so that a true 360° phase shift can be obtained [18]. An integrated amplifier sums up the I and Q channel and provides a differential output.

The CCU input signal from the transmitter is connected to the COMP_INPUT connector. The vector modulator IC has a differential input, but can be used single-endedly as it is done here. C12 and C13 are coupling capacitors, L1 and L2 improve input matching.

The output pins are connected to the collectors of the output transistors and require an external DC path to the 5 V supply rail. This path is realized with inductors L3 and L4. The differential output is converted back to an asymmetric output with an ETC1-1-13 transformer.

The vector modulator IC is controlled by two symmetrical baseband input line pairs, IBBM and IBBP to set the gain of the inphase channel and QBBM and QBBP for the quadrature channel. Operational amplifiers are used to convert a single drive signal in the range of 0 - 1 V to a differential signal with 0.5 V maximum deflection that is biased at 0.5 V. R8 and R16 set the reference voltages for the I and Q channels and can be used to adjust the minimum gain point of both channels to exactly 0.5 V input voltage at V_IBB and V_QBB. Instead of using external control voltages it is also possible to set the vector modulators state with the local variable resistors R18 and R20, when the jumpers JP1 and JP2 are set.

The vector modulator offers high speed control up to 200 MHz that is not necessary for this application, so C1 and C2 are used to reduce the cut-off frequency of the internal control circuitry to about 4.5 kHz to suppress phase noise.

Between the vector modulator and the amplifier capacitors C5, C28 and C34 enable to route the output of the vector modulator to test point TESTLOOP1 or use this point as a source for the amplifier. The amplifier is realized with an ADL5322 that is also used at the transmitter's last stage, see Section 3.2.3. The reasons for using this amplifier are the low noise figure of 5 dB and the high output 1 dB compression point of 27 dBm, so the suppression of high power direct coupled carrier components is possible.

When the CCU is used in context with the UHF frontend, C35 is used to couple the amplifiers output signal to the TESTLOOP2 connector for insertion at the receiver. To explore the possibilities of active carrier compensation, the

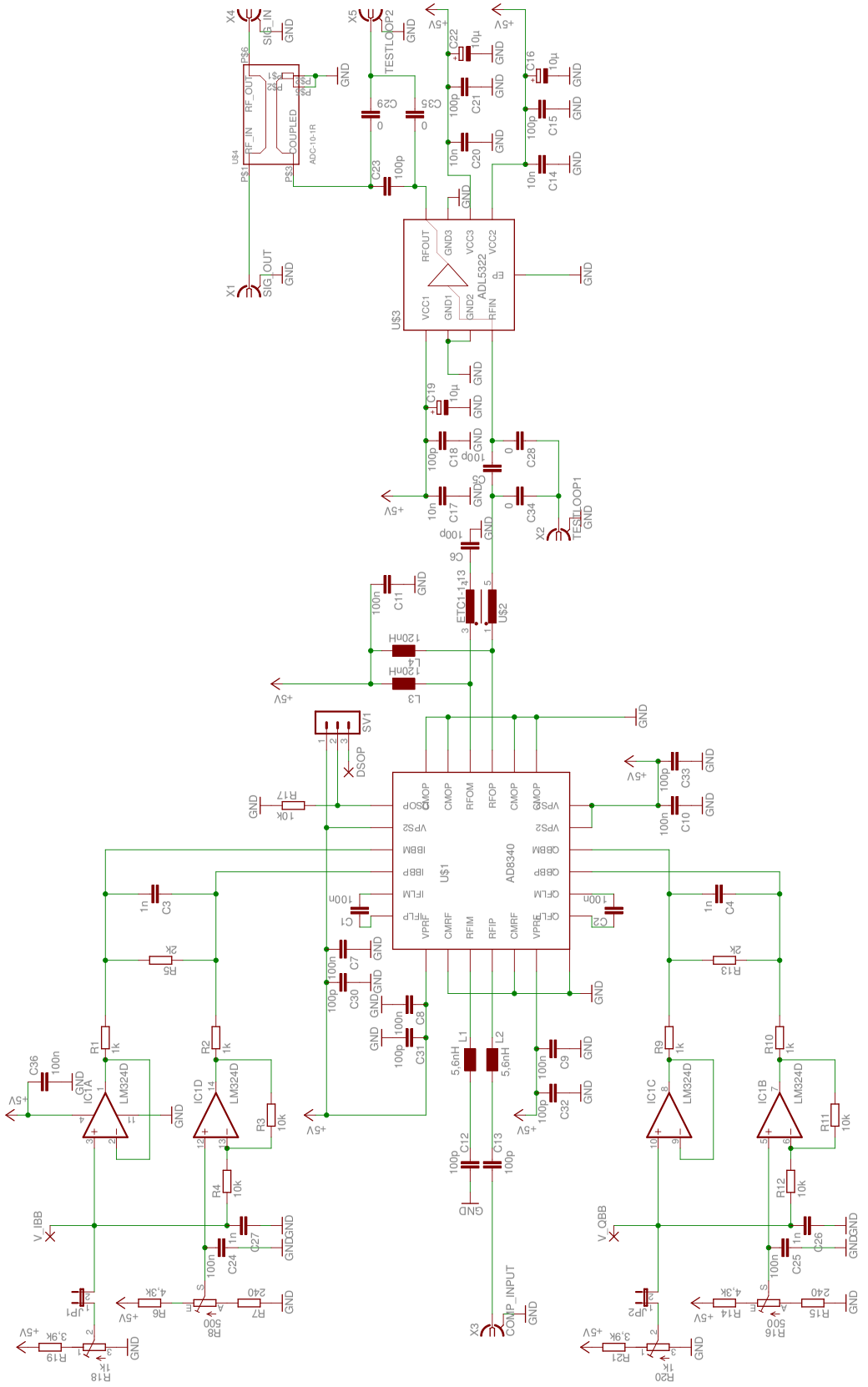

Figure 5.1: CCU schematic

amplifier's output is routed through C23 to an ADC-10-1R directional coupler with 10 dB coupling loss. Here the amplifier's output is merged with the signal being applied at the SIG_IN connector. The resulting output signal can be picked up for observation at the SIG_OUT jack.

Both RF-ICs and the op-amps operate on a common 5 V supply line. For proper operation a stable voltage source must be provided to supply this line.

5.2.2 Circuit Board Layout

Standard FR4 material of reduced thickness was used to lower the width of 50 Ω microstrip lines, as summarized in Table 5.1.

Parameter		Value	Unit
Relative permittivity	ε_r	4.7	
Dielectric loss	$\tan\delta$	0.014	
Height	h	0.8	mm
Copper plating thickness	d	35	µm
50 Ω microstrip line width for 866 MHz	w	1.421	mm

Table 5.1: Properties of FR4 PCB material used at the CCU (typical values)

The upper part of the PCB is covered with the op-amp level converter and the manual control elements, as can be seen in Figure 5.2. The RF part is situated at the lower half of the CCU board, and the PCB's lower edge is covered with RF connectors and power supply soldering pads. The assembled CCU board is depicted in Figure 5.3.

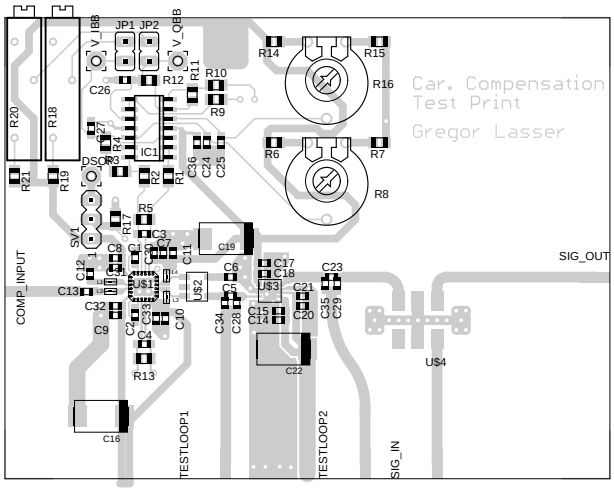

Figure 5.2: CCU PCB layout

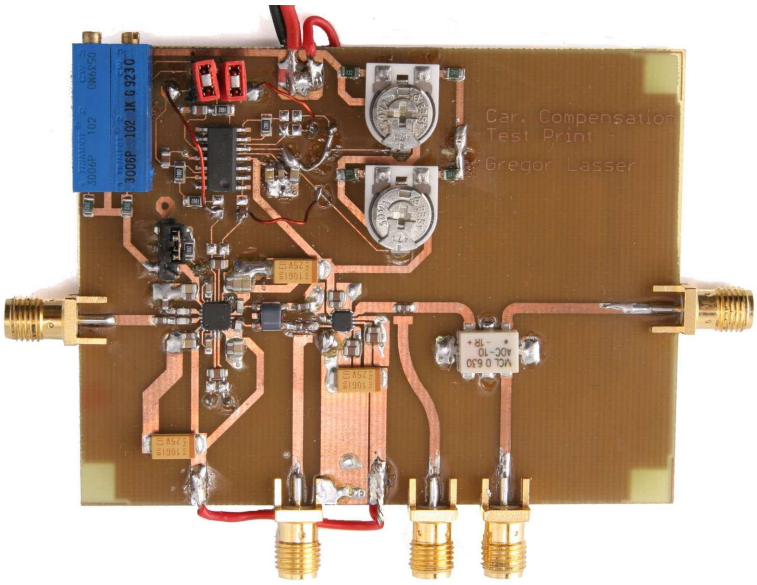

Figure 5.3: CCU board

5.3 Measurements

Two measurement series were carried out to characterize the CCU. In the first one, presented in the following two subsections, a VNA was used to verify the carrier suppression capabilities of the CCU and take its phase response. In the second one the CCU's noise suppression performance was analyzed.

5.3.1 Carrier Suppression

To measure the realizable suppression ratio the following test setup was used. The vector network analyzer available provides direct access to the source ports of the internal measurement coupler. This access was used to insert a directional coupler with 10 dB coupling loss to provide a reference signal for the CCU's COMP_INPUT port. To compensate for the coupling losses an attenuator of equal loss was inserted in the source path. The SIG_IN and SIG_OUT connectors were now conventionally connected to the ports 1 and 2 respectively. This setup is graphically presented in Figure 5.4.

The VNA was calibrated using a regular SOLT[1] method, but taking the SIG_IN–SIG_OUT path of the deactivated CCU as "Thru".

Figure 5.5 and Figure 5.6 represent two representative results from a long series of measurements conducted. The CCUs trimmer resistors R18 and R20 were adjusted for maximum suppression at about 866 MHz. At both measurements a suppression ratio of about 50 dB was accomplished. Top values of 70 dB suppression have been reached.

[1] Short, Open, Load, Thru (calibration method)

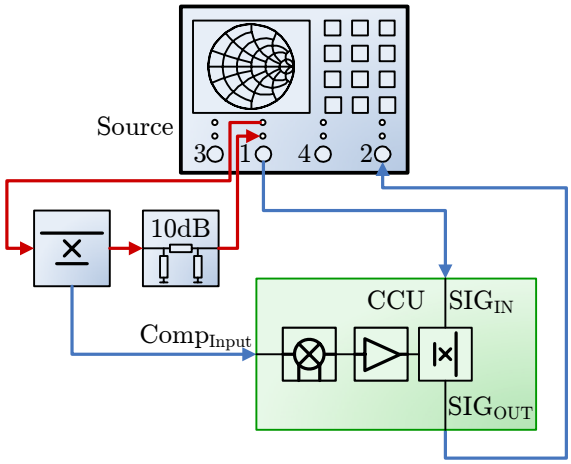

Figure 5.4: CCU suppression measurement setup

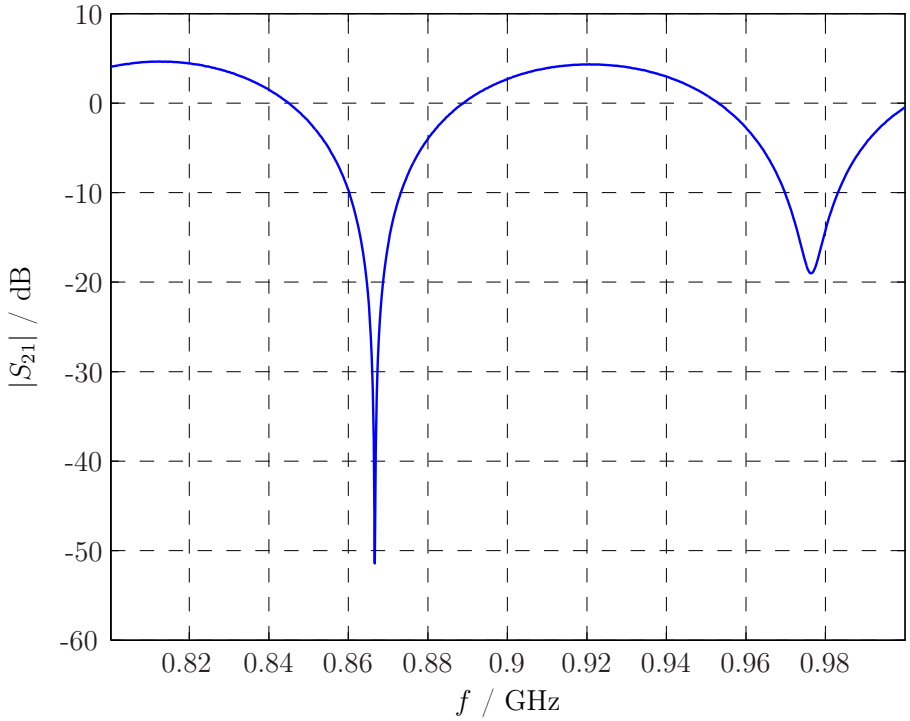

Figure 5.5: CCU suppression measurement with poor compensation path delay match.

A noticeable difference between Figure 5.5 and Figure 5.6 is the suppression bandwidth provided. The reason for this behavior lies in the different compensation path cable lengths used for these experiments.

To suppress a single frequency, the suppression signal needs to be exactly 180° out of phase to the signal to be suppressed. For broad-band signals this condition can only be established if the transit times of the regular and the

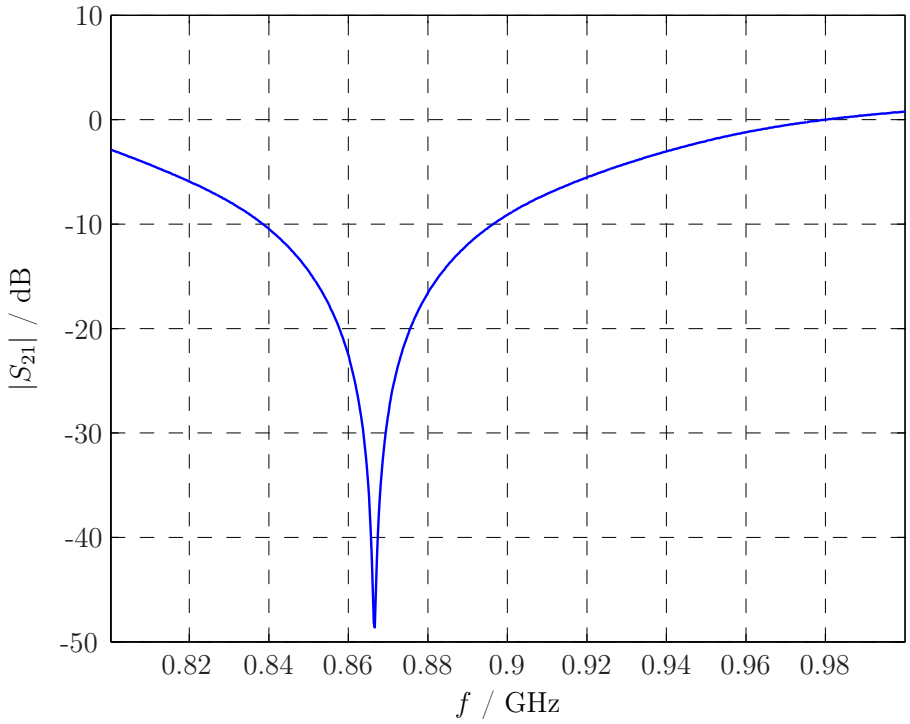

Figure 5.6: CCU suppression measurement with good compensation path delay match.

compensation path are equal. The phase measurement of the CCU described in the next subsection (Figure 5.7) revealed, that the CCU's phase response is very linear over a wide frequency range. Therefore the CCU is not really a limiting factor for broad-band suppression performance. To achieve high suppression ratios over larger bandwidth intervals the cable lengths have to be matched to ensure equal delay in the main and the suppression path.

The 20 dB suppression bandwidth achieved were 18 MHz in the case of Figure 5.6 and 4 MHz in Figure 5.5. During the test series even larger suppression bandwidths could be achieved.

5.3.2 Phase Error

To explore the possibilities of broad-band compensation, the relative phase error of the CCU was measured. Figure 5.7 represents the phase offset relative to 866 MHz measured from the COMP_INPUT to the SIG_OUT port. When observed over a frequency range from 800 to 1000 MHz the phase error is smaller than 3.5°. Over the UHF RFID band the phase error is almost negligible. This is also true when other output phase settings are observed, as long as the signal amplitude does not get to small.

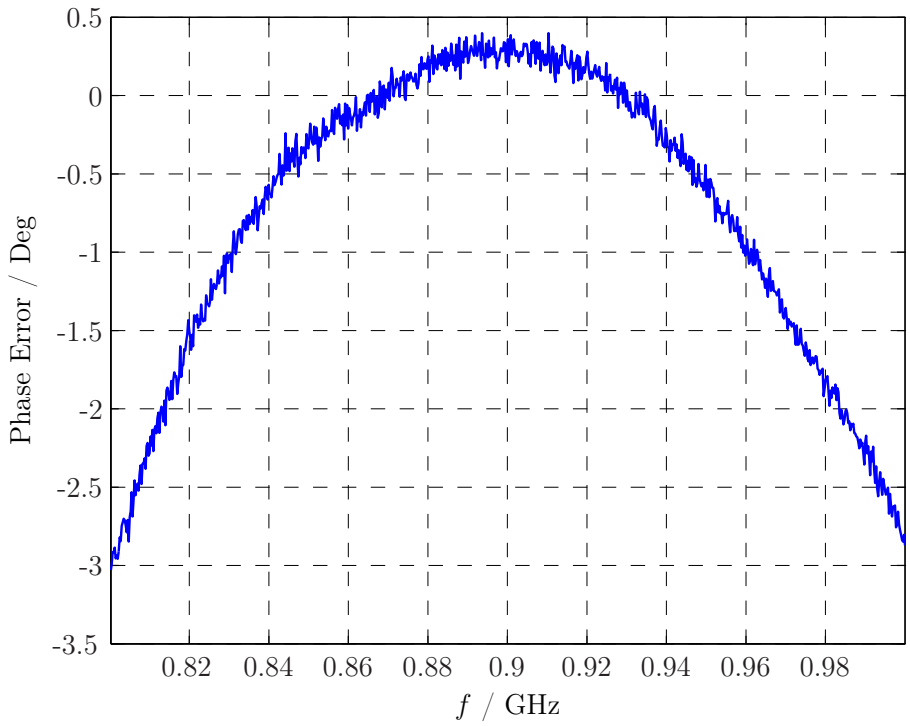

Figure 5.7: CCU phase error

5.3.3 Broad-band Noise Suppression

One might suggest that broad-band suppression is irrelevant for RFID systems, because only a sinusoidal carrier component is present during reception. However, when the noise floor is also taken into account, this is not the case.

The transmitter not only produces a clear carrier signal but also noise. This noise is not only a product of the transmitter itself, but the first IF signal leaving the rapid prototyping board is noisy, too.

When only the carrier is being suppressed by the CCU, the transmit signals noise components increase the receiver input noise floor. With a CCU optimized for broad-band suppression, transmitter noise components are reduced, too.

To verify these suppression properties, the following measurements were carried out. Figure 5.8 presents the setup used to conduct these tests. As signal source

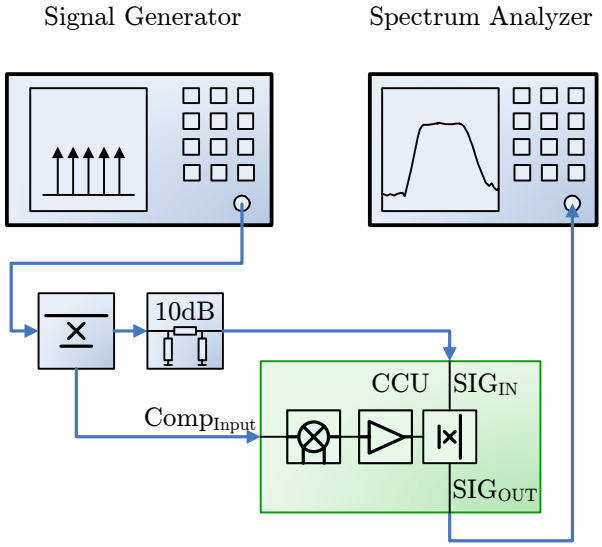

Figure 5.8: CCU broad-band noise measurement setup

a vector signal generator has been utilized. It was set to generate a broad-band noise signal. The generator output was again split up using a directional coupler and an attenuator as indicated in Figure 5.8. The output of the CCU coupler was observed with a spectrum analyzer.

Figure 5.9 presents the results of the measurement. The first blue trace is for reference only, it shows the spectral shape of the noise signal. To obtain a smooth curve averaging has been used on this and all other measurements of this series.

The red graph represents a well aligned CCU, with perfectly matched cable lengths and 50 dB of suppression between 862 and 868 MHz. The lowest suppression ratio in the whole frequency range is 36.6 dB.

In contrast to this result the green curve represents the same measurement setup except that the signal generator–COMP_INPUT port path was physically

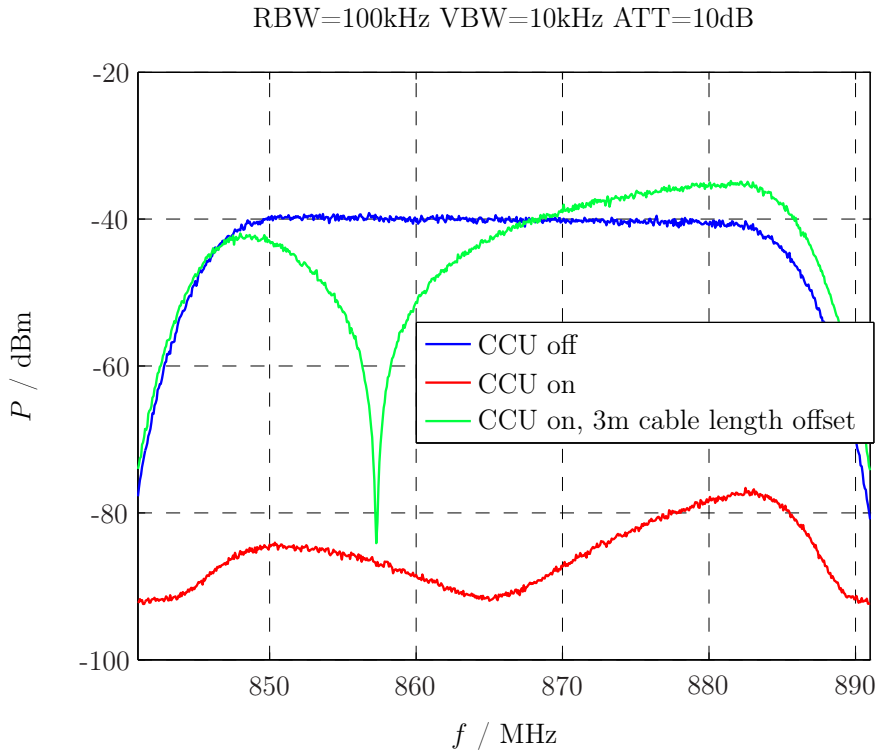

Figure 5.9: CCU noise suppression test

extended by 3 m of coaxial cable. At frequencies above 870 MHz even constructive interference takes place and the green curve raises above the blue one.

Chapter 6

Experiment

To proof the functionality of the UHF RFID frontend the test setup depicted in Figure 6.1 was used.

A VSG[1] acts as signal source for the transmitter, it was set to produce a query command fully compliant to the EPCglobal standard [19]. The query command was generated in MATLAB using the parameters as indicated in Table 6.1. The baseband sequence calculated in MATLAB was then sent to the VSG, a SMU200A from Rhode&Schwarz, to generate the modulated RF output at 13.56 MHz according to this data.

Name	Value	Unit
Delimiter	17	µs
Tari	12.5	µs
Pulsewidth	0.265	
Lengthone	1.75	
RTcal	2.75	
TRcal	2	
Moddepth	0.9	
Leadin	2	ms
Leadout	1	ms
Pause	4	ms

Table 6.1: EPCglobal standard parameters used for the experiment

For the tag to reader communication FM0 baseband signaling was requested in the query command. The Leadin and Leadout parameters specified in Table 6.1 correspond to the duration of the pure carrier transmitted before and after the query command. This Leadin–Query–Leadout sequence was followed by a pause of 4 ms to reset the tag and enable continuous observation of its response. This is necessary, because after the tag detects a query command it sends back a pseudorandom number called RN16, and is waiting for an acknowledge message containing this number. If the tag does not receive this acknowledging signal it will remain silent [19, p. 35].

[1] Vector Signal Generator

The IF1 signal from the VSG is amplified and upconverted to UHF frequencies by the transmitter. The external local oscillator generators were set for a resulting center frequency of 866 MHz. The output of the transmitter is now amplified by an external power amplifier module. For that purpose a ZHL-2-12 from Mini-Circuits has been used. The specification parameters of this amplifier can be found in Table 6.2. Although the amplifiers 1 dB compression point $P_{1\text{dB}}$ is rated to be 29 dBm, an output power of 33 dB is easily accomplished under slight compression.

Parameter	Value	Unit
f_{min}	10	MHz
f_{max}	1.2	GHz
min. Gain	24	dB
$P_{1\text{dB}}$	29	dBm
$P_{IN_{MAX}}$	10	dBm
F	4	dB

Table 6.2: Mini-Circuits ZHL-2-12 amplifier specification

The transmit and receive signals are combined in a circulator from Raditek. This device provides 25 dB of isolation. Between the circulator and the antenna a directional coupler and a tuner was placed.

The directional coupler and the 20 dB attenuator attached to it are drawn white in Figure 6.1 to illustrate that these components are not directly necessary for testbed operation, but were inserted to measure the power during transmit time periods. To achieve this, trigger pulses are generated by the VSG which are used to gate the powermeter connected to the 20 dB attenuator. The powermeter gate was chosen to measure the carrier power during leadin to give a true peak power reading. The pulses generated at the VSG are also used to trigger an oscilloscope for tag message observation.

The tuner mentioned above, a SF-11N from Microlab/FXR, was necessary to improve the antenna's return loss. A circular polarized SAA06-290010 patch antenna from SmartAnt with 8 dBi gain and 14 dB return loss was used [20].

The tags are linear polarized, so 3 dB are lost due to polarization mismatch with the antenna. When this loss and the cable and circulator losses are taken into account 33 dBm are needed at the measurement coupler to reach 33 dBm ERP at the testbed's antenna.

Before the actual measurements had been conducted the measurement setup was adjusted: First the gain of the transmitter had been reduced and the VSG, transmitter, receiver and power amplifier were turned on. Then the tuner was adjusted for minimum receiver input power. In a second step the output power was increased and the tuner was again adjusted, followed by alignment of the CCU. The last step was to further increase the output power up to 33 dBm as

observed on the power meter.

After setting up the testbed a commercially available RFID tag, a Rafsec G2, was placed in the antenna field. The tag was fixed to a wooden ladder which was moved backward to increase reader–tag distance, while the readers antenna, which had been mounted on a wooden mast, remained on a constant position. This experiment was carried out at the fifth floor corridor of our institute, as depicted in Figure 6.2.

This picture shows the ladder and the tag at the maximum distance where a tag answer could be observed: 11.4 m. It should be noted that this relatively long reading range was likely based on reflections at the corridor walls. It is clear that serious tag sensitivity measurements should be taken out in a suitable absorber room, but the tenor of these measurements was to verify the testbed's functionality and not to measure the tag.

The received signals corresponding to this setup are drawn in Figure 6.3. The CCU was slightly readjusted to increase the receiver output and overcome the threshold of the envelope detector.[2]

The upper yellow trace of Figure 6.3 represents the IF1 receiver output. The left part of the trace shows the effect of the last bits of the query command: The mismatched CCU cable length but also the cable between tuner and antenna prohibit proper suppression of the modulated leaking carrier signal. Here this signal is suppressed with a delayed inverse copy which results in big spikes at the beginning and end of each keyed signal period. These spikes appear at the left part of both traces.

The lower trace results from the envelope detector output being displayed at the oscilloscope. In contrast to the IF1 output signal the backscattered signal can be clearly spotted in the middle of the graph.

[2]In a receiver redesign positive bias for the detector diodes could be considered to increase detector sensitivity.

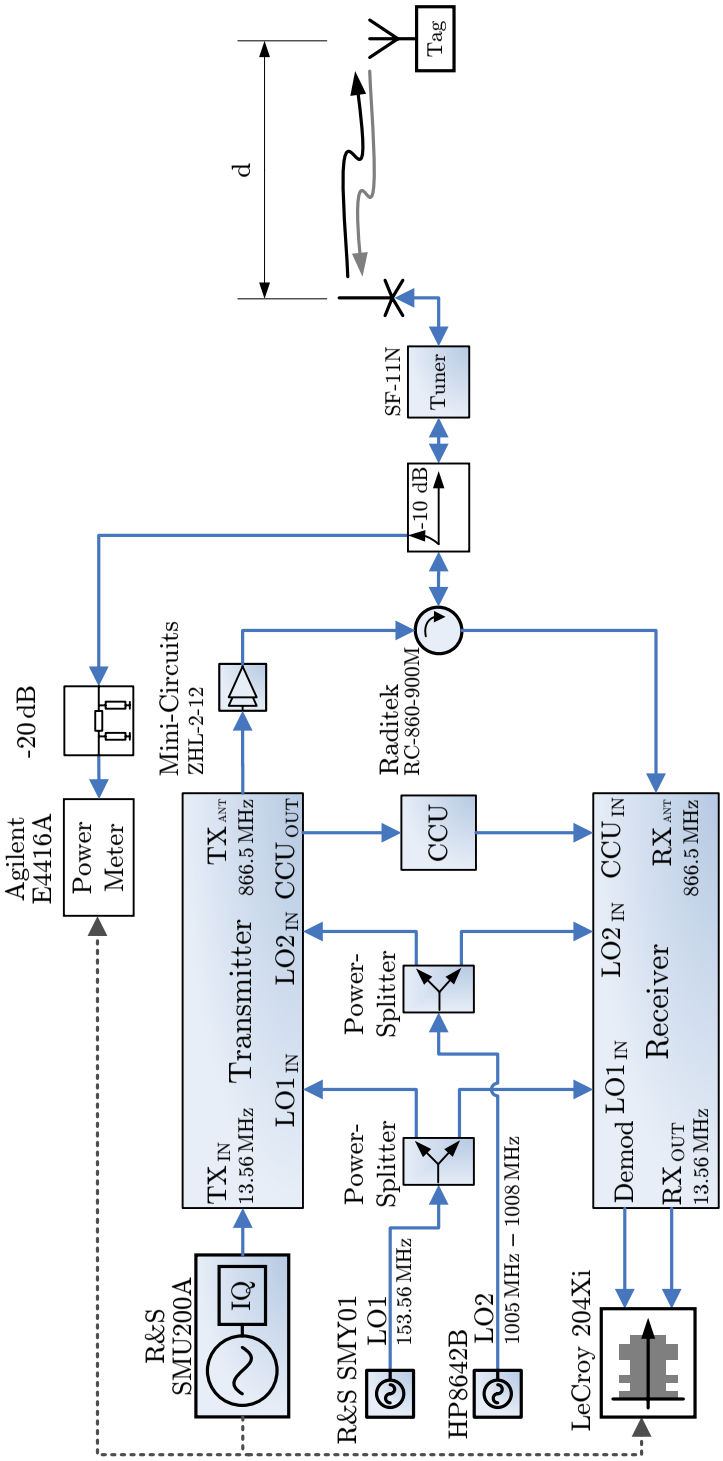

Figure 6.1: Experiment Setup

Figure 6.2: Fifth floor corridor with experiment setup

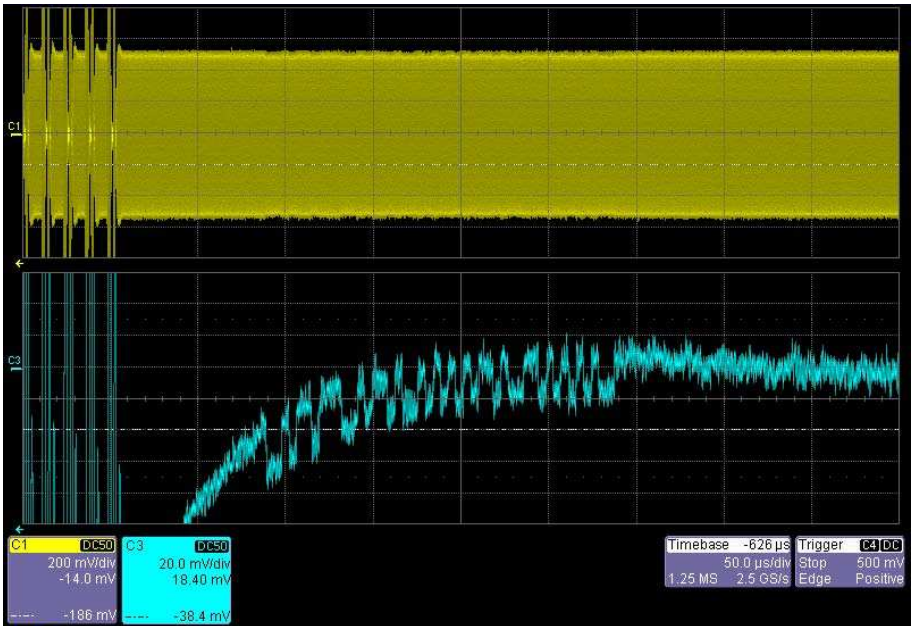

Figure 6.3: Received tag answer at 11.4 m read distance

Chapter 7

Conclusion

In this diploma thesis I described the frontend design of an extremely flexible UHF RFID testbed. The system concept developed incorporates an already existent digital baseband board, transmitter, receiver, CCU, power amplifier, antennas, a circulator, signal generators and power splitters.

While the latter components were acquired from RF manufacturers, I have developed transmitter, receiver and CCU from scratch. Critical components were tested on separate testprints, the layouts of the main modules were engineered and the externally manufactured printed circuit boards were equipped with components. The assembled receiver, transmitter and CCU modules were again tested to characterize their most important parameters and to verify that the key design criterions were met.

Finally, I built up the RFID testbed from the components acquired and developed before and carried out an experiment to illustrate the frontend's capabilities.

In the first part of this thesis some specific fundamentals relevant to RFID were described. With some feasible assumptions the theoretical limits of current passive RFID systems in general and this testbed in particular were calculated. It was shown that by design this testbed frontend enables measurements up to these theoretical limits.

The UHF testbed frontend designed in this diploma thesis has not only been described here but was also presented on a conference [21].

Appendix A

Schematics

On the following pages the full schematics of transmitter, receiver and CCU are listed.

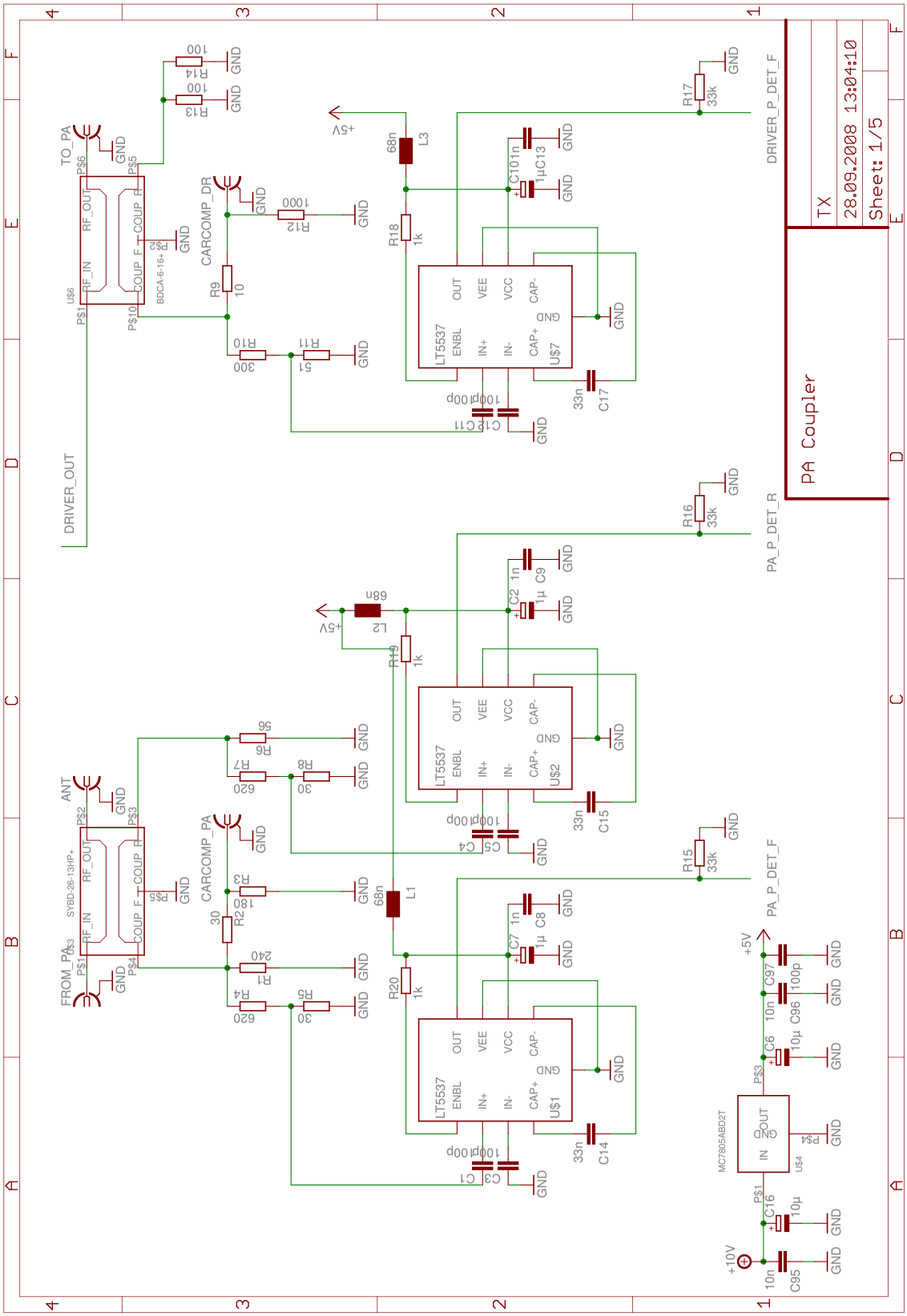

Figure A.1: Transmitter schematic 1/5

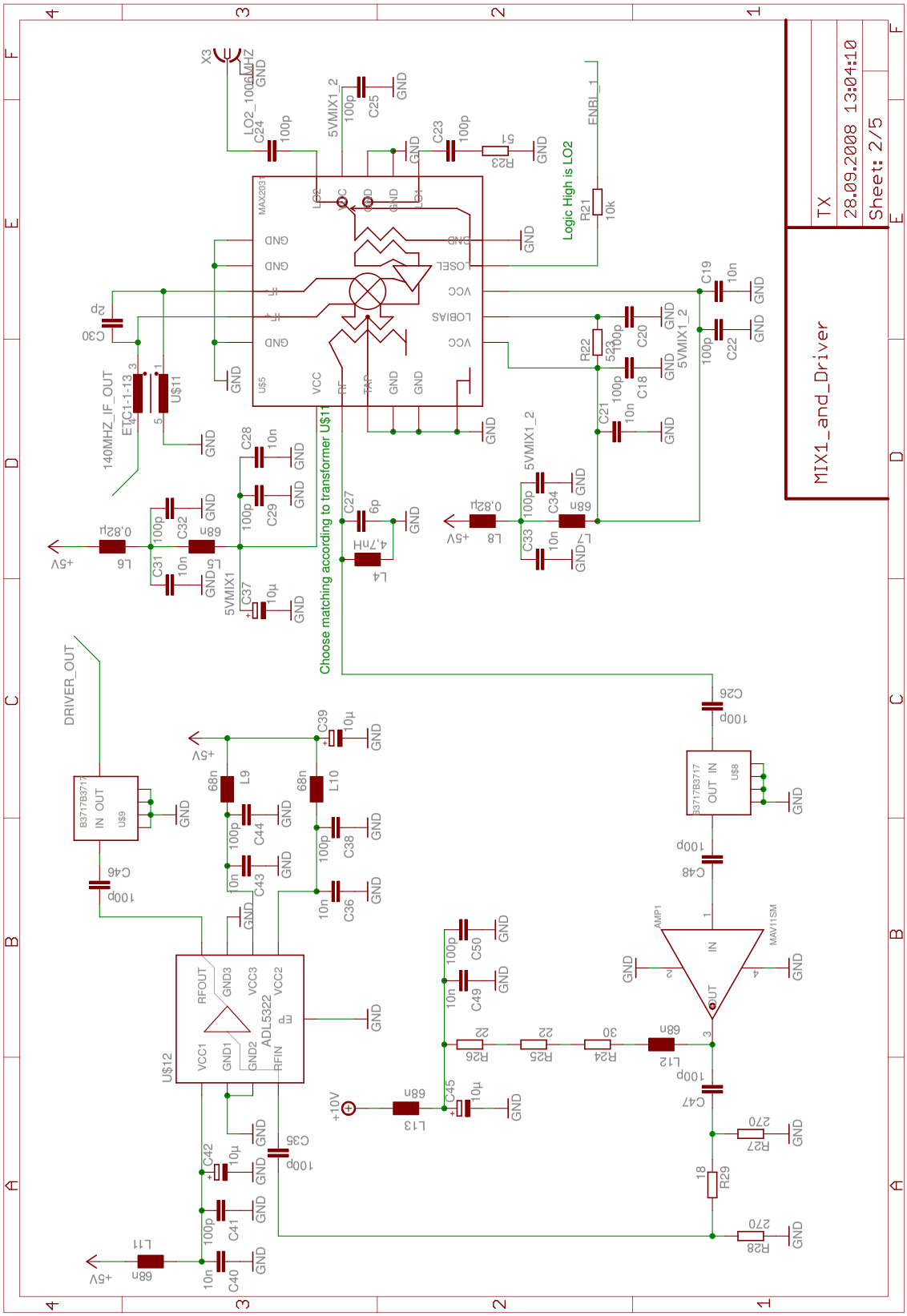

Figure A.2: Transmitter schematic 2/5

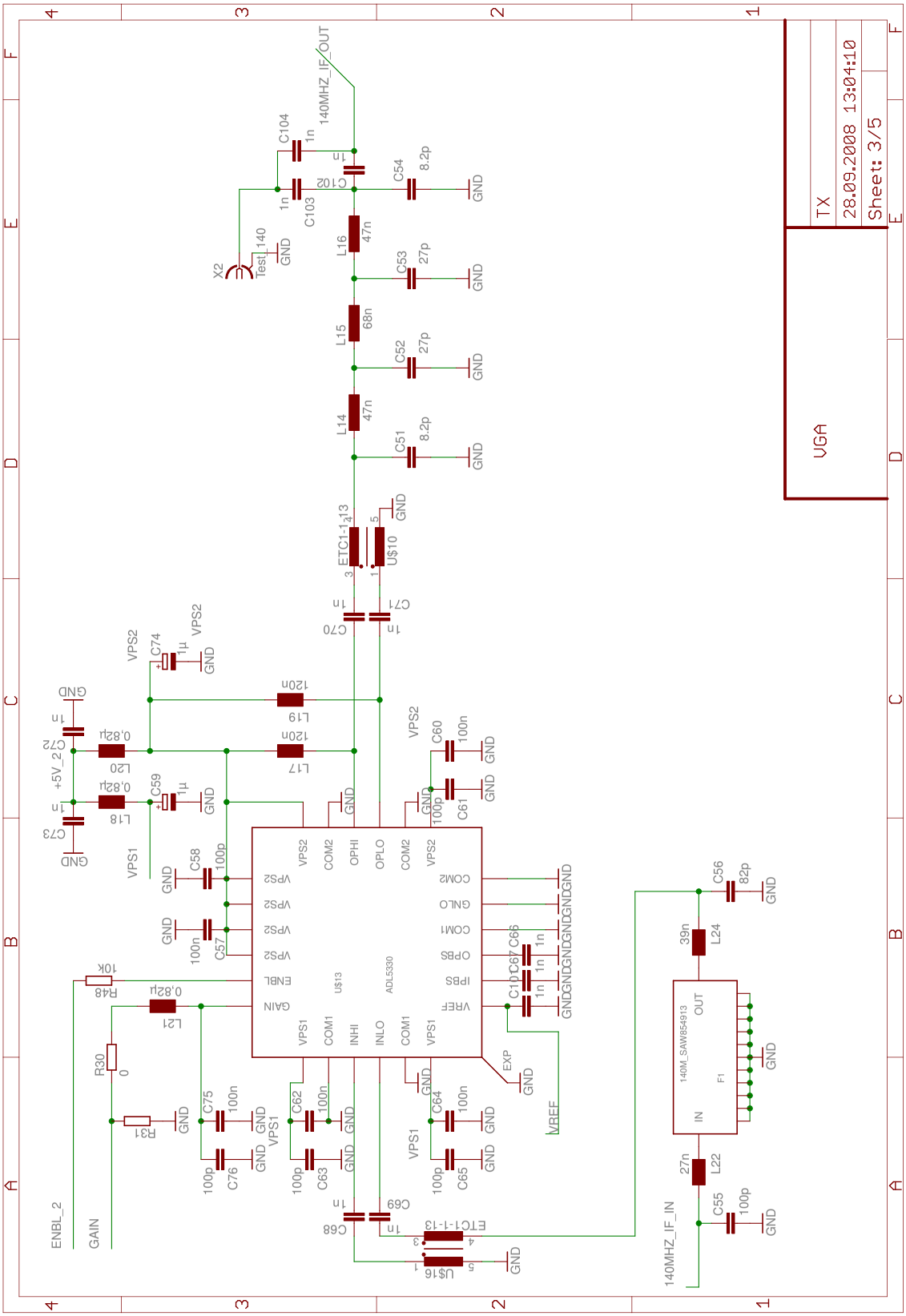

Figure A.3: Transmitter schematic 3/5

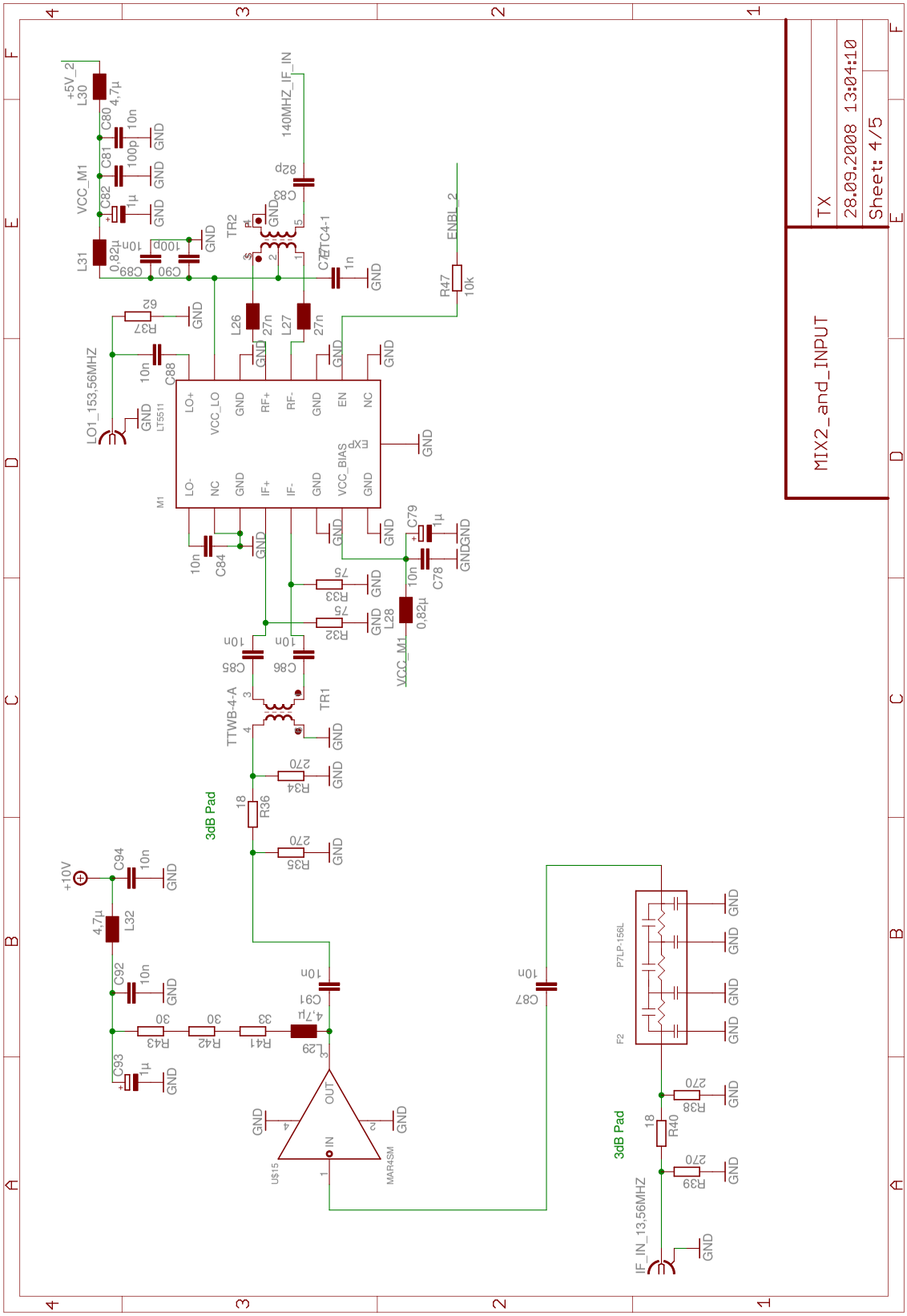

Figure A.4: Transmitter schematic 4/5

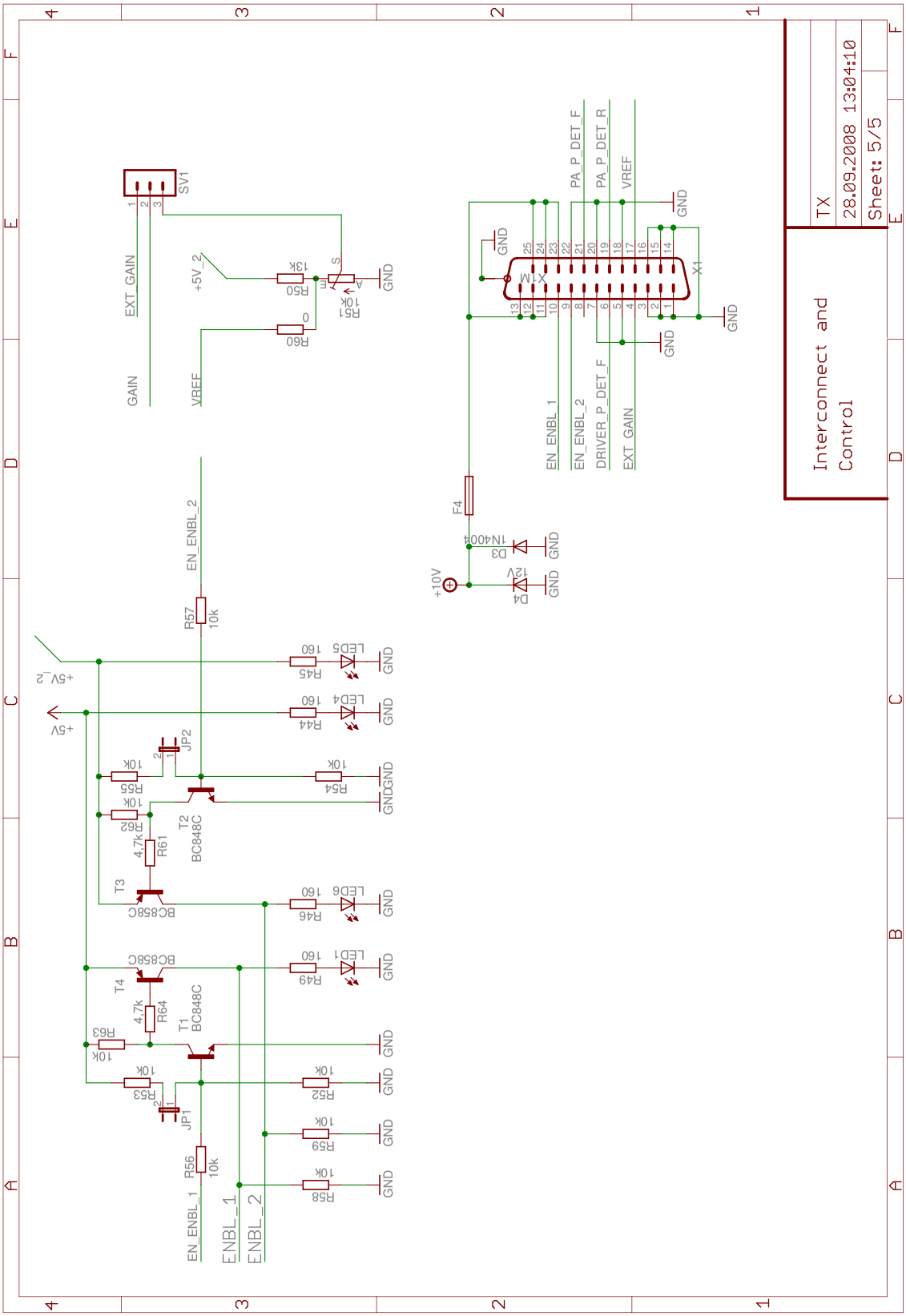

Figure A.5: Transmitter schematic 5/5

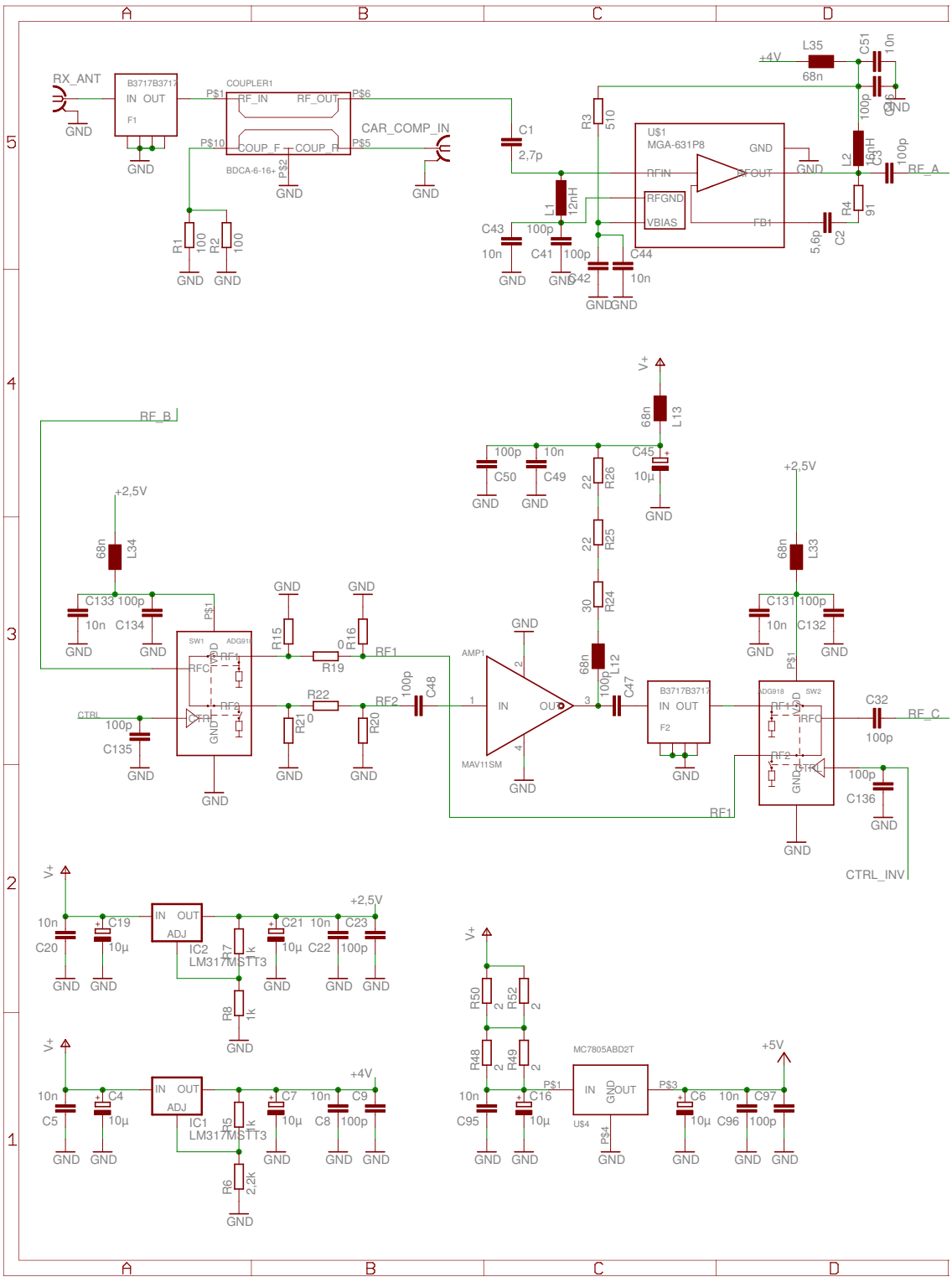

Figure A.6: Receiver schematic 1A/3

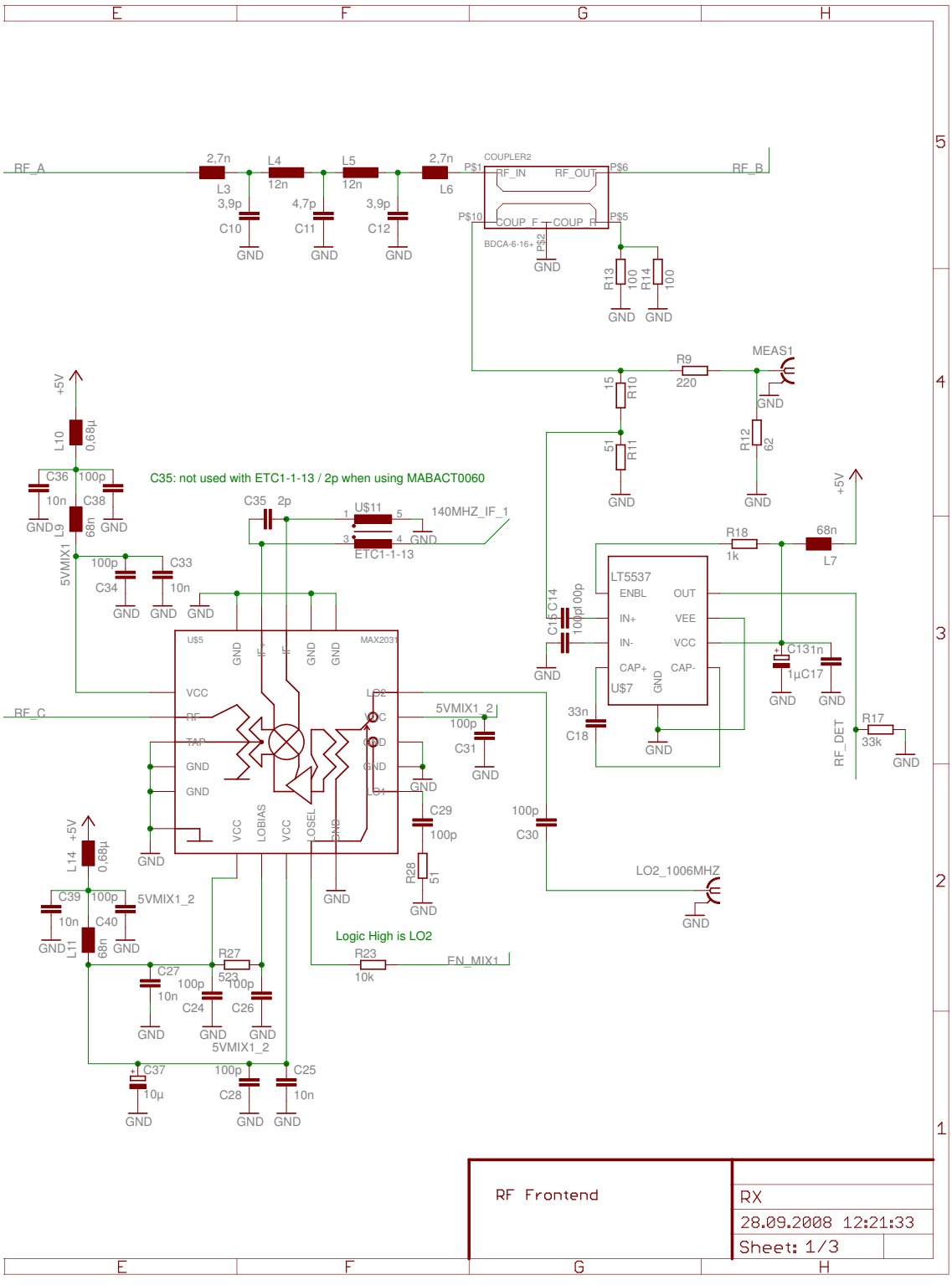

Figure A.7: Receiver schematic 1B/3

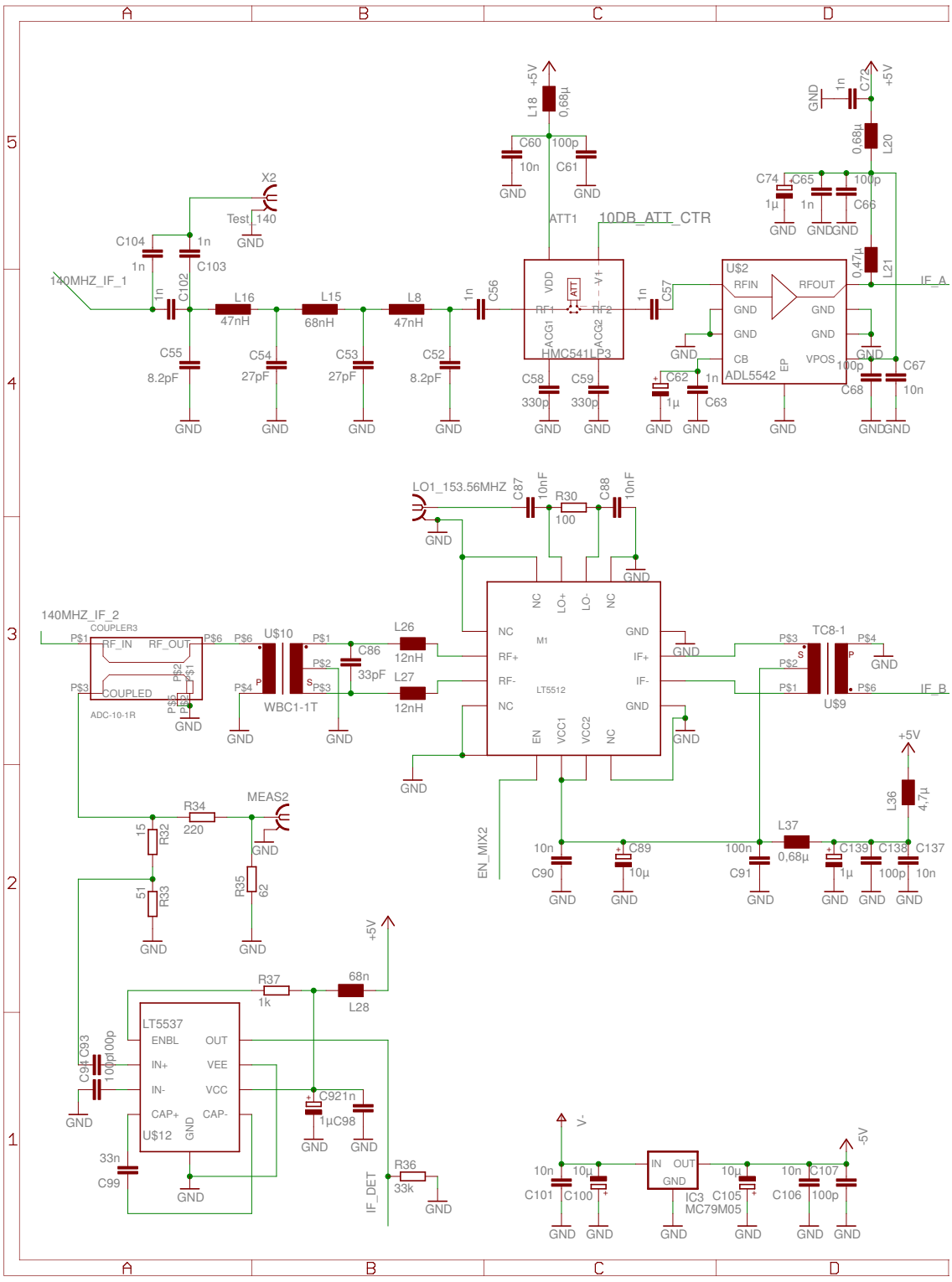

Figure A.8: Receiver schematic 2A/3

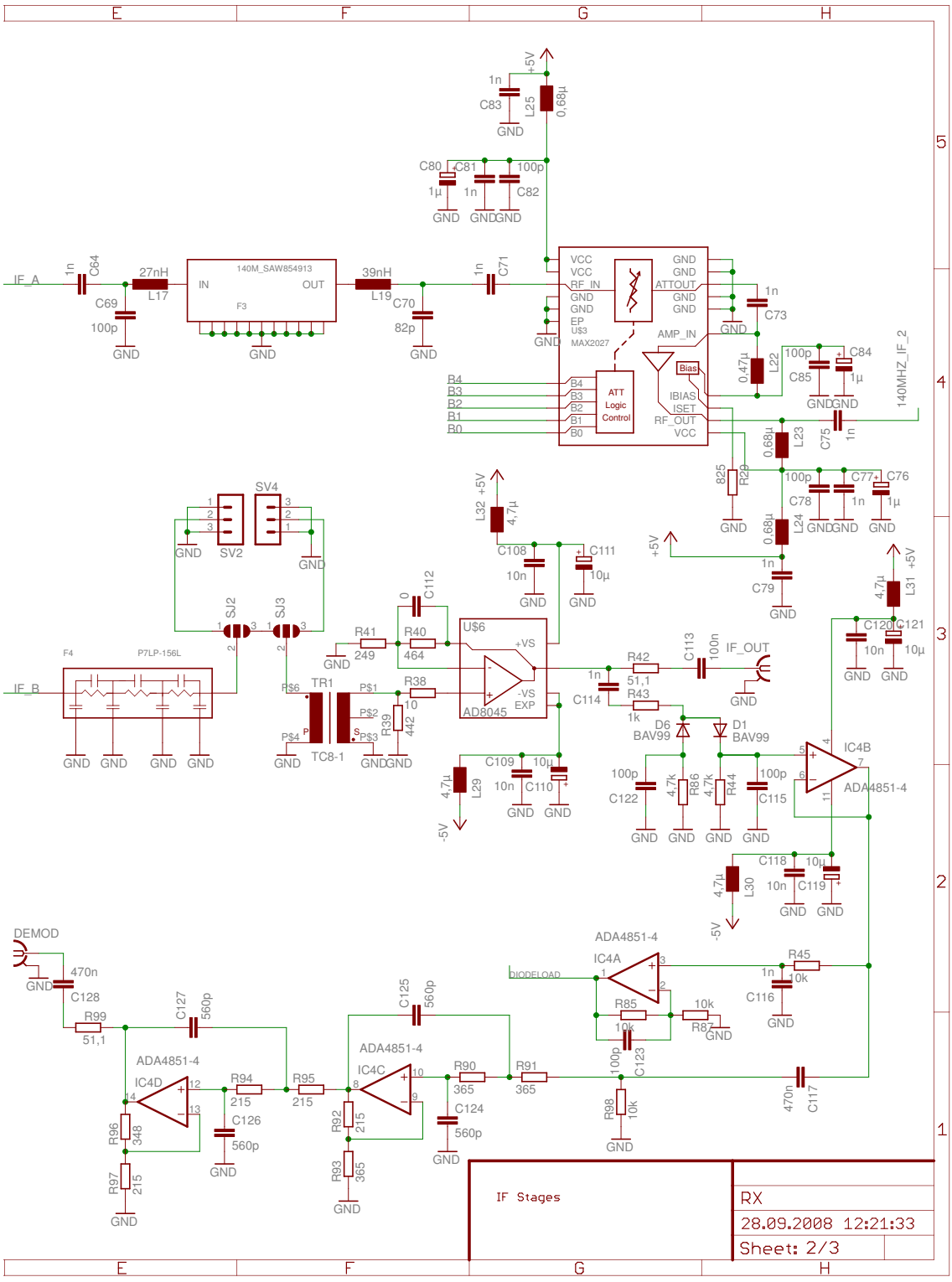

Figure A.9: Receiver schematic 2B/3

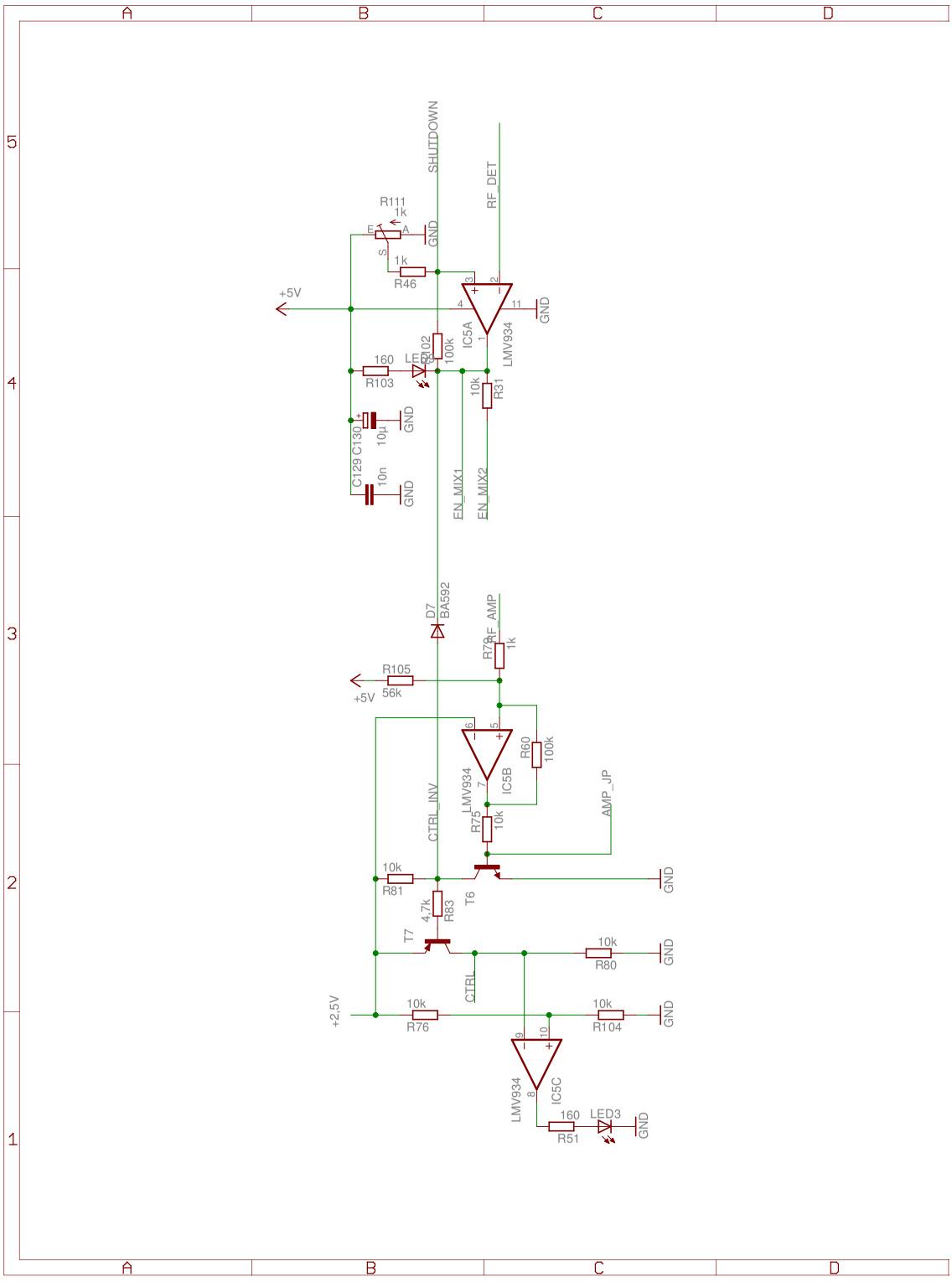

Figure A.10: Receiver schematic 3A/3

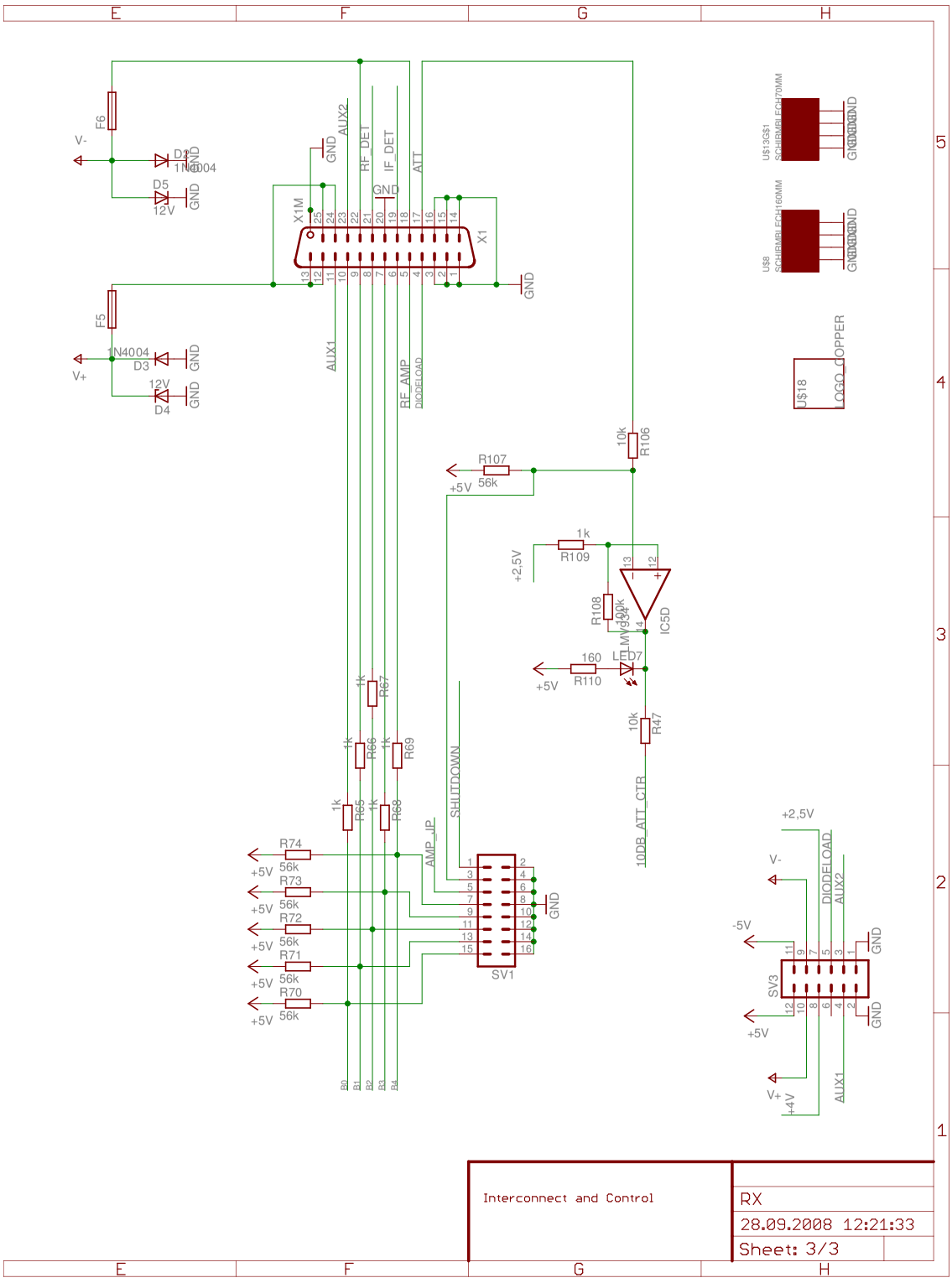

Figure A.11: Receiver schematic 3B/3

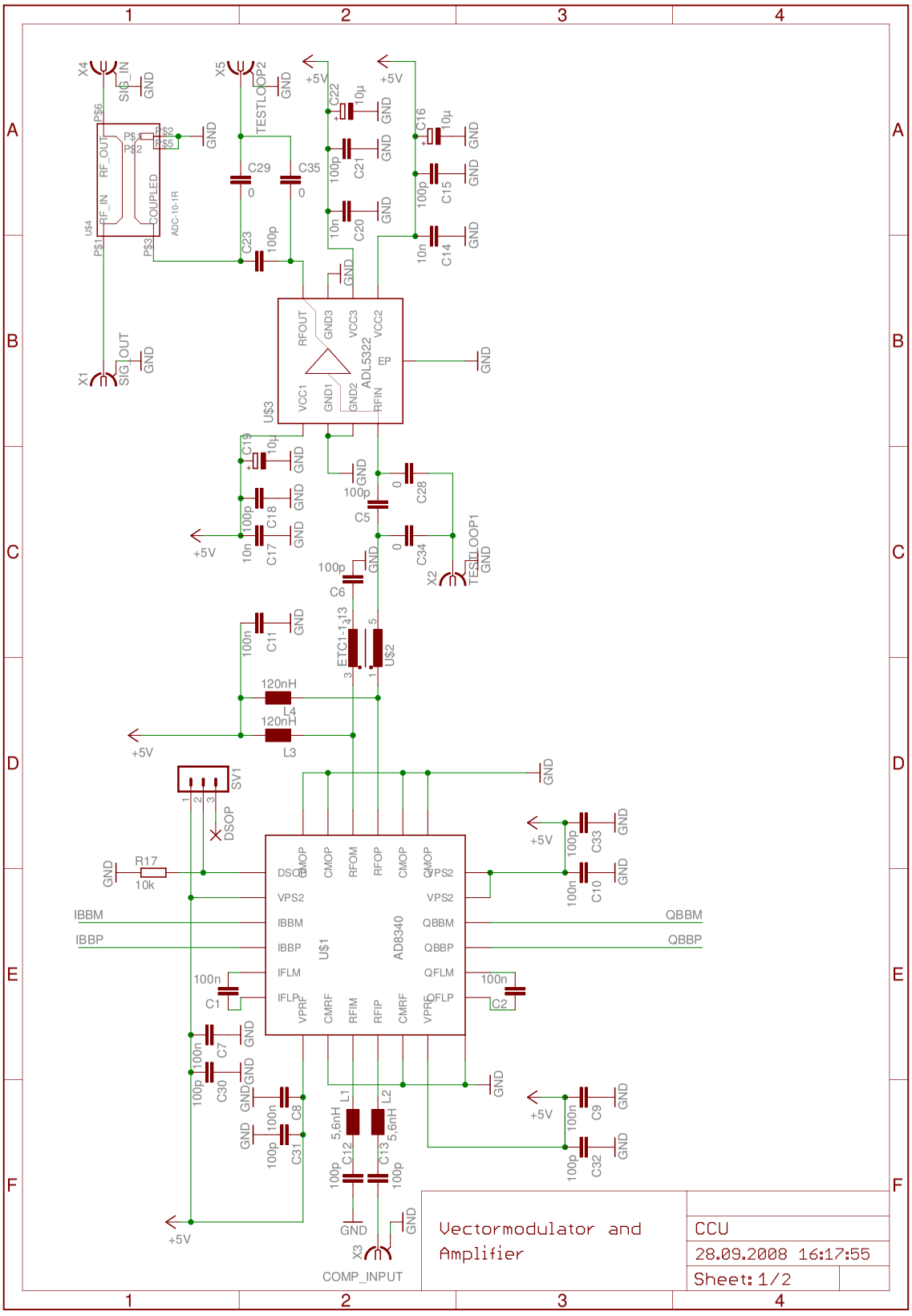

Figure A.12: CCU schematic 1/2

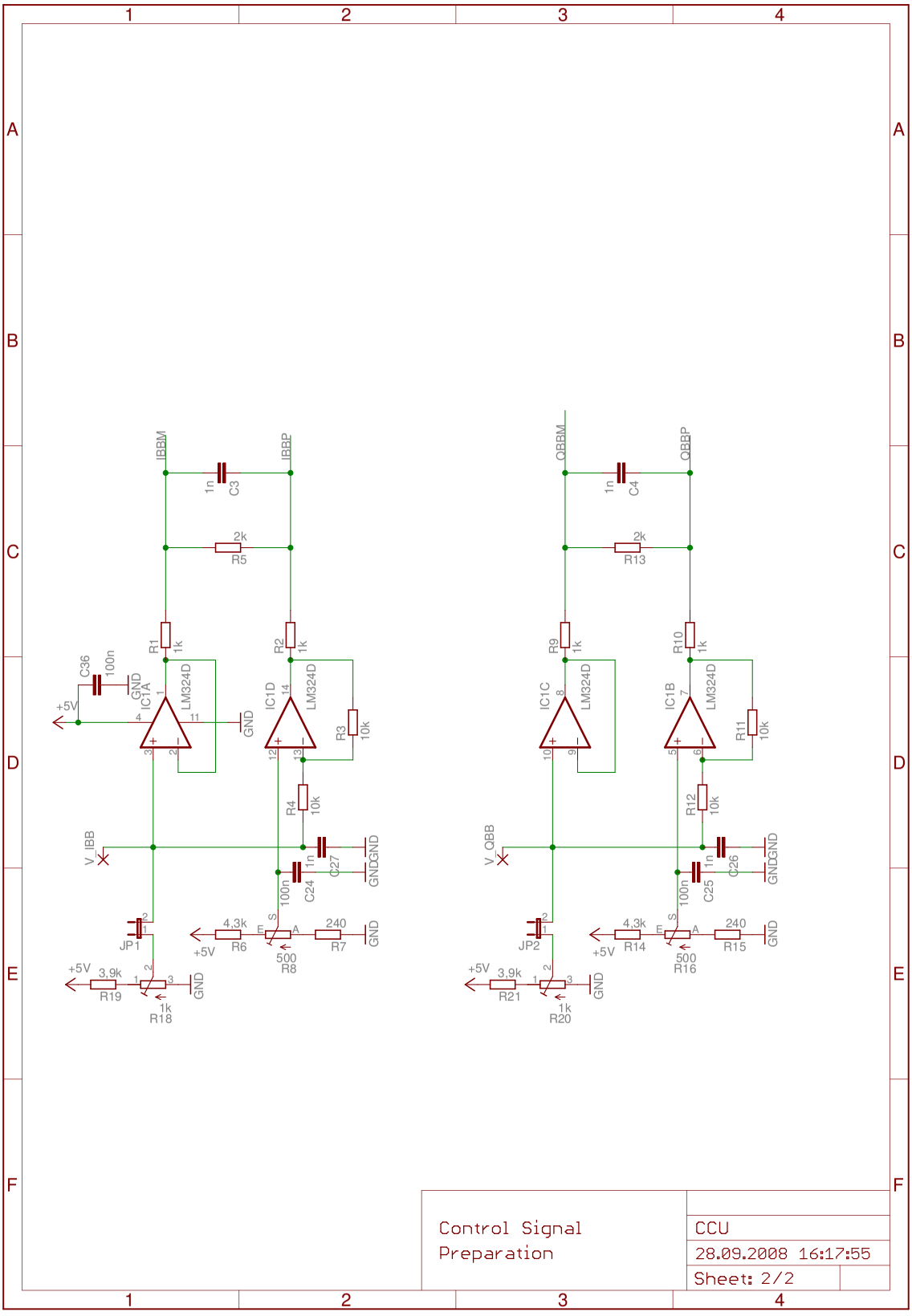

Figure A.13: CCU schematic 2/2

Acknowledgments

I would like to thank my supervisors Robert Langwieser and Arpad L. Scholtz for their guidance and support throughout this diploma thesis. Special thanks also go to Michael Fischer and Lukas W. Mayer for many inspiring discussions.

I would also like to thank my friends and my colleagues from university for their encouragement and help during my studies.

Last but not least I would like to thank my parents for giving me valuable support to finish my studies, and my sister for her understanding and giving me so much motivation.

Bibliography

[1] J. Landt. The history of RFID. *IEEE Potentials*, 24(4):8–11, October-November 2005.

[2] Jari-Pascal Curty, Michael Declercq, Catherine Dehollain, and Norbert Joehl. *Design and Optimization of Passive UHF RFID Systems*. Springer, first edition, 2007.

[3] ERC recommendation 70-03 relating to the use of short range devices (SRD), May 2007.

[4] Pavel V. Nikitin and K. V. S. Rao. Theory and measurement of backscattering from RFID tags. *IEEE Antennas and Propagation Magazine*, 48(6), December 2006.

[5] R. C. Hansen. Relationships between antennas as scatterers and as radiators. *Proceedings of the IEEE*, 77(5):659–662, May 1989.

[6] W. K. Kahn and H. Kurss. Minimum-scattering antennas. *IEEE Transactions on Antennas and Propagation*, 13(5):671–675, September 1965.

[7] P.V. Nikitin, K.V.S. Rao, and R.D. Martinez. Differential RCS of RFID tag. *Electronics Letters*, 43(8):431 – 432, April 2007.

[8] R. E. Collin. Limitations of the thevenin and norton equivalent circuits for a receiving antenna. *IEEE Antennas and Propagation Magazine*, 45(2):119–124, April 2003.

[9] Jørgen Bach Andersen and Rodney G. Vaughan. Transmitting, receiving and scattering properties of antennas. *Antennas and Propagation Magazine, IEEE*, 45(4):93 – 98, August 2003.

[10] Yu Liu, Qishan Zhang, and Ming Zheng. Signal analysis and design criteria for UHF RFID reader. *ITS Telecommunications Proceedings*, pages 233–236, June 2006.

[11] Lukas W. Mayer and Arpad L. Scholtz. A dual-band HF/UHF antenna for RFID tags. VTC2008 Fall, to be published.

[12] C. Angerer, M. Holzer, B. Knerr, and M. Rupp. A flexible dual frequency testbed for RFID. In *Tridentcom08: proceedings of the 4th International Conference on Testbeds and Research Infrastructures for the Develpment of Networks and Communities*, March 2008.

[13] Gottfried Magerl. Messtechnik. Skript, May 2004.

[14] Mini-Circuits. *MAR-4SM+*. P.O. Box 350166, Brooklyn, New York, rev. b edition.

[15] Linear Technology Corporation. *LT5537*. 1630 McCarthy Blvd., Milpitas, CA 95035-7417, rev. a edition, 2005.

[16] Linear Technology Corporation. *LT5512*. 1630 McCarthy Blvd., Milpitas, CA 95035-7417, rev. a edition, 2005.

[17] Paul Horowitz and Winfield Hill. *The Art of Electronics*. Cambridge University Press, 1980.

[18] Analog Devices. *AD8340*. One Technology Way, P.O. Box 9106, Norwood, MA 02062-9106, U.S.A., rev. b edition, 2007.

[19] EPCglobal. Epc radio-frequency identity protocols class-1 generation-2 UHF RFID protocol for communications at 860 MHz – 960 MHz version 1.2.0, March 2007.

[20] SmartAnt Telecom Co. Ltd. *SAA06-290010*. 2F, No. 669, Sec. 4, Chung Hsing Rd., Chutung, Hsinchu,310 Taiwan R.O.C., preliminary 0.1 edition.

[21] Robert Langwieser, Gregor Lasser, Christoph Angerer, Markus Rupp, and Arpad L. Scholtz. A modular UHF reader frontend for a flexible RFID testbed. In *RFID2008*, Budapest, Hungary, July 2008.

List of Abbreviations

AC	Alternating Current
ADC	Analogue to Digital Converter
AGC	Automatic Gain Control
ASIC	Application-Specific Integrated Circuit
ASK	Amplitude-Shift Keying
BALUN	BALanced - UNbalanced converter
BPF	Band Pass Filter
BPSK	Binary Phase Shift Keying
CCU	Carrier Compensation Unit
CW	Continous Wave
DAC	Digital to Analogue Converter
DC	Direct Current
DSP	Digital Signal Processor
DUT	Device Under Test
EIRP	Equivalent Isotropically Radiated Power
ERP	Equivalent Radiated Power
GPIB	General Purpose Interface Bus (IEEE 488)
GSM	Global System for Mobile Communications
HF	High Frequency
HPF	High Pass Filter
IC	Integrated Circuit
IF	Intermediate Frequency
LAN	Local Area Network
LED	Light Emitting Diode
LF	Low Frequency
LO	Local Oscillator
LNA	Low Noise Amplifier
LPF	Low Pass Filter
MIMO	Multiple Input Multiple Output
op-amp	operational amplifier
PA	Power Amplifier
PC	Personal Computer
PCB	Printed Circuit Board
RCS	Radar Cross Section
RF	Radio Frequency
RMS	Root Mean Square
RX	Receiver

SAW	Surface Acoustic Wave
SMA	SubMiniature version A (connector)
SNR	Signal to Noise Ratio
SOLT	Short, Open, Load, Thru (calibration method)
TX	Transmitter
UHF	Ultra High Frequency
VGA	Variable Gain Amplifier
VNA	Vector Network Analyzer
VSG	Vector Signal Generator

List of Symbols

Att	Attenuator Level
BW	Bandwidth
$\tan\delta$	Dielectric Loss Tangent
ε_r	Relative Permittivity
$EIRP$	Equivalent Isotropically Radiated Power
f_c	Center Frequency
F	Noise Figure
G	Gain
g	Normalized Conductance
h	Thickness, Height
I	Current
IM_3	3$^{\text{rd}}$ Order Intermodulation Ratio
IP_3	3$^{\text{rd}}$ Order Intercept Point
λ	Wavelength
P	Power
$P_{1\text{dB}}$	1 dB Compression Point
ϱ	Reflection Coefficient
RBW	Resolution Bandwidth (of Spectrum Analyzer)
S	Power Density
U	Voltage
VBW	Video Bandwidth (of Spectrum Analyzer)
w	Width
Z	Complex Impedance
z	Normalized Complex Impedance
Z_w	Characteristic Impedance of Transmission Line
Z_0	Characteristic Impedance of System

List of Figures

List of Tables